Fluvial geomorphic elements in modern sedimentary basins and their potential preservation in the rock record: a review

Weissmann, G.S.[a,*], Hartley, A.J.[b], Scuderi, L.A.[a], Nichols, G.J.[c], Owen, A.[b], Wright, S.[a], Felicia, A.L.[a], Holland, F.[a], and Anaya, F.M.L.[a]

[a] Department of Earth and Planetary Sciences, MSC03 2040, 1 University of New Mexico, Albuquerque, New Mexico 87131-0001, U.S.A.

[b] Department of Geology and Petroleum Geology, School of Geosciences, University of Aberdeen, Aberdeen, AB24 3UE, U.K.

[c]Nautilus Limited, Ashfields Farm, Priors Court Road, Hermitage, Berkshire, RG18 9XY, U.K.

[*] Corresponding Author Email: weissman@unm.edu (G. Weissmann)

Fluvial geomorphic elements in modern sedimentary basins and their potential preservation in the rock record: areview

Weissmann, G.S.[a,*], Hartley, A.J.[b], Scuderi, L.A.[a], Nichols, G.J.[c], Owen, A.[b], Wright, S.[a], Felicia, A.L.[a], Holland, F.[a], and Anaya, F.M.L.[a]

[a] Department of Earth and Planetary Sciences, MSC03 2040, 1 University of New Mexico, Albuquerque, New Mexico 87131-0001, U.S.A.

[b] Department of Geology and Petroleum Geology, School of Geosciences, University of Aberdeen, Aberdeen, AB24 3UE, U.K.

[c]Nautilus Limited, Ashfields Farm, Priors Court Road, Hermitage, Berkshire, RG18 9XY, U.K.

[*] Corresponding Author Email: weissman@unm.edu (G. Weissmann)

Abstract

Since tectonic subsidence in sedimentary basins provides the potential for long-term facies preservation into the sedimentary record,analysis of geomorphic elements in modern continental sedimentary basins is required to understand facies relationships in sedimentary rocks. We use a database of over 700 modern sedimentary basins to characterize the fluvial geomorphology of sedimentary basins. Geomorphic elements were delineated in 10representativesedimentary basins, focusing primarilyon fluvial environments. Elements identified includedistributive fluvial systems (DFS), tributive fluvial systems that occur between large DFS or in an axial position in the basin, lacustrine / playa, and eolian environments. The DFS elements includelarge DFS (>30km in length), small DFS (<30 km in length), coalesced DFS in bajada or piedmont plains, and incised DFS. Our results indicate that over 88% of fluvial deposits in the evaluatedsedimentary basins are present as DFS, with tributary systems covering a small portion (1-12%) of the basin. These geomorphic elements are commonly arranged hierarchically, with the largest transverse rivers forming large DFSand smaller transverse streams depositing smaller DFS in the areas between the larger DFS. These smaller streams commonly converge between the large DFS, forming a tributary system. Ultimately, most transverse rivers become tributary to the axial system in the sedimentary basin, with the axial system being confined between transverse DFSentering the basin from opposite sides of the basin, or a transverse DFS and the edge of the sedimentary basin. If axial systems are not confined by transverse DFS, they will form a DFS.Many of the world's largest rivers are located in the axial position of some sedimentary basins. Assuming uniformitarianism, sedimentary basins from the past most likely had a similar configuration of geomorphic elements.

Facies distributions in tributary positions and those on DFS appear to display specific morphologic patterns. Tributary rivers tend to increase in size in the downstream direction. Because axial tributary rivers are present in confined settings in the sedimentary basin, they migrate back and forth within a relatively narrow belt (relative to the overall size of the sedimentary basin). Thus, axialtributary riverstend to display amalgamated channel belt form with minimal preservation potential of floodplain deposits. Chute and neck cutoff avulsions are also common on meandering rivers in these settings. Where rivers on DFS exit their confining valley on the basin margin, sediment transport capacity is reduced and sediment deposition occurs resulting in development of a 'valley exit' nodal avulsion point that defines the DFS apex. Rivers may incise downstream of the basin margin valley because of changes in sediment supply and discharge through climatic variability or tectonic processes. We demonstrate that rivers on DFS commonly decrease in width down-DFS caused by infiltration, bifurcation, and evaporation. In proximal areas, channel sands are amalgamated through repeated avulsion, reoccupation of previous channel belts, and limited accumulation space. When rivers flood on the

medial to distal portions of a DFS, the floodwaters spread across a large area on the DFS surface and typically do not re-enter the main channel. In these distal areas, rivers on DFS commonly avulse, leaving a discrete sand body and providing high preservation potential for floodplain deposits.

Additional work is needed to evaluate the geomorphic character of modern sedimentary basins in order to construct improved facies models for the continental sedimentary rock record. Specifically, models for avulsion, bifurcation, infiltration, and geomorphic form on DFS are required to better define and subsequently predict facies geometries. Studies of fluvial systems in sedimentary basins are also important for evaluating floodpatterns and groundwater distributions for populations in these regions.

Keywords: distributive fluvial systems; sedimentary basins; tributary fluvial systems; fans

1. Introduction

Sedimentologists focused on continental environments (e.g., fluvial, alluvial, eolian, and lacustrine deposits) seek modern analogs to betterunderstand processes that may have been responsible for forming the facies distributions observed in the rocks and for improved prediction of facies connectivity and geometries for applications in natural resource development (e.g., petroleum reservoirs, groundwater, and aggregate). To this end, geomorphic studies of rivers and other continental environments have served to help formulate facies models of these depositional systems (e.g., Collinson,1996; Miall, 1996, 2010; Bridge, 2006).

A fundamental concept in sedimentary geology is that sediments that ultimately become sedimentary rocks must be buried and preserved at a depth, and this occurs primarily in sedimentary basins where tectonic subsidence occurs (Miall, 2000; Allen and Allen, 2013). Not all geomorphic studies used in understanding continental environments for facies models, however, have been conducted in sedimentary basins (Weissmann et al., 2011). In order to evaluate sedimentary basin-scale (e.g., 10^4 – 10^6 km^2) processes of continental sedimentary fill and the geomorphic processes responsible for facies distributions observed in the rock record, we must evaluate the geomorphic processes of modern sedimentary basins. Studies of continental geomorphology outside these sedimentary basins may be useful for understanding channel-scale depositional processes and upstream catchment contribution to sediment supply and stream discharge. However, these will not further the understanding of sedimentary basin-scale processes and overall geometries of deposits responsible for sedimentary basin fill and evolution (Hartley et al., 2010b).

In the continental realm, tectonic subsidence exists in sedimentary basins located in divergent, intraplate, convergent, and transform settings (e.g., Ingersoll, 2012; Allen and Allen, 2013).In these continental areas, long-term subsidence occurs and sediments are lowered below a level where erosion is possible (e.g.,*preservation space*of Blum and Törnqvist, 2000). Nyburg and Howell (2015) showed that modern continental sedimentary basins cover only ~16% of the current continental area if one excludes the passive margin setting, thus only deposits from a relatively small portion of the modern continental area will ultimately be preserved in the sedimentary rock record.

Weissmann et al. (2010) identified 724 continental sedimentary basins (e.g., basins primarily located on the continents with minimal marine influence, thus excluding the passive margin setting) globally, a compilation that coversmost climatic and tectonic settings. Though this has been reported as excluding all rivers that enter the ocean (e.g., Sambrook Smith et al., 2010; Fielding et al., 2012), this designation only denotes that sea level change did not affect deposition in most of these sedimentary basins. However, some of the axial rivers may exit the sedimentary basin and ultimately terminate in the ocean.Active subsidence in these sedimentary basins is indicated by relatively thick (10s to 100s of meters in many basins) accumulation of young (Quaternary and Neogene) sediments. Though subsurface data are not available for all 724 sedimentary basins identified by Weissmann et al. (2010), compilations describing sedimentary basins indicates that sediments are accumulating in these tectonic settings (e.g., Busby and Ingersoll, 1995; Busby and Azor Peréz,2012; Allen and Allen, 2013). In our recentwork (e.g., Hartley et al., 2010a,b, 2013; Weissmann et al., 2010, 2011, 2013; Davidson et al., 2013), we indicated that distributive fluvial systems (DFS) cover large areas in these sedimentary basins and comprise most but not all of the fluvial deposits in these basins. Additionally, wenoted that deposits of tributive fluvial systems comprise a much smaller percentage of the basin area.

The term, DFS,wasdefined as ’the *deposit* of a fluvial system which in planform displays a radial distributive channel pattern’ (Hartley et al., 2010b, P. 168, emphasis added). In 2010 (Hartley et al. 2010a,b; Weissmann et al., 2010), we proposed the DFS term in order to encompassfluvial and alluvialdistributive landforms at all scales. Thus, alluvial fans, fluvial fans, megafans, avulsive channel systems where the avulsions occur from a node at an apex (e.g., Richards et al., 1993), or alluvial cones (e.g., Geddes, 1960) are all different types of DFS. Wedeveloped the generalized term DFS rather than *fan* to avoid the confused terminology in response to concepts put forward by Blair and McPherson (1994) on what constitutes a fan. All of these landforms display apices where the stream enters the sedimentary basin at a point source (e.g., the upland valley) below which the riverdistributes sediment on fan-shaped landforms, thus filling accommodation produced by tectonic subsidence. The channel system on a DFS typically moves to new locations on the DFS through nodal avulsions at the DFS apex.

The term *distributive* was specifically selected (as opposed to *distributary*) to describe these landforms and is not ’a redundancy’, as suggested by Fielding et al. (2012). The term *distributive* is defined as ’…having the property of distributing; characterized by dealing portions or by spreading; given to engaged in distribution’ (Brown, 1993, P. 707-708). Thus, the rivers on the DFS have the property of distributing sediment wherever accommodation exists in the sedimentary basin, accomplishing this through deposition on alluvial fans, fluvial fans, and fluvial megafans. We specifically did not use the term *distributary*, as this implies that coeval flow exists in several channels (Neuendorf et al., 2005). Not all channel belts are coevally active on the DFS (Hartley et al., 2010b), nor is it possible to evaluate whether channels were coeval from the rock record.

The purpose of this review article is to examine the geomorphic character of fluvial systems in continental sedimentary basins using imagery and literature sources. We begin by delineating and describing various geomorphic elements found in sedimentary basins, offering a quantified assessment of the aerial coverage of these landforms and a possible interpretation of how these deposits may be represented in the sedimentary record. We use the term *geomorphic elements* to describe regions covered by different landform types found in the sedimentary basins (e.g., DFS, tributive fluvial systems, eolian, and lacustrine areas). We then review literature describingprocesses and deposits that occur on some of these geomorphic elements. Significant discussion of fluvial successions and their potential for preservation in the long-term rock record has occurred since Weissmann et al. (2010, 2011) and Hartley et al. (2010a,b) suggested that DFS deposits mostlikely comprise most of the fluvial sedimentary rock record from continental sedimentary basins; thus we follow the discussion on geomorphic elements in sedimentary basins with a review of the controversy surrounding this concept. This review paper is presented in *Geomorphology* with the hope that it will spawn new detailed analysis of the geomorphic processes that are present in sedimentary basins, thus significantly enhancing our understanding of fluvial successions from the past.

2. Terminology and methods of analysis

We delineated geomorphic elements from 10sedimentary basins around the world, representing a range of different tectonic (e.g., compressional, extensional, and transtensional) and climatic settings, in order to quantify the aerial significance of each geomorphic element type in the sedimentary basin setting and to evaluate typical positions of these geomorphic elements in the sedimentary basin context (Fig. 1; Table 1). Six fluvial elements were identified in the sedimentary basins. These include:

- Several types of distributive fluvial systems (DFS):
  - Megafans, or large DFS (>30km length), as described by Hartley et al. (2010b) (Fig. 2A). The 30-km minimum length for a megafandefined by Leier et al. (2005) and Hartley et al. (2010b) was used as a basis to distinguish megafans from smaller fans;
  - Fluvial fans and alluvial fans, or smaller DFS (<30km length) (Fig. 2B);
  - Bajada or piedmont, where fans are coalesced and cannot be readily distinguished from each other (Fig. 2C);
  - IncisedDFS (these may be large or small DFS), where under current climatic conditions the DFS contain an incised valley that cuts across all or part of the DFS (Fig. 2D);
- Tributive fluvial systems:
  - Axial tributary river systems, held in the axial position of the sedimentary basin and typically are orientedparallel to the long axis of the basin (Fig. 2E);
  - Interfan tributary rivers, where smaller streams are focused between large DFS (Fig. 2F).

In addition to the fluvial geomorphic elements, we noted the presence of two other geomorphic elements in the basins:

- Eolian depositional areas, specifically ergs that cover a significant area in the sedimentary basin (Fig. 2G);
- Lacustrine and playa depositional areas (Fig. 2H). Swamps and wetlands associated with DFS or tributive fluvial systems were included in the DFS or tributive system, though we recognize that wetlands may significantly affect facies locally (Hartley et al., 2010b).

Upland areas or internal uplifted areas within a sedimentary basin were also identified. These are typically found where intrabasinal faults have uplifted a small portion of underlying sediments and basement rock. None of the systems we have reviewed terminate in the marine realm, thus avoiding inclusion of areas where recent sea level change may have influenced depositional patterns.

To conduct this work, we used relatively cloud-free satellite images of the sedimentary basins. LANDSAT images and Shuttle Radar Topography Mission (SRTM) data were obtained from the Global Land Cover Facility (GLCF; http://glcf.umd.edu) or the U.S. Geological Survey EarthExplorer (http://earthexplorer.usgs.gov) databases and compiled for each sedimentary basin. We created false color images of each basin to create scenes that provide sufficient contrast in order to manually delineate and identify the geomorphic elements. We typically use the false color combination of LANDSAT bands with red=band 7, green = band 5, and blue = band 4 to reduce the influence of hazy atmospheric conditions and to display a primarily blue-yellow combination to clarify features for red-green colorblind individuals.Boundaries of geomorphic elements were digitized manually based on apparent orientation and connection of fluvial deposits to their source at their entry point to the sedimentary basin. This compilation was completed using ArcGIS software (ESRI, 2015). We projected this imagery in Equal Area projections appropriate to the location in order to preserve the area for comparison between different locations.

3. Geomorphic elements of modern sedimentary basins

Geddes (1960) described the distribution of fluvial deposits in the Ganges Plain as a series of large alluvial cones, later called megafans, with *intercone* fluvial deposits lying between the megafans. DeCelles and Cavazza (1999) later generalized foreland basin depositional form showing that the Himalayan and Andean foreland basins were covered by megafan deposits, fluvial deposition of inter-megafan rivers that converge to a stream forced between the megafans, and deposits of an axial fluvial trunk system, where all transverse streams ultimately become tributary.

Extensional basins have been shown to have similar character, with transverse streams forming alluvial fans of various sizes that are tributary to an axial river system (e.g., Leeder and Gawthorpe, 1987; Leeder et al., 1996; Gawthorpe and Leeder, 2000; Connell et al., 2012, 2013). Connell et al. (2012) used an experimental basin to show that the width of the axial stream system is dependent on the relative sediment supply in the axial system versus the transverse systems, where a narrower axial channel belt is observed when the transverse systems carry a relatively higher sediment load. The axial river will also form a large fan as it enters the basin if space is available (Connell et al., 2012).

In an expansion of previous work on sedimentary basins, Weissmann et al. (2010) used satellite imagery to evaluate fluvial form in over 700 modern sedimentary basins from different tectonic and climatic settings, recognizing that the pattern of transverse fans of varying sizes filling the sedimentary basins with sediment and discharge from DFS feeding the axial system are consistent in all sedimentary basins and that the area covered by DFS typically is much greater than that covered by tributary systems in the basin (e.g., see Fig. 3 from Weissmann et al., 2010). Many of the axial rivers in these basins are commonly considered to be some of the world's largest rivers (e.g., Gupta, 2007; Tandon and Sinha, 2007; Latrubesse, 2015). We also observed that the arrangement of fluvial geomorphic elements to be consistent with the distributions described by DeCelles and Cavazza (1999) in most sedimentary basins around the world (Fig.3).

In this section, we present geomorphic element delineation for10sedimentary basins that represent a range of different climatic and tectonic settings (Fig. 1) and review literature on depositional systems in these basins. To avoid redundancy in describing the features of sedimentary basins, we first describe the Himalayan and Andean foreland basins in greater detail since significant work has been completed on the geomorphology of these basins. Subsequent discussions of other basins focused on features that are unique to these basins while referring back to the Himalayan or Andean forelands for features that are similar between the basins studied.

3.1. Features of foreland basins:

Foreland basins are sedimentary basins that lie between a mountain front and the adjacent craton in compressional settings (Allen et al., 1986; Covey, 1986; DeCelles, 2012). We delineated geomorphic elements in portions of three foreland basins– the Himalayan foreland basin in India (Fig.4), the Chaco Plain of the Andean foreland basin, South America (Fig. 5), and the Tanana foreland basin located south of Fairbanks, Alaska (Fig. 6). We chose these basins as they comprise different climatic regimes from continental to subtropical monsoon influenced (Himalaya), subtropical to drylands (Andes), and continental to polar (Tanana). In all three foreland basins, DFS cover more than 90% of the land surface, with tributary inter-DFS or axial systems covering between 2 and 7% of the area (Table 1).

Many geomorphic studies have been conducted on the fluvial deposits in the Himalayan foreland basin (e.g., Geddes, 1960; Gole and Chitale, 1966; Wells and Dorr, 1987; Mohindra et al., 1992; Singh et al., 1993; Sinha and Friend, 1994; Sinha, 1996, 2009; Lahiri, 1996; Gupta, 1997; Shukla et al., 2001; Kale, 2002; Jain and Sinha, 2003, 2004, 2005; Sarma, 2005; Sinha et al., 2005, 2007, 2014; Singh et al., 2006; Tandon et al., 2006; Singh, I.B., 2007; Singh, S.K., 2007; Chakraborty and Ghosh, 2010; Chakraborty et al., 2010; Wilkinson et al., 2010; Sinha and Tandon, 2014) and the Andean foreland basin (e.g., Iriondo, 1993, 2007; Horton and DeCelles, 1997, 2001; DeCelles and Cavazza, 1999; Leier et al., 2005; Wilkinson et al., 2006, 2010; Iriondo and Paira, 2007; Iriondo et al., 2007; May, 2011; Latrubesse et al., 2012). This previous work described fluvial processes and landforms on the large DFS (or megafans) and axial streams of these basins.

The configuration of fluvial depositional landforms in all three foreland basins mapped in this work corresponds to the geomorphic model suggested by DeCelles and Cavazza (1999). In these basins, large DFS, or megafans, develop where rivers with relatively large drainage basins enter the sedimentary basins (Figs. 4, 5, and 6; Table 2). These large DFS coalesce to form a broad alluvial plain covering the area adjacent to the mountain belt arc. Sinha and Friend (1994) termed rivers that feed these large DFS as *mountain-fed streams*asthese are sourced from high in the adjacent mountain range. Some groundwater-fed rivers develop on the distal portion of these large DFS, termed *plains-fed streams* by Sinha and Friend (1994). These plains-fed streams are typically underfit streams held in larger paleochannels that represent a previous position of the main river on the DFS.

Smaller DFS fill the sedimentary basin in areas between the large DFS (inter-megafan area of DeCelles and Cavazza, 1999). These are developed from rivers that have smaller drainage basins (Table 2) and have been called *foothills-fed streams* by Sinha and Friend (1994). Many of these *smaller* DFS still exceed 30km in length and would thus be classified as a large DFS, but they are smaller than the DFS formed from the mountain-fed rivers. A tributary river system may develop in a zone of convergence that is present where the foothills-fed rivers are forced between the larger mountain-fed DFS. Ultimately, all of these rivers are tributary to the axial river system in the basin.

In all three foreland basins delineated for this project, stream width measurementsderived from satellite images of the rivers in these basins indicate that the axial rivers are the widest (and thus largest) rivers in the sedimentary basin (e.g., the Ganga and Brahmaputra Rivers in the Himalayan Foreland, the Paraguay and Paraná Rivers in the Chaco Plain, and the Tanana River in the Tanana Foreland) while the transverse rivers that feed the large DFS appear to carry significantly less discharge. Accurate discharge data for these rivers are difficult to acquire; however, data available for the Ganga River at Farakka (located just before the river enters Bangladesh) indicates this river has a mean annual discharge of ~4.59 billion m^3 (Rao, 1975) while the major tributaries on DFS (e.g., the Ghaghra, Gandak, and Kosi rivers) range in mean annual discharge between 52 and 94 million m^3 (Dhar and Nandargi, 2002).

3.1.1. Himalayan foreland basin, India

In the Ganges Plain of the Himalayan foreland basin, several transverse rivers built large DFS, including the Ganga (56,664 km^2), the Sarda/Ghaghra (79,518 km^2), Gandak (26,757 km^2), Kosi (12,839 km^2), and Tista (18,227 km^2) DFS on the north side of the basin and the Son (8361 km^2) from the south (e.g., cratonic) side of the basin. Between several of the large DFS are smaller interfan DFS (Fig. 2F). Rivers that form these smaller DFS have apices that exist at the mouths of relatively steep drainage basins and thus tend to deposit a mix of grain sizes with a relatively higher percentage of coarser material, on average, such as boulder and gravel grade material (Roy, 1981; Fig. 7) than the rivers on large DFS (Geddes, 1960; Sinha and Friend, 1994; Sinha, 1996; Singh et al., 2006), where the deposits of the large DFS are dominated by medium sand and finer. The rivers from these small interfan DFS converge between the larger DFS, thus creating inter-megafan tributary systems (Fig.8). These inter-megafan rivers can be quite large and the sandy channel belt very wide. For example, the Mahananda River, located between the Kosi and Tista large DFS, is ~2 km wide. Where the interfan Mahananda River reaches an area where accommodation is present between the distal toes of the large DFS, it forms a smaller DFS that fills accommodation between these megafans (Fig. 8).

The transverse rivers are tributary to the axial Ganges River in this portion of the basin. Depending on their position in the basin, the large DFS have varying orientations across the basin. For example, the Tista and Kosi DFS lie across the basin in an orientation relatively perpendicular to the axial Ganges River (Wilkinson et al., 2010). In contrast, DFS located in the western portion of this basin (including the Gandak, Ghaghra, and Ganga DFS) are oriented and elongated eastward with increasing degrees of incision into DFS to the west (Wilkinson et al., 2010; Sinha and Tandon, 2014; Fig.4).

Several large, incised DFS are present on the west side of this basin (e.g., the Yamuna, Ganga, and Ghaghra DFS). Rivers on these DFS are presently held in deep (10-20 m) incised valleys cut through older fluvial deposits (e.g., Shukla et al., 2001; Gibling et al, 2005; Tandon et al., 2006; Roy et al., 2012). Though interfluve deposits are significantly modified by human development, several paleochannels are observed on the interfluve areas that appear to radiate outward from the different apices (e.g., Shukla et al., 2001; Fig. 9). Therefore, we interpret these deposits as incised large DFS.

Several authors have indicated that incision in the western Ganges plain is related to changes in stream power and sediment supply caused by variation in monsoon strength (e.g., Gibling et al., 2005; Tandon et al., 2006; Kale, 2007; Roy et al., 2012), where periods of monsoon intensification lead to incision and erosion in the western Ganges Plain. Additionally, Roy et al. (2012) used OSL dating from the Ganga Valley and surrounding interfluve deposits to show that periods of aggradation in the western Ganges Plain were correlative to times of declining monsoonal strength.

The large DFS are tributary to the axial Ganges River in this portion of the sedimentary basin. This axial system increases in width to the west as the river gains discharge from its tributary rivers, expanding from 1 km wide to about 15 km wide. The axial Ganges River is confined between the large transverse DFS to the north and either the sedimentary basin edge to the south or large DFS entering the basin from the south.

In the Brahmaputra Valley portion of the Himalayan foreland basin, the Brahmaputra River forms a very large anabranching, multichannel, and multipattern axial tributary river (Gilfellon et al., 2003; Sarma, 2005; Sarma and Phukan, 2006; Singh, 2007; Latrubesse, 2008; Lahiri and Sinha, 2012). The Brahmaputra River is held between a piedmont plain of coalesced DFS to the north and either large DFS or the Shilong Plateau to the south (Lahiri and Sinha, 2012; Fig. 10). All rivers that enter the eastern end of this sedimentary basin form a piedmont plain of coalesced DFS, including the Brahmaputra River as it enters the basin (Fig. 11).

The DFS on the two sides of this basin display different form (Sarma, 2005; Lahiri and Sinha, 2012). Tributary rivers on the south side of the Brahmaputra River constructed large DFS, including the Noadihang (3219 km^2), Burhi Dihing (1816 km^2), and the Dikhow (602 km^2) DFS (Table 2). The rivers on these tributary DFS display sinuosities ranging between 1.37 and 2.06 (Lahiri and Sinha, 2012) with river morphology commonly displaying classic meanderbelt form with alternating point bars and common neck cut off avulsions, indicated by the presence of oxbow lakes (Fig. 10). Lahiri and Sinha (2012) suggested that much of this channel belt shifting is through lateral meander migration, with no apparent preferred direction of this migration.

In contrast, the rivers on the northern side of the Brahmaputra River tend to have smaller DFS, ranging in size from <200 to 737 km^2 (Table 2). These rivers display sinuosity ranges between 1.2 and 2.0, with paleochannels on the DFS surface displaying generally lower sinuosities than their modern counterparts (Lahiri and Sinha, 2012). Avulsive shifts on these DFS currently tend to be westward in response to local subsidence (Lahiri and Sinha, 2012).

The axial Brahmaputra River is characterized by high discharge (mean annual discharge of 21,200 m^3/s; Lahiri and Sinha, 2012) and sediment supply (mean annual sediment discharge of 852.4 $t/km^2/yr$; Latrubesse, 2008), with bankfull flows and peak sediment movement occurring during the monsoon (Goswami, 1985). Channels switch frequently in the active channelbelt plain, and the sides of the channel belt have migrated and widened into the surrounding DFS through time (Goswami, 1985; Sarma, 2005; Lahiri and Sinha, 2012). Sinuosity along this river is relatively low, ranging from 1.02 to 1.05 (Lahiri and Sinha, 2012). Much of the channel belt evolution is controlled by local tectonic features through local regions of higher subsidence or faulting (Lahiri, 1996; Lahiri and Sinha, 2012). The bed material and bar deposits of the Brahmaputra River typically range in grain size between silt and fine sand with some coarse sand (Goswami, 1985; Sarma, 2005).

3.1.2. Andean foreland basin, Chaco Plain

Similar to the Himalayan foreland basin deposits, the Chaco Plain portion of the Andean foreland basin of Bolivia, Paraguay, and Argentina contains several large DFS, or megafans (Iriondo, 1993, 2007; Horton and DeCelles, 1997, 2001; DeCelles and Cavazza, 1999; Leier et al., 2005; Wilkinson et al., 2006, 2010; Iriondo and Paira, 2007; May, 2011; Latrubesse et al., 2012), including the three largest DFS in the world – the Pilcomayo River DFS (216,115 km^2), the Bermejo DFS (83,475 km^2), and the Salado DFS (184,819 km^2) (Fig.5). These, along with other large DFS, coalesce to form a regional alluvial plain that covers an area of over 700,000 km^2 in the Chaco Plain (Fig. 5; Table 1). The axial Paraguay and Paraná Rivers lie on the far eastern side of this basin and are held between the large DFS to the west and the basin edge to the east.

The mountain-fed rivers on the large DFS have large drainage basins, ranging in size from 7400 to over 900,000 km^2, that reach into the high Andes (Table 2). Rivers on these large DFS tend to enter the sedimentary basin as broad, braided channel belts. Down-DFS, many of the channel belts diminish in width, caused by infiltration, bifurcation, or evaporation, becoming single-thread channels with higher sinuosity (Iriondo, 2007; Hartley et al., 2010b; Weissmann et al., 2011). For example, the Bermejo River has an average width of about 2500m and average sinuosity of 1.08 across the upper 100 km of the DFS. The river becomes narrower and more sinuous downstream of a point located about 140 km from the apex, narrowing to an average width of 440 m and average sinuosity of 1.64 (Fig. 12). Interestingly, the change in sinuosity observed at ~140 km from the apex is not coincident with a change in the gradient (Fig.12C). Instead, the transition from a low-sinuosity channel to a high-sinuosity channel is coincident with the area below which paleochannel belts are no longer connected, with paleochannel belts are shown by lighter colors on the satellite imagery (Fig. 12A).

Rivers on the Pilcomayo, Parapetti, and Rio Grande DFS ultimately decrease in size such that they disappear into wetlands on the distal DFS surface, never reaching the axial Paraguay or Paraná rivers as a single, connected channel. However, the presence of paleochannels on the distal portions of these

DFS indicate that rivers on these DFS were larger in the Pleistocene and reached farther into the basin (e.g., Iriondo, 1993, 2007; Iriondo and Paira, 2007; Latrubesse et al., 2012). Iriondo et al. (2007) and papers held within that volume describe details of the geomorphology of the Chaco Plain, focusing especially on the axial Paraná River.

Similar to observations from the Himalayan foreland basin, smaller, foothills-fed DFS - developed from rivers with smaller drainage basins that do not extend far into the Andes Mountains (Table 2) - fill the accommodation between the large DFS (Fig.5). The tributary system formed as these foothills-fed rivers on the smaller DFS coalesce between the larger mountain-fed DFS is not as pronounced in the Chaco Plain as in the Himalayan foreland basin. Similar to the small, foothills-fed DFS in the Himalayan Foreland, the smaller foothills-fed DFS in the Chaco Plain typically have steeper gradients (Table 2).

Though some eolian deposits are observed in the basin, these appear to form a thin veneer on top of the large DFS deposits and thus were not delineated as eolian deposits in this review (e.g., for example, on the Parapetti DFS several eolian regions are observed; Iriondo and Paira, 2007; Latrubesse et al., 2012).

Below a spring line, groundwater-fed rivers emerge on the DFS plains (Iriondo, 1993; Weissmann et al., 2011; Hartley et al., 2013). Vegetation and soil character act as a proxy to mark this springline and moisture conditions in the soils, where vegetation in the western portion of the Chaco Plain (above the springline) reflect dryland species whereas vegetation below the springline in the east Chaco reflect wetter, swampy conditions (Zak and Cabido, 2002; Iriondo and Paira, 2007; Hartley et al., 2013).

At the toe of the alluvial plain, the axial Paraguay and Paraná rivers form a large tributary system along the eastern edge of the basin, collecting discharge from the transverse DFS. As these rivers enter the sedimentary basin from the east, they construct large DFS before forming the axial drainage in the basin (Fig. 13). Once in the basin, the axial system is confined between the eastern edge of the basin and the large DFS to the west and covers an area of ~14,500 km^2 (Table 1).

The axial Paraguay River is confined to an 8-15 km wide meanderbelt held between the very large DFS (e.g., Pilcomayo and Bermejo DFS) and the eastern edge of the sedimentary basin in the northern part of the Chaco Plain. Scroll bar topography is dominant in the floodplain surrounding the active river, indicating that much of the deposit consists of an amalgamation of point bar deposits.

As the Paraná River enters the foreland basin, it forms a large DFS and then joins the Paraguay River as the axial river in the southern portion of the Chaco Plain (Iriondo, 2007; Iriondo and Paira, 2007). The combined river forms a very broad anabranching channel belt and floodplain complex covering a width of up to 45km (Orfeo and Stevaux, 2002; Iriondo, 2007; Lewin and Ashworth, 2014; Fig. 13). This axial system is confined between the transverse large DFS and the eastern edge of the sedimentary basin. Orfeo and Stevaux (2002) divided the floodplain into two portions: the proximal floodplain, which receives annual floods, and the distal floodplain, which receives only *extraordinary* floods (these authors do not indicate a return period for the extraordinary floods). This channel/floodplain complex is composed of amalgamated bar forms consisting of primarily medium- to fine-grained sand (Orfeo and Stevaux, 2002). Small lakes and wetlands commonly fill the scroll bar topography in the floodplain (Paira and Drago, 2007). The axial Paraná River flows across several structural blocks that control the position of the river, causing the axial channel belt to widen from ~5-10 km width near the Paraná-Paraguay confluence to over 100 km width in the province of Santa Fe (Iriondo, 1993, 2007).

3.1.3. The Tananaforeland basin, Alaska

The Tanana foreland basin displays similar features to the Himalayan and Andean foreland basins, although developed under a significantly colder climatic regime. This indicates that the configuration of DFS and tributary rivers is similar in foreland basins, no matter the climatic setting.Five large DFS enter the Alaska Range foreland basin from the south, with the tributary axial Tanana River held between the distal end of these coalesced DFS and the northern edge of the sedimentary basin (Fig.6). Smaller DFS are present between these large DFS, with rivers and streams from these smaller interfan DFS coalescing between the large DFS in interfan tributary rivers. As observed in the Himalayan foreland basin, several of the interfan tributary rivers form DFS near the toes of the adjacent large DFS where accommodation exists.Similar to the other foreland basins, the transverse DFS systems comprise most of the depositional area covered by the sedimentary basin (5670 km^2, or 93.9%), while the interfan tributary and axial river deposits cover a significantly smaller area of the basin (365 km^2, or 6.1%) (Table 1).Longitudinal stream profiles on several of the DFS show active deformation from transpression in this sedimentary basin (e.g., Lesh and Ridgeway, 2007), indicating contemporaneous deformation with fluvial deposition.

3.2.Rift basins

We delineated geomorphic elements in portions of two modern rift basins:the Okavango Basin located in Botswana and Namibia, and the Rio Grande Rift Basin located in New Mexico, USA (Figs.14 and 15). We selected these basins because significant previous work has been conducted on fluvial deposits in them. As observed in the foreland basins, coalesced DFS comprise most of the deposits that cover the sedimentary basin (Table 1).

3.2.1. Okavango rift basin

In the case of the Okavango Rift Basin, large DFS are formed by the Eiseb and Epukiro (10,010 km^2), Okavango (35,452 km^2), Kwando (8000 km^2), and Zambezi (3167 km^2)rivers as these rivers enter the rift from the west and northwest (Fig.14). When these rivers reach the basin edge to the southeast, they form tributary rivers (the Linyati and Chobe rivers) that either ultimately join the Zambezi River and leave the sedimentary basin to the northeast, flow toward lacustrine regions near the Okavango DFS (e.g.,the Savuti Marsh located northeast of the Okavango DFS or Lake Ngami located southeast of the Okavango DFS), or leave the basin through the Boteti River near the Okavango DFS. In the northern portion of this basin, some smaller DFS are present in the inter-large DFS area.The DFS cover ~94% of the sedimentary basin, with <1% of the basin covered by the small axial tributary rivers and about 5% of the basin covered by lacustrine deposits (DFS comprise 99% of the fluvial depositional area in this basin; Table 1).

Of these large DFS, the Okavango DFS has been widely studied (e.g., McCarthy et al., 1988,1991, 1992, 1993, 2002; Stanistreet and McCarthy, 1993; Stanistreet et al., 1993; Shaw and Nash, 1998; Gumbricht et al., 2001, 2004; Ellery et al., 2003; Tooth and McCarthy, 2004; McCarthy, 2006; Ramberg et al., 2006;Wolski and Murray-Hudson, 2006; Wolski and Savenije, 2006;Milzow et al., 2009; Reiser et al., 2014), while other DFS in the basin have not been as extensively studied (e.g., Moore et al., 2007).

The Okavango DFS is perennially flooded in its proximal reaches, with seasonal flooding in the more distal regions (Wolski and Murray-Hudson, 2006; Milzow et al., 2009). These floods take 3-4 months to traverse the DFS (Milzow et al., 2009). Distributary channels avulse frequently, distributing sediment across the DFS (McCarthy et al., 1988, 1992) and depositing ribbon sand bodies that are surrounded by finer-grained deposits (Stanistreet et al., 1993). Becausethe catchment for the Okavango DFS is dominated by eolian deposits, the Okavango River carries a bedload of fine- to medium-grained sand with very little suspended load (McCarthy et al. 1991); therefore, the fine-grained floodplain sediments are not deposited from suspended load but instead consist of sediment-laden peat deposits (Stanistreet et al., 1993; McCarthy and Cadle, 1995). Many of the sedimentary subenvironments are reflected by vegetation subcommunities on this DFS (Ellery et al., 2003).

Groundwater and evapotranspiration play important roles in the water budget of the Okavango DFS (McCarthy, 2006; Ramberg et al., 2006; Milzow et al., 2009). Up to 90% of the floodwater entering the fan is infiltrated into the groundwater system, with most of the recharge occurring during seasonal floods (McCarthy, 2006; Ramberg et al., 2006). Ultimately, most of this groundwater is transpired by wetland vegetation on the DFS, causing accumulations of salts and production of dense brine that sinks into the basin aquifer (McCarthy, 2006). Lateral flow from flood channels toward vegetated islands is important locally, with salt deposition occurring beneath these islands (e.g., McCarthy, 2006; Wolski and Savenije, 2006; Milzow et al., 2009). Additionally, under the present climate, very little sediment reaches the distal portion of the DFS; therefore sedimentation in the distal reaches of the DFS is currently dominated by chemical deposition of calcretes and silcretes as a result of evapotranspiration of groundwater (McCarthy and Ellery, 1995).

Farther east in the basin, the Kwando and Zambezi rivers form large DFS. The Kwando DFS is blocked at its downstream end by the Linyanti Fault (a large normal fault), thus forcing flow eastward to the Zambezi River (Gumbricht et al., 2001). This river forms a relatively broad wetland with channels that appear to be similar to those on the Okavango DFS. The Zambezi River also forms a broad wetland, with a wide (~5-10 km) channel belt composed of amalgamated point bar deposits. Multiple distributary channels are apparent on the Zambezi DFS.

3.2.2. Rio Grande rift basin

The Rio Grande Rift consists of a series of interconnected half-graben basins that contain a relatively thick (>1000m) succession of Pliocene-Pleistocene fluvial deposits interpreted as alluvial fan (small DFS) and axial fluvial deposits (e.g., Mack and Seager, 1990; Hawley and Haase, 1992; Hawley et al., 1995; Connell et al., 2013). Subsidence rates in the southern Rio Grande Rift have been estimated to average~0.03mm/yr (Leeder et al., 1996).

Satellite imagery shows that DFS (in the form of alluvial fans) cover most of the surface area in the sedimentary basin (89.4% of the area), with deposits from the axial Rio Grande covering the remaining 10.6% of the area (Fig,15; Table 1). Subsurface data, however, indicate that in the past the axial Rio Grande system covered a much larger area of the sedimentary basin (Hawley and Haase, 1992; Connell et al., 2013). Two types of DFS, or alluvial fans, have been identified in the Rio Grande Rift – lateral and axial DFS (Frostick and Reid, 1987; Leeder and Gawthorpe, 1987; Mack et al.,1997, 2003, 2006, 2008; Leeder and Mack, 2001; Connell et al., 2013). Lateral DFS are derived from the hanging-wall and from footwall sides of the half graben, with hanging-wall systems typically being much larger than their footwall counterparts (e.g., Frostick and Reid, 1987; Leeder and Gawthorpe, 1987; Mack et al., 2003). Axial DFS occur where a half-graben is filled and the axial system spills into an adjacent (downstream) half-graben if accommodation exists between the lateral DFS (Mack et al., 1997, 2006). This *fill and spill* type scenario is considered to have occurred a number of times, resulting in linkage of half-grabens to form a throughgoing axial river system thatfeeds an axial DFS in the terminal half-graben (Mack et al., 1997). Depending on the difference in baselevel when the axial river spills into an adjacent basin, the river may either incise through older lateral DFS deposits if baselevel is significantly loweror, if it is close to grade, the axial system will rework the toe of the footwall-derived lateral DFS as the axial system migrates toward the area of greatest subsidence adjacent to the footwall (e.g. Leeder and Mack, 2001).

During the past 0.8 Ma, the Rio Grande has responded to Quaternary climate and related sediment supply and discharge changes by incising into the older deposits (Connell et al., 2013), therefore most of the lateral DFS are presently incised. While channels are currently incised completely through most of the DFS, radial patterns of paleochannels are clearly observed (Fig.15A). These incised valleys are relatively narrow, ranging in width between 0.5 and 2.5 km. The axial Rio Grande is currently held in a valley that ranges in width between 0.4 and 3 km.

3.3. Other sedimentary basins

In addition to the foreland and rift basins, we also measured the areal extent of geomorphic elements in several other sedimentary basins in different tectonic settings, including the Pantanal Basin of Brazil, Death Valley in the USA, the Tarim Basin of western China, a transtensional basin in Mongolia (Basin N4330E10270 from Weissmann et al., 2010), and the northern portion of the San Joaquin Basin of California (Table 1). Our goal in doing this work was to quantify the aerial extent that DFS cover relative to other fluvial deposits in different types of sedimentary basins rather than describe the fluvial features in detail. In all of these basins, except the Tarim Basin where eolian deposits dominate the basin surface, DFS cover more than 89% of the basins and comprise most of the area of fluvial deposition. Though the Tarim Basin is primarily covered by a large eolian sand sea, traces of radiating paleochannels from the Hotan River and adjacent rivers are apparent under the dunes in imagery, suggesting this may be a covered large DFS (Fig.16).

The fluvial geomorphology and sedimentology has been described in many of these sedimentary basins, including in the Pantanal Basin (e.g., deSouza et al., 2002; Assine, 2005; Assine and Silva, 2009; Buehler et al., 2011; Assine et al., 2014), Death Valley (e.g., Denny, 1965; Blair and McPherson, 1994; Fordham et al., 2010), and the San Joaquin Basin (e.g., Janda, 1966; Marchand, 1977; Huntington, 1980; Marchand and Allwardt, 1981; Lettis, 1988; Bartow, 1991; Weissmann et al., 2002, 2005).

3.4. Summary

In all the sedimentary basins where we delineated geomorphic elements, DFS deposits from transverse streams form a significant percentage of the area covered by fluvial deposits (88-99%; Table 1). Wilkinson et al. (2010) made a similar finding for foreland basins along the east side of the Andes. Hartley et al. (2010b) and Davidson et al. (2013) described the planview characteristics of large DFS that are present in many of these sedimentary basins.Though we did not measure geomorphic elements in all 724 sedimentary basins identified by Weissmann et al. (2010), visual inspection of the global sedimentary basin database imagery indicates these observations are consistent in most modern sedimentary basins. Additionally, tributary rivers are specifically found in an axial position or in inter-megafan positions in these basins. This may lead toward a basin-scale predictive model of different fluvial depositional types. Therefore, in order to understand these fluvial rocks, we must evaluate the geomorphic form and processes on the DFS, in the interfan regions, and along the tributary axial systems.

Assuming uniformitarianism, geomorphic elements observed in these basins are representative ofelements that would be found in ancient sedimentary basins. Thus, we expect that DFS form a significant percentage of fluvial sedimentary rocks observed globally. This inference has been debated by several other workers (e.g., Sambrook Smith et al., 2010; Fielding et al., 2012; Latrubesse, 2015). We will discuss this debate in section 5.4 of this paper.

4. Processes on geomorphic elements

4.1. Distributive fluvial systems

The DFS primarily occur where a stream leaves the confines of a highland valley into a sedimentary basin and distributes its sediment load across the basin to fill the accommodation available. Nodal avulsions occur at the apices of these DFS as the stream leaves the highland valley that we term *valley-exit* avulsions.The DFS may also occur in the axial position of a basin if accommodation exists and the river is not confined by transverse fans (e.g., the Amargosa River in Death Valley (Fig. 17), the Rio Grande, Mack et al., 1997, and the San Joaquin River, Weissmann et al., 2005).Sweeping of the channel system across the DFS distributes sediment onto a generally fan-shaped landform. As noted for alluvial fans, fluvial fans, and megafans, the DFS landforms typically are convex upward in cross fan profile and concave upward in longitudinal profile (e.g., Hooke, 1967; Gumbricht et al., 2001;Blair and McPherson, 2009; Charkraborty et al., 2010). The size, gradient, and alluvial or fluvial processes of a DFS are dependent on the drainage basin characteristics (e.g., size, geology, gradients), climate, and the size and geometry of the receiving sedimentary basin (Gordon and Heller, 1993; Stanistreet and McCarthy, 1993; Whipple and Trayler, 1996; Dade and Verdayen, 2007).

Stanistreet and McCarthy (1993) described a spectrum of scales and processes on fans (or DFS) ranging between debris-flow-dominated fans (commonly called alluvial fans), braided fluvial fans, and low sinuosity/meandering river (losimean) fans. The debris–flow-dominated fans have higher gradient and typically are smaller than the other fan systems. Blair and McPherson (1994) suggested that a natural slope break existed between these fan types; however,Hashimoto et al. (2008) clearly showed no such break exists. Instead, a continuum of forms exists for DFS, with the potential for a mix of processes to be present on any given fan. Fluvial planform and processes on different styles of DFS have been reviewed, including reviews of alluvial fans (Harvey, 1984, 1997, 2005, 2011; Lecce, 1990; Rachocki and Church, 1990; Blair and McPherson, 2009) and megafans or large DFS (e.g., Leier et al., 2005; Nichols and Fisher, 2007; Hartley et al., 2010b; Davidson et al., 2013); therefore we will not go into detail on alluvial or fluvial planform in this paper and instead focus on major processes that influence DFS development and filling of sedimentary basin accommodation.

Two processes appear to be important for the development of DFS landforms: (i) avulsions and associated flooding, and (ii) loss of stream discharge downstream caused by infiltration, evaporation, and bifurcation (though not all rivers on DFS lose discharge downfan). We describe these processes in this section.

4.1.1. Avulsions and flooding

As the river system migrates back and forth across the DFS through a series of avulsions, it typically builds depositional lobes on different parts of the DFS (McCarthy et al., 1988, 1992; Assine, 2005; Mack et al., 2008; Chakraborty and Ghosh, 2010;Zani et al., 2012). Avulsion frequency has been shown to be generally related to aggradation rate (Bryant et al., 1995) and, as observed on the Okavango DFS, the rate of aggradation typically increases downfan (McCarthy et al., 1992). Thus, avulsions tend to occur more frequently downfan during aggradational periods, often building small progradational lobes with each avulsion (e.g., Assine, 2005; Assine and Silva, 2009; Buehler et al., 2011; Assine et al., 2014). Less frequent nodal avulsions near the apex or intersection point switch deposition from one large-scale lobe to another (e.g., Chakraborty et al.,2010).

Flooding over the super-elevated alluvial ridge becomes more frequent before a river system avulses to a new position on the DFS (Buehler et al., 2011). The avulsive patterns observed on DFS are similar as those described for axial-trunk systems (e.g., the Cumberland Marshes described by Smith et al., 1989, 1998;Pérez-Arlucea and Smith, 1999); however,in contrast to flooding along tributary rivers held in valleys in degradational terrain or along the axial portions of a sedimentary basin, once flood waters leave the confines of the channel they typically never return to the main channel but instead spread across the DFS surface (Fig.18). Levees along the active channel prevent flow from returning to the main stem channel, except potentially at the distal end of the DFS where the channels are not highly superelevated (e.g., Bernal et al., 2013). Thus, depth of flood waters in a channel along a DFS is controlled only by the height of the natural levees, and flows cannot get deeper than this height. This contrasts with rivers in valleys where flow depths can continue to increase as floodwaters fill their valleys.

The causes of avulsions have been hypothesized as primarily being related to superelevation of the channel belt over the adjacent floodplain, producing a gradient advantage for avulsion (e.g., Slingerland and Smith, 1998, 2004; Jones and Schumm, 1999; Mohrig et al., 2000; Makaske, 2001; Makaske et al., 2002, 2007; Törnqvist and Bridge, 2002; Ashworth et al., 2004; Jerolmack and Paola, 2007). Field (2001) noted that low bank height along a superelevated reach may create optimal conditions for avulsions on alluvial fans, especially along channel bends. Similar conditions for an avulsion were found along the Kosi River during a recent near avulsion of that system (Sinha, 2009). However, channel-capacity limitations (e.g., Schumm et al., 1996; Jones and Schumm, 1999; Makaske, 2001), substrate conditions (e.g., Aslan et al., 2005; Makaske et al., 2012), or channel blockage by vegetation or ice dams (e.g., King and Martini, 1984; Schumann, 1989; McCarthy et al., 1992; Harwood and Brown, 1993; Ethridge et al., 1999; Gibling et al., 2010) can also lead to forced shifts.

The sedimentology of avulsion deposits has been studied on several rivers; however,documented examples of avulsions are relatively rare so only a handful of studies exist as analogs for the rock record. Detailed work has been conducted on the Saskatchewan River (e.g., Smith et al., 1989, 1998; Perez-Arlucea and Smith, 1999; Slingerland and Smith, 2004), the Mississippi River (e.g., Aslan and Blum, 1999; Aslan et al., 2005), and the Rhine-Meuse delta (e.g., Stouthamer, 2001; Makaske et al., 2007). Other studies have used satellite imagery to evaluate the evolution of avulsions at a large scale, with most of these studies focused on avulsions on DFS (e.g., Sinha, 1996, 2009; Assine, 2005; Sinha et al., 2005; Buehler et al., 2011; Zani et al., 2012; Assine et al., 2014). Several workers have suggested that avulsion deposits constitute a large portion of the fluvial stratigraphic record (e.g., Kraus, 1996; Kraus and Wells, 1999; Davies-Vollum and Kraus, 2001; Kraus and Davis-Vollum, 2004; Jones and Hajek, 2007; Makaske et al., 2007; Gibling et al., 2010), thus additional mapping and evaluation of the sedimentology of modern avulsions is needed in order to understand facies distributions and geometries that may be found in the sedimentary record.

Three forms of avulsion were described by Slingerland and Smith (2004): avulsion by annexation, avulsion by incision, and avulsion by progradation. In avulsions by annexation, preexisting channels on the floodplain surface capture the flow of the main channel belt. Avulsions commonly reoccupy abandoned channels on the floodplain surface because these tend to be relatively low elevation locations (Jerolmack and Paola, 2007). An example of such an avulsion almost occurred on the Kosi River DFS, where the river broke through an embankment in Nepal and was captured by several large paleochannels on the DFS before it was impounded by human intervention (e.g., Sinha, 2009; Chakraborty et al., 2010). Avulsion by incision occurs where the flows leave the confines of the parent channel, eroding into the floodplain. Such avulsions may be most common in areas of very low or no aggradation and on floodplains that drain quickly (Slingerland and Smith, 2004). Avulsions through progradation are formed as a prograding splay lobe moves down the DFS. As flow leaves the confines of the parent channel through a crevasse splay, it loses competence and sediment-carrying capacity; thus sediment is deposited in a splay lobe. As sediment fills the low elevation areas on the floodplain, the splay progrades basinward. Buehler et al. (2011) produced a time-series of satellite images on the Taquari DFS showing this type of avulsion.

In the rock record, two end member realizations of avulsion types have been suggested, termed incisional avulsion or aggradational avulsion by Mohrig et al. (2000) or stratigraphically abrupt or stratigraphically transitional avulsions (Jones and Hajek, 2007). These probably correspond to avulsions by annexation or incision and avulsions by progradation, respectively. We believe the avulsion by annexation on the Kosi River (e.g., Chakraborty et al., 2010) represents an avulsion that would create a stratigraphically abrupt avulsion deposit, where the progradational avulsions on the Taquari River DFS and the São Lourenço DFS (e.g., Assine, 2005; Buehler et al., 2011; Makaske et al., 2012; Assine et al., 2014) represent the stratigraphically transitional avulsion type.

4.1.2. Loss of stream discharge due to infiltration, bifurcation, and evaporation

Rivers on many DFS appear to significantly decrease in size downfan because of infiltration, bifurcation, and evaporation (e.g., Hartley et al., 2010b; Weissmann et al., 2010, 2011, 2013; Davidson et al., 2013). The relative proportion of flow loss caused by each of these is unknown and, to our knowledge, has not been measured; however, infiltration loss on the Okavango DFS, as noted earlier, is significant (McCarthy, 2006). Of these factors, evaporation is especially difficult to quantify. We expect significant variability on the importance of these factors on stream discharge for different DFS, even between DFS located in the same sedimentary basin.

Infiltration of flows near the apex of alluvial fans has long been known to be an important factor for groundwater recharge in many sedimentary basins (e.g., Bull, 1977; Hendrickx et al., 1991; Munévar and Mariño, 1999; Houston, 2002; Weissmann et al., 2004; Fleckenstein et al., 2006; McCarthy, 2006; Ramberg et al., 2006; Li et al., 2007; Blainey and Pelletier, 2008; Milzow et al., 2009). Weissmann et al. (2011) described significant channel size decrease downstream on the Pilcomayo DFS, where the channel belt decreases in average width from1600 m within 20 km of the apex down to an average width of 245 m ~130 km from the apex. Ultimately, the channel belt terminates in splays, thus the channel does not directly reach the axial Paraguay River. Weissmann et al. (2011) suggested that the highpermeability sediments present near the apex of the DFS caused by amalgamation of channel belt deposits is optimal for infiltration. As noted previously, a similar pattern of decreasing width down-DFS is observed on the Bermejo River DFS (Fig.12).

This recharged groundwater commonly exits the DFS near the distal toes along a springline (Weissmann et al., 2011, 2013; Hartley et al., 2013). Below this point, many paleochannels become spring fed across the DFS surface (Gohain and Parkash, 1990; Fig.19). Commonly, agriculture and small communities depend on springs near the distal portion of a DFS. The amount of recharge may vary across the sedimentary basin, but such mountain-front streams may provide significant aquifer recharge in sedimentary basins (e.g., Munévar and Mariño, 1999; Fleckenstein et al. 2006).

Because of this water table configuration where the water table tends to be shallow near the distal portion of the DFS and deeper near the apex, soils on DFS tend to show a predictable trend of drainage characteristics downfan (e.g., Hartley et al., 2013; Weissmann et al., 2013). Near the apex, soils tend to be welldrained. This is reflected by vegetation or crop patterns. In the Chaco Plain, vegetation in well-drained portions of the DFS tend to be dominated by dryland species; while below the springline, vegetation is dominated by wetland species and species that require significant water supply (Zak and Cabido, 2002;Iriondo, 2007; Hartley et al., 2013). On the Tista DFS in India, tea (which requires well-drained soils) is grown on the upper portion of the DFS (Hartley et al., 2013; Weissmann et al., 2013). In the medial portions of the Tista DFS, rice is grown during the monsoon season when water table rises, but pineapple and other crops that require better drainage are grown as the water table falls during the dry season. At the distal end of the DFS, rice is typically grown all year asconditions remain saturated during much of the year. This proximal to distal dry to wet configuration appears to be a common feature of DFS around the world, irrespective of climatic setting (e.g., Gohain and Parkash, 1990; Fontana et al., 2014).

Bifurcation may also cause significant downfan decreases in channel size (e.g., McCarthy et al., 1988,1991). Causes of bifurcations and formation of distributary channels have been well documented on deltas and have been correlated to sea level rise (e.g., Jerolmack,2009). However, becausemostcontinental DFS are not influenced by sea level change, this must not be a control on most DFS. Further evaluation of bifurcation processes on DFS is needed. Some controls may include the presence of shallow water table distally on the DFS, slight gradient advantages for some channels, reacquisition of older, abandoned channels on the floodplain where this did not lead to full avulsion, and channel blocking and anastomosis by vegetation or high sediment load.

4.1.3. Incised DFS

Rivers on DFSin many of the investigated sedimentary basins are incised into their fans under current climatic and tectonic conditions; however, most of these DFS experienced aggradational episodes during the Quaternary and Pleistocene (e.g., Lettis,1988; Weissmann et al., 2002, 2005; Assine, 2005; Tandon et al., 2006;Iriondo, 2007; Fontana et al., 2008, 2014; Zani et al., 2012; Assine et al., 2014). Incision into modern DFS has caused some confusion in the literature about whether several modern rivers contributed to basin sediment fill, where workers have evaluated current flood maps and noted that several rivers in DFS are not currently distributive (e.g., Fielding et al., 2012). Yet, evaluation of deposits surrounding these incised valleys shows the presence of a pattern of paleochannels radiating away from an apex near the sedimentary basin edge (e.g., Shukla et al., 2001; Weissmann et al., 2002, 2005, 2011; Fontana et al., 2008; Zani et al., 2012; Fig.2D). In the following section, we describe several cases where climate change or tectonics has caused the river system to incise into its DFS.

Harvey (1996) noted two distinct classes of incision: incision that is initiated near the fan apex and incision that is initiated at the distal end of a fan. He also noted that a fan can take many different morphological forms given these different modes of dissection. Incision at the apex, or fan-head trenching, is common on DFS and described for many alluvial fans (e.g., Hooke, 1967; Bull, 1977, 1991;Schumm, 1977; Harvey, 1987, 1996, 2005;Schumm et al., 1987; Blair and McPherson, 1998). The intersection point marks the location where the stream intersects the DFS surface, below which aggradation occurs on the DFS (e.g. Hooke, 1967). Here, we call these *top down* incisions. Base-level change at the toe of the DFS - caused by river, lake, or sea level change or by tectonic uplift - may also cause incision from the distal end of the DFS upward, where incision typically follows the active channels and the paleochannels on the DFS. In this paper, we call these *bottom up* incisions. The geomorphic literature holds many studies that evaluate controls on fluvial incision and dissection (e.g., Stokes and

Cunha, 2012), and we will not attempt to review this vast literature here. Instead, we focus on the morphologic results of incision on DFS.

*Top-down incised DFS:*Changing sediment supply and stream discharge from Quaternary climate change caused cycles of aggradation and degradation on many DFS, resulting in top-down incisions. Many modernriver systems on DFS experienced incision and aggradation caused by stream power changes resulting from glacial cyclicity (e.g., Lettis, 1988; Harvey, 1996; Weissmann et al., 2002, 2005; Fontana et al., 2008; 2014), but monsoonal strength variability has also been identified as controlling aggradational cycles (e.g., Gibling et al., 2005; Tandon et al., 2006). The depth of incision into the DFS sediments ranges from a few meters on systems that were not linked to drainage basins influenced by Quaternary glaciation (e.g., Assine,2005; Assine and Silva, 2009; Assine et al., 2014) to tens of meters on systems with rivers directly linked to glaciated drainage basins (e.g., Weissmann et al., 2002, 2005; Gibling et al., 2005; Tandon et al., 2006;Fontana et al., 2008, 2014); however, the incision in either case is deep enough such that the DFS surface no longer receives flows even during the largest floods. In these cases, the DFS surface is 'detached'(Gibling et al., 2005)from the forming river under the present climate regime. During periods of incision, the DFS surface is exposed to weathering, allowing the possible formation of laterally extensive soils (e.g., Weissmann et al., 2002); however, gullying in response to incision may also be present across this exposure surface (e.g., Gibling et al., 2005, 2011). Maps of recent flooding (e.g., Dartmouth Flood Observatory maps, http://floodobservatory.colorado.edu/Archives/index.html) show that flooding occurs only in the confines of the incised valley.

Rivers held in the incised valleys may display a different morphology than those on the open fan. For example, the upper 100km of the Taquari River below the DFS apex is held in an incised valley (Figs.2D and 20). Above this intersection point, the meandering form is dominated by chute and neck cutoff avulsions, similar to that described for rivers held in degradational terrain (e.g., Jackson,1978; Levey, 1978; Nanson, 1980; Miall, 1996, 2010). The river channel sweeps back and forth across the valley and the deposits consist of amalgamated and overprinted point bar deposits (Fig.20A). Below the intersection point, the river channel shows little evidence of chute and neck cutoff avulsions, but instead shifts position on the floodplain through nodal avulsions (Fig.20B). The single channel migrated laterally but did not build an amalgamated channel belt before the current avulsion. This single channel is surrounded by levees and is superelevated above the surrounding floodplain. The contrasting styles above and below the intersection point will lead to very different channelbelt deposit form.

Bottom-up incisions: Base level fall, in response to axial river, lake, or sea level change or in response to tectonicallygenerated uplift, may cause *bottom-up* incision into DFS, where head-cut erosion typically follows paleochannel pathways as incision works upward onto the DFS. Harvey (1996) also demonstrated that distal incision may occur under conditions of stream power change if the fan surface experiences early cementation. Base-level fall results in two different geomorphic responses on DFS. The first is a generation of a tributary drainage network migrating upstream from the toe of the DFS.The second is downcutting of existing channel networks (e.g., paleochannels) into the underlying DFS, resulting in a radiating drainage network cut into the underlying DFS. In cases where top-down incision cuts through the entire DFS, the drop in baselevel associated with this new position of the main channel can induce bottom-up incision.

The Beni River DFS is currently undergoing uplift at its toe along with base-level drop in the Amazon Basin (Fig. 21). The upper portion of the DFS shows at least two abandoned meanderbelts and the active meanderbelt radiating outward from an apex located at the mountain front (Fig.21). At the distal end of the DFS, a dendritic tributary drainage pattern is observed where incision from uplift of the

Fitzcarrald Arch extending beneath the DFS is taking place(Fig. 21; Dumont 1996; Regard et al. 2009). Accordingly, theactive channel and radial paleochannels have been incised and sit inside small valleys; thus rivers are confined to these valleys through this portion of the uplifted DFS.

Coincident with the onset of northern hemisphere glacial cyclicity at about 780,000 ka, stream power of the Rio Grande River increased and the river incised in the axial portion of its rift basin (Connell et al., 2013). With this base-level drop, the transverse DFS have been incising from the toe upward (Fig.15). Headcut erosion into the DFS typically follows paleochannels, thus forming a radiating pattern of gullies and arroyos that progress toward the DFS apex. Ultimately, the main channels incised completely through the DFS, leaving the DFS surface exposed to weathering and erosion.

4.2. Tributary fluvial systems

Tributary systems are present in two primary locations in sedimentary basins: in the inter-DFS convergence areas and as axial stream systems that parallel the strike of the sedimentary basin.

4.2.1. Inter-DFS tributary systems

Little work has been done on inter-DFS convergence areas and river dynamics and sedimentation in these sites. In foreland basins, DeCelles and Cavazza (1999) called this region the 'inter-megafan'area; however, areas of convergence also occur between adjacent larger fans in basins where the DFS may not be classified as megafans (e.g., Death Valley). Imagery indicates that the tributary area is relatively diffuse, with a gradational change between the distributive systems on smaller DFS to a tributary system of converging channels as the rivers are directed between two adjacent larger DFS (Figs. 2F and8). Converging channels are observed in a roughlytriangular wedgelocated above the point where the larger DFS meet. Tributary channels are located along the uphill boundaries of the larger DFS (herein we call these *boundary* rivers), with the channel belt increasing in size downstream as more streams merge into the boundary river. In the inter-megafan area between the Kosi and Tista large DFS in India, this zone of convergence is located 10-20 km north of these boundary rivers (Fig.8). This convergence zone consists of a complex mix of tributary, converging streams, and distributive streams, with all streams ultimately being tributary into the boundary rivers.

Where large DFS meet, the boundary rivers converge and form a potentially large inter-megafan river. For example, the Mahananda River, which lies between the Kosi and Tista large DFS, consists of a sandy channel belt that ranges between 1 and 2 km wide (Fig.8). Channel size in this location will be controlled by the number of tributary systems entering the sedimentary basin in this inter-megafan area and the climate.

4.2.2. Axial tributary systems

Some of the largest rivers in the world are present in the axial position of sedimentary basins (e.g., the Yukon, Paraná, Paraguay, Ganges, and Brahmaputra rivers), though we note that many large rivers do not cross actively subsiding continental basins (e.g., the Lena, Amur, Yesiney, Volga, and Danube rivers). Large rivers in sedimentary basins are confined between opposing DFS or between a DFS and the basin edge. In this constrained position, the river channels tend to migrate across this confining area, leaving a deposit consisting of amalgamated channel belts, point bars, and braid bars, depending on geomorphic form of the channel belt (e.g., Goswami, 1985; Sarma, 2005; Iriondo et al., 2007).These channel belts tend to be coarse-grained dominated and may produce substantial sheet sandstones that range from 10 to 30 km in width.

Rivers in the axial position tend to take on similar form to those in degradational terrains because they are confined. Chute and neck cutoff avulsions, leading to an amalgamated form, dominate meanderbelts in this position. Floodplains adjacent to the main channel commonly display scroll bar topography, with small lakes and wetlandscoveringmany of the low areas in the floodplain (e.g., Iriondo, 2007; Paira and Drago, 2007). Preservation potential of lacustrine units in these deposits needs further evaluation becauseas the river sweeps back and forth across its confined valley it may rework many of these deposits, potentially leaving behind the sand associated with underlying point bar deposits. Conversely, these mud-dominated units are mostlikely cohesive and may prevent lateral migration, thus increasing preservation potential; however, many of the axial systems are so large that they will rework these deposits.

5. Discussion

As noted in all the sedimentary basins evaluated for this work, DFS cover a significantly larger area of the sedimentary basin than tributary rivers. Typically over 90% of the fluvial depositional area is covered by DFS deposits. In this section, we describe some implications of this finding for evaluating the geomorphology of fluvial systems in sedimentary basins and for understanding facies observed in the sedimentary rock record.

5.1. Differences between DFS and tributary rivers in sedimentary basins

In most cases, the degree of confinement of rivers on DFS is much less than that of rivers in a tributary position in a sedimentary basin. Rivers on DFS are able to shift across a relatively wide area of the DFS while tributary rivers in axial positions are commonly confined between opposing DFS or a DFS and the basin edge and inter-megafan tributary rivers are confined between adjacent DFS. This difference in confinement causes differences in character between rivers on DFS and those in tributary positions.

Meandering rivers in confined positions in the sedimentary basins (e.g., tributary rivers and rivers in incised valleys) appear to be similar to those in degradational terrain, where chute and neck cutoff avulsions create an amalgamation of point bar deposits and display an overprinted mix of scroll bar topography (e.g., Iriondo, 2007; Paira and Drago, 2007). In contrast, meandering rivers on DFS commonlyhave less amalgamation and form alluvial ridges without evidence of overprinted scroll bars, probably avulsing before these rivers have time to create an amalgamated form. For example, the Taquari River displays no amalgamation of point bar deposits along its channel belt in the aggradational portion of the DFS, while in the confined, incised valley portion of the DFS the river displays the overprinted mix of scroll bars (Fig.20). Similarly, the Burhi Dihing DFS shows multiple individual paleochannels across the DFS with little evidence of neck and chute cutoff avulsions (Fig.10), thus these coalesce on the fan surface as individual channels that may overprint other individual channels; however, these are not amalgamated in the same manner as observed in tributary rivers in the axial position or other rivers held in confined valleys (e.g., incised valleys). An exception to this meanderbelt form is observed on the Beni River DFS, where the channel belts remained in a location for long enough to produce an amalgamated channel belt form (Fig.21C). These different forms of meander belts will produce very different sand body geometries in the rock record, where lack of amalgamation will result in discrete ribbon sandstone geometries (e.g., Owen et al., 2015b) and an amalgamated meander belt will produce a complex sheet sandstone with multiple pointbar accretion directions (e.g., Hartley et al.,2015). Thus, channel belt sandstone geometries offer clues as to the position or process in the sedimentary basin.

Braided rivers on DFS also display different character than their counterparts in the axial position. On many braided DFS, the river system bifurcates downfan, producing a broad active depositional area with significant vegetated floodplains between individual braided channel belts. Distally on braided DFS, the individual channel belts may be separated by significant floodplain deposits, thus allowing for preservation of floodplain fines adjacent to braided channel belt materials. In contrast, braided rivers held in the confined axial position are more similar to those in degradational terrains, commonly filling the entire axial valley between opposing DFS or the DFS and the basin edge. Very little floodplain material is preserved in this setting because the channel belts are constantly shifting across the entire width of their valley, reworking and removing any floodplain sediments that do get deposited. Ultimately, with removal of these floodplain deposits, a relatively coarse-grained, broad channel belt deposit is left.

5.2. River network and other modeling on DFS

River network mapping on DFS cannot be accomplished using common river network tools available in GIS software. In our attempts to delineate the river networks on DFS, we found that the algorithms currently available are unsuccessful in defining the diverging river networks present on DFS. Most of the models used to delineate channels and map river networks (e.g., D8, with single flow direction toward one of the eight (cardinal and diagonal) neighboring grid cells, and D∞, where an infinite number of flow directions are possible; Tarboton, 1997)are based on flow over a terrain surface represented by a grid digital elevation model (O'Callaghan and Mark, 1984). The underlying assumption of constantly accumulating flow down gradient (e.g., flow accumulation, ESRI, 2015) does not work on DFS, where topography leads to a distributive pattern of channels rather than the tributary accumulating network assumed by these models. As noted by Pelletier (2008), depth modeling of flooding on fans is challenging, with active channels spreading out from an apex. New algorithms are needed to predict river networks on DFS that allow for distributive drainage patterns, especially in low-gradient regions typical of many large DFS.

Additionally, other numerical models for prediction of channel depth based on drainage basin characteristics or area (e.g., Leopold et al., 1964; Reinfelds and Bishop, 1998; Davidson and North, 2009) will not work on DFS. Because rivers on DFS experience significant discharge loss from infiltration, bifurcation, and evaporation, the drainage basin contribution is potentially reduced down-DFS, thus channel size may decrease rather than increase with distance down-DFS. Most models do not capture this change. Thus, new models must be developed that account for decreasing flows on distributive systems in order to make predictions on upstream properties based on sandstone geometries in the rock record. Pelletier (2008) suggested that diffusion equations may be used for modeling large-scale DFS development, but other governing equations are needed for characterizing smaller scale DFS development and channel evolution.

Several models are available for predicting bifurcation and avulsion on deltas; however, these commonly call upon backwater effects (e.g., the influence on sedimentation caused by the retardation of flow as the river meets standing water in deltaic settings) as the cause of bifurcation (e.g., Jerolmack and Swenson, 2007). Because of the typically high gradients of DFS (Hartley et al., 2010b), backwater typically has minimal to no impact on DFS;different models for bifurcation and avulsion on DFS must be developed. As noted previously, superelevation of the active channel belt, though important, may not be the only cause for bifurcation or avulsion. The relative importance of superelevation, vegetation, channel substrate conditions, and channel-capacity limitations must be considered in these models.

Clearly, changes in sediment supply and discharge, commonly caused by climate change, control aggradational and degradational cyclicity on DFS (e.g., Weissmann et al., 2002, 2005; Gibling et al., 2005; Fontana et al., 2008, 2014; Pelletier, 2008), yet a clear understanding of feedbacks and timing of these cycles is not availablebecause we lack good age control on these sediments. The process of valley filling upon the start of aggradation is not well understood nor is the process of incision. Quantitative models that capture controls on aggradation and degradation are needed in order to evaluate conditions necessary for large-scale aggradation and filling of incised valleys. In many cases, this valley filling is quite substantial, with valleys connected to glaciated terrain being anywhere from 10 to 20m deep (e.g., Weissmann et al., 2002, 2005; Gibling et al., 2005; Fontana et al., 2008).

5.3. DFS in the Quaternary as analogs for the past

The substantial Quaternary climate changes significantly affected river systems in these sedimentary basins (e.g., Weissmann et al., 2002; Gibling et al., 2005, 2011; Fontana et al., 2014), and similar high-amplitude climate variability has not occurred during most other periods in Earth's history. Many of the modern drainage basins that feed rivers in the sedimentary basins appear to have experienced glaciation in some portion of the drainage basin, thus causing significant increases or decreases in sediment supply and stream discharge during the Quaternary. During glacial episodes and as glaciers receded, the sediment supply and discharge were relatively high from glacial erosion and melting in the drainage basins, thus creating conditions for aggradation in many basins (e.g., Weissmann et al., 2002; Tandon et al., 2006; Iriondo and Paira, 2007; Latrubesse et al., 2012; Roy et al., 2012; Fontana et al., 2014). During the interglacial periods, the sediment supply and discharge in many rivers decreased dramatically, creating conditions for fluvial incision into previously deposited fluvial sediments. Therefore, the modern river, held in an incised valley, may not represent the aggradational mode of the river. Paleochannel distributions on the interfluve areas between incised valleys must be evaluated in order to understand the aggradational landform condition. Additionally, even in systems that are not directly linked to glaciated drainage basins, several studies have shown that the extreme climate changes associated with Quaternary glacial cycles have significantly affected aggradation/degradation cycles on fans and along rivers (e.g., Bull, 1991; Weissmann et al., 2005; Stokes and Cunha, 2012).

Though modern systems that have developed through the Quaternary are the only analogs available for interpreting the rock record, we must be cautious in doing so. Analyses on how the Quaternary fluvial systems may be different than those of the past are needed in order to better understand the limitations of these modern analog rivers.

5.4. Implications for the rock record

In a review of over 700 modern continental sedimentary basins around the world, Weissmann et al. (2010, 2011) recognized that DFS covered most of the fluvial depositional area in these basins. Work presented herein supports that finding, showing that DFS comprise over 90% of the fluvial depositional areas in most of the basins evaluated for this report. Thus, Weissmann et al. (2010, 2011) concluded that DFS deposits may be the most common fluvial form found in the rock record.

Significant debate over this concept has ensued since publication of those papers, with several workers presenting arguments that conflict with the suggestion that DFS dominate the rock record (e.g., Sambrook Smith et al., 2010; Ashworth and Lewin, 2012; Fielding et al., 2012; Latrubesse, 2015). Many of the concepts offered in these papers, however, present misconceptions about work of Weissmann et al. (2010, 2011) and Hartley et al. (2010a,b). In this section, we present some of the concepts explored by Sambrook Smith et al. (2010), Fielding et al. (2012), and Latrubesse (2015) in an attempt to clarify some of these misconceptions and highlight areas that are in need of additional work. The arguments from these papers can be classed into several areas:

- River size decrease on DFS.
- Large rivers and their preservation potential.
- Continental areas important for preservation of fluvial deposits.
- Use of satellite imagery to make conclusions about depositional systems.
- Classification of landforms that are DFS.
- Examples of sedimentary successions that are not DFS.
- Criteria for recognition of DFS in the rock record are not unique.

5.4.1. River size decrease on DFS

Fielding et al. (2012) suggested that the only way for rivers to decrease downstream on DFS is for bifurcation to occur, thus making the term *distributive* and *distributary* redundant. However, as shown previously by Weissmann et al. (2011) for the Pilcomayo DFS and herein on the Bermejo DFS and stated by Hartley et al. (2010a), single channel rivers can and commonly do decrease in size downstream on DFS even without bifurcation; however, bifurcation may be present on a DFS. The apparent reason for this decrease in size is the presence of relatively permeable sediments of amalgamated channel belts in the proximal portions of the DFS, thus infiltration can readily occur along these reaches. Evaporation may also contribute to some water loss in these areas. An observed decrease in width of channels downstream is a common occurrence on DFS, though it may not happen on all DFS.

Fielding et al. (2012) and Latrubesse (2015) cite the Kosi DFS asan example where the river channel size remains relatively constant downstream. However, image analysis clearly shows that the active channel belt width decreases from ~7000 m just below the barrage down to 1500-3000 m width near the toe of this DFS (Fig.22). Much of the reason for this decrease in active channel width is from bifurcation, where floodwaters are routed into the floodbasin located between the Kosi and the Gandak DFS. Some of this width change may also be caused by anthropogenic influences, as the Kosi channel width is ~4500m above the barrage (still wider than the river at the distal portions of the DFS).

5.4.2. Large rivers and theirpreservationpotential

Large rivers are defined in numerous ways (see Latrubesse, 2015, for a discussion of this); however, an assessment of large rivers based on discharge, as suggested by Latrubesse (2015), may be used as a proxy for the sizes of bedforms and deposits that may be preserved from these channel systems. Sambrook Smith et al. (2010), Fielding et al. (2012), and Latrubesse (2015) incorrectly suggested that large rivers were excluded from the databases presented by Weissmann et al. (2010) and Hartley et al. (2010b).

A critical evaluation of the database presented by Hartley et al. (2010b) shows that several large rivers form large DFS and are included in the large DFS database (e.g., the Ganges, Indus, Brahmaputra, Paraná, Paraguay, and Zambezi rivers). The database of Weissmann et al. (2010) did not include specific rivers (as incorrectly suggested by Fielding et al., 2012), but instead showed locations of active continental sedimentary basins. Included in this database are many of the world's largest rivers that cross the sedimentary basins. For example, the Paraguay, Paraná, Ganges, Brahmaputra, Magdalena, Orinoco, Indus, Zambezi, Yukon, and Niger rivers all cross sedimentary basins highlighted by Weissmann et al. (2010).

As noted by Hartley et al. (2010a) and shown herein, these large rivers enter the sedimentary basins and form large DFS (e.g., the Magdalena, Paraná, Paraguay, Ganges, Brahmaputra, and Zambezi rivers; Figs. 2A, 4, 5, 10, and 13). Below the DFS, these rivers often become the axial tributary system in the basin, as is the case of the Ganges, Indus, Brahmaputra, Paraguay, and Paraná rivers. Thus, these large rivers are very present in the continental sedimentary basin and have potential for preservation in the rock record. Many of the examples presented by Fielding et al. (2012) of sandstones produced by large rivers mostlikely came from large rivers in either the axial position or on their DFS as they entered the sedimentary basin.

5.4.3. Continental areas important for preservation of fluvial deposits

Much discussion in Sambrook Smith et al. (2010), Fielding et al. (2012), and Latrubesse (2015) was devoted to showing that DFS cover less area of the overall continent than drainage basins of large rivers (e.g., Fielding et al.'s Fig. 3). In this discussion, these authors infer that large areas of the continent were excluded from analysis by Weissmann et al. (2010, 2011) and Hartley et al. (2010a,b), and in this statement they are correct. As shown by Nyburg and Howell (2015), however, only ~16% of the continental area holds sedimentary basins and only in these sedimentary basins, where tectonic subsidence is present, do sediments have the potential to be buried and ultimately lithified. Sediment stored along rivers outside these sedimentary basins is only temporarily stored *en route* to the oceans. Thus, Weissmann et al. (2010, 2011) focused on identifying locations where these sedimentary basins are present in the continents. Therefore, many of the large regions shown by Fielding et al. (2012) were not included in the database asthey are located outside active sedimentary basins and have little or no long-term preservation potential.

In focusing on sedimentary basins, Weissmann et al. (2010, 2011) applied a fundamental principle of sedimentary geology, specifically that accommodation space must be available in order to preserve sediments as sedimentary rocks (e.g., Jervey, 1989;Reading and Levell, 1996). In marine settings, accommodation space exists anywhere below sea level; therefore, most marine sediments have the potential to be preserved as sedimentary rocks. However, in continental settings, only specific regions will be preserved. Blum and Törnqvist (2000) followed use of the terms *accumulation* space and *preservation* space from Kocurek and Havholm (1993) and Kocurek (1998) to define components of accommodation space in continental settings, where accumulation space is defined as '…the volume of space that can be filled within present process regimes, and is fundamentally governed by the relationship between stream power and sediment load, and how this changes in response to geomorphic base level', and preservation space exists where '…subsidence lowers these deposits below possible depths of incision and removal' (Blum and Törnqvist, 2000, p. 20). Sedimentary basins are the primary locations on the continents where sufficient subsidence exists for long-term preservation of continental sediments, and in fact may be the only locations where *significant* long-term preservation is possible. Therefore, we must look at modern sedimentary basins and the fluvial styles within these basins in order to understand fluvial form in past sedimentary basins now represented by fluvial sedimentary rocks.

A critical review of Ashworth and Lewin (2012) and Fig. 3 in Fielding et al. (2012) shows areas of supposed significance included in the large river drainage basins where fluvial successions can never be preserved. The drainage basins outlined in this figure include the Rocky Mountains and

AppalachianMountains that surround the Mississippi drainage basin, the Andes Mountains surrounding the Amazon drainage basin, the Himalayas in the Ganges/Brahmaputra and Indus drainage basins, and other mountainous areas of the Nile and Lena drainage basins. Additionally, most of the drainage basin areas include highlands where hillslope processes associated with erosion are dominant and major rivers are cutting into significantly older (e.g., older than Miocene) deposits in an erosional setting. Sediments along the rivers in these areas have very little chance of preservation, thus including these large regions outside sedimentary basins as significant for preservation of sedimentary successionsfrom large rivers is misleading, at best.

Latrubesse (2015) uses the Amazon River network as an example of a system that is clearly larger than megafans (large DFS), thus questioning whether the claim of DFS dominance in sedimentary basins is valid. He computes the area of relatively young sediments in the Amazon drainage network to cover an area of ~686,000 km^2. An evaluation of a DEM covering the present Amazon River system, however, clearly shows that this river is incised into older deposits and is presently in an overall degradational mode. This is shown by the dendritic pattern of the river system as it crosses the Amazon intercratonic basin (Fig.23). In other work, Latrubesse et al. (2010) showed that the surrounding deposits of the Solimoes Formation (Miocene) were sourced from megafans (or large DFS) and that the Amazon River and its tributaries are presently incised into these deposits. Additionally, Latrubesse (2015) indicated that the megafans of the Solimoes Formation covered an area of over 7,000,000 km^2, a much greater area than the present Amazon tributary network covers.Therefore, even in this case, the DFS deposits appear to cover a much larger area than the tributary system.

5.4.4. Use of satellite imagery to make conclusions about depositional systems

A criticism of Weissmann et al. (2010, 2011) and Hartley et al. (2010b) is that satellite images are a ’snapshot in time’ and do not represent the ultimate evolution of the sedimentary basin fill (Sambrook Smith et al., 2010; Fielding et al., 2012). However, this could be said of applying any geomorphic study to the sedimentologic record. Imagery used by Weissmann et al. (2010, 2011) and Hartley et al. (2010b) displayed the same range in ages as any geomorphic study would, with surface sediments ranging from Pleistocene to Recent. Paleochannels on the DFS surfaces represent geologically recent expressions of the river channel form, and incised systems represent the dynamic changes in the relatively recent past (usually from the end of the recent glaciation) where the sediment supply and discharge on the rivers significantly changed with the changing climate (e.g., Weissmann et al., 2002, 2005).

Thus, if interpreted properly, this ‘snapshot’ in time from imagery represents more than just the instant the image was taken. River stages and morphologic form of the present river are instantaneous, and successive images show change. For example, a time series of images clearly shows the evolution of the avulsion on the Taquari DFS (Buehler et al., 2011). To infer that imagery cannot be used to evaluate regional patterns of geomorphology is to discard an important tool for analysis of remote locations.

Several studies of subsurface deposits in several basins indicate that the landforms observed at the surface do correlate to deeper deposits (e.g., Lettis, 1988; Hawley et al., 1995; Weissmann et al., 2002; Fontana et al., 2008; Connell et al., 2013; Reiser et al., 2014; Sinha et al., 2014).However, caution is needed when applying facies distributions observed in the modern systems directly to the rock record without considering facies preservation potential. For example, a higher proportion of coarse-grained facies were observed in the subsurface of the San Joaquin Basin than what was observed on the surface (Weissmann et al., 1999). Thus, additional subsurface work is needed to help develop a better understanding of the preservation potential of various facies as the fluvial systems evolve and are buried. Improved understanding of how the geomorphic elements observed at the surface will be preserved with burial may be captured in the future using new technology, such as geophysical methods (e.g., 3D seismic).

5.4.5. Classification of landforms considered to be DFS

As noted previously, the term DFS was developed as a collective name to include fluvial landforms that are distributive in nature. Thus, alluvial fans, fluvial fans, and fluvial megafans are all classified as different types of DFS. Latrubesse (2015) distinguished avulsive river systems (e.g., the Beni River) as being different than a DFS. However, since nodal avulsion at the apex is an important aspect of any DFS, the difference between an 'avulsive river' and a river on a DFS is unclear. Instead, avulsive rivers are integral parts of a DFS, where, as noted previously, rivers on DFS commonly move through avulsion. Latrubesse (2015) used the example of the Beni River as an avulsive river, dismissing the interpretation by Wilkinson et al. (2006) and Weissmann et al. (2011) that this river system is forming a megafan. However, the avulsions on this system take place at a point located as the river enters the sedimentary basin, and this river is distributing sediment across the basin in a radial pattern. Thus, we interpret the deposits from this river as a megafan, or large DFS.

As noted earlier in this paper, the Beni River has a different form than many rivers on other DFS around the world, where the Beni River meander belts uniquely show a high degree of amalgamation through chute and neck cutoff avulsions (Fig. 21C). This indicates that the river remained in place for a sufficient period of time to develop the amalgamated meanderbelt form prior to avulsion. The reasons for this difference in fluvial style are unclear at this time, but this could form an interesting problem for future study.

5.4.6. Examples of sedimentary successions that are not DFS

Sambrook Smith et al. (2010), Fielding et al. (2012), and Latrubesse (2015) described situations where fluvial sediments are preserved and where no evidence is presented that these were deposited on DFS. Many of the successions identified by these workers occurred where high-amplitude sea level change has caused development of incised valleys. For example, the canyon fill of the Eeonile is related to rapid sea level decline that led to significant incision, with later sea level rise creating conditions for valley fill. We agree that these successions are important in the sedimentary record (Hartley et al.,2010a); however, the work of Weissmann et al. (2010, 2011) specifically focused on river deposits in sedimentary basins that were not influenced by sea level change. Therefore, these examples are irrelevant to the present discussion.

Other examples used by Sambrook Smith et al. (2010), Fielding et al. (2012), and Latrubesse (2015) include the aulocogen fills of the Mississippi River embayment and the Paraná River. These basins contain thick successions of sedimentary fill that do not have the form of a DFS. Latrubesse (2015) also highlights the Bananal Basin in Brazil, a basin that was missed by Weissmann et al. (2010), noting that this modern basin does not display a DFS form on rivers entering the basin. In all of these cases, the river system is large relative to the width of the basin and no space exists for a distributive system to form. Instead, the river system trends parallel to the sides of the basin and no radial pattern is developed. Thus, the width of the sedimentary basin relative to the river size and orientation may have some control on whether a DFS can develop (Hartley et al., 2010b).

5.4.7. Criteria for recognition of DFS in the rock record are not unique

Weissmann et al. (2010) suggested four criteria that are important for recognition of DFS deposits in the rock record. These include (i) a radial pattern of channels from the DFS apex, (ii) common down-DFS channel size decrease, (iii) down-DFS grain size decrease, and (iv) lack of lateral channel confinement. As noted by Sambrook Smith et al. (2010) and Fielding et al. (2012) and acknowledged by Hartley et al. (2010a), some of these criteria may overlap with observations of tributary systems. Weissmann et al. (2010) intended these to be initial observations based on the evaluation of satellite imagery, with the expectation that future work would refine these concepts.

An example of evolving concepts is given in Weissmann et al. (2013), where the signature of DFS prograding into the sedimentary basin was proposed. Weissmann et al. (2013) suggested that a drying upward and coarsening upward succession would develop as the DFS progrades into the basin, and they provided rock record examples that supported this hypothesis.

Many rock record examples also exist within the literature (e.g., Friend and Moody-Stuart, 1972; Friend, 1978; Kelly and Olsen, 1993; Horton and Decelles, 2001; Cain and Mountney, 2009, 2011; amongst others), all of which broadly agree with the trends cited in Weissmann et al. (2013). However, until recently very few studies provided quantified data that enables the trends cited to be vigorously tested. Owen et al. (2015b) recently published an assessment of the Salt Wash Member of the Morrison Formation, SW USA, presenting an example of how DFS may be recognized in the rock record.

A clear downstream change in architecture is evident in this succession that allows a system-scale overview. Proximal regions are dominated by amalgamated channel belt deposits thatdownstream pass into channel belt deposits that are separated by laterally extensive floodplain deposits in the medial area. In the distal area, floodplain deposits dominate the succession, with channel deposits in the form of isolated ribbon channels forming only a minor amount of the succession. Owen et al. (2015b) were able to test the trends cited by Weissmann et al. (2013) by quantifying parameters across the Salt Wash fluvial system. For example, the authors demonstrated a downstream decrease in the proportion (from 67% of the succession to 0%) and average thickness of channel belt deposits (15 to 3.8m), while the proportion of floodplain deposits increased (from 38% to 94%) on the Salt Wash DFS. The proportion of sandstone to mudstone also decreases downstream from 70% to 8%, demonstrating a downstream decrease in DFS grainsize. Additionally, paleocurrent analyses demonstrated a radial pattern of channels from an apex that is statistically estimated to be located in northwestern Arizona (Owen et al. 2015a).

Quantified data are also available from the Huesca DFS, Spain (Hirst, 1991), and although data are from a substantially smaller DFS deposit (the Huesca DFS has an apex to toe length of ~70 km while the Salt Wash DFS is ~550 km), cited trends are remarkably similar.

Not all trends cited by Weissmann et al. (2013) could be statistically established. For example, a downstream decrease in channel belt grainsize is not found on the Salt Wash DFS. Owen et al. (2015b) related this observation to bypass of sediment during progradation phases, thus allowing influxes of coarser-grained material into the distal realms.

6. Conclusions

Becausetectonic subsidence exists in sedimentary basins, as shown by a thick succession of relatively recent fluvial deposits in these basins, preservation space exists for sediments to accumulate and be preserved. Therefore, in order to understand the processes that may have formed the facies of the continental sedimentary rock record, we need to better understand the geomorphic processes that occur in these sedimentary basins. Though fluvial geomorphic studies focused on rivers in erosional terrains outside sedimentary basins may help us gain understanding on channel-scale processes, these may have limited application for understanding sedimentary processes in the context of the sedimentary basin that may be used as a predictive framework for evaluating continental sedimentary successions.

The key geomorphic elements in modern sedimentary basins consist of DFS, tributive fluvial, eolian, and lake/playa. Of the fluvial elements, DFS by far comprise the main component of most modern continental sedimentary basins and are likely to have done so in the past. In the basins delineated for this work, DFS comprise about 90% or more of the fluvial deposits.

Many of the current approaches to understanding fluvial systems are based on work undertaken on tributive systems located outside sedimentary basins, and in some instances the key differences between tributive and distributive systems mean that these approaches are inappropriate as they do not take into account downstream decreases in discharge or differences in avulsion and associated flooding processes. Process-based predictive models for DFS need to be developed that account for these differences.

Future work is required to describethe variability on modern DFS related to climatic and tectonic settings.Understanding the controls on channel belt morphology (e.g., sinuosity and planview) on DFS is required, especially in modeling and characterizingthe transition between different morphologic forms down-DFS. The morphology of channel belts and their associated floodplains appears to be controlled by upstream conditions in the drainage basin for the DFS. Measurements of flow conditions on DFS are needed in order to understand controls on morphologic change.

At a system scale, avulsion frequencies at channel and DFS lobe scale must be better understood. This controls the return period of channel belts on a DFS and may aid in a more complete understanding of the evolution of fluvial basin fill. Additionally, an understanding of changes in meander belt development in different parts of a DFS, particularly bifurcation and avulsion and how these may change downstream on a DFS, is required in order to better interpret ancient fluvial successions.

Groundwater distributions and the presence of springlines areimportant for human habitation on DFS and for recognition of soil and channel characteristics that may be present in the rock record (e.g., Hartley et al., 2013; Weissmann et al., 2013). Thus, regional-scale groundwater modeling is needed in order to better understand controls on the location and variability of the groundwater system in DFS. Such models could lead to a predictive framework on where and when emergent groundwater features may be present on distal portions of DFS, and they may help in evaluation of impacts of water development on communities that depend on the groundwater and springs.

Further work should examine the importance of differences in the nature of incision on DFS particularly the importance of variability in discharge and sediment supply in the catchment generating *top-down* incision or base-level control in generating *bottom-up* incision. Incisional/aggradational cyclicity appears to play a key role in the development of modern and Pleistocene-aged DFS, and channel belt morphology inside incised valleys may be different than channel belt morphology in the open fan setting. Controls on aggradation or degradation, quantified for modeling, should be better understood in order to construct reasonable models of DFS evolution.

Most reaches of large rivers have no preservation potential in many continental settings as they do not commonly occur in actively subsiding sedimentary basins. Where these rivers cross a sedimentary basin, they build a large DFS as they enter the basin, then downstream of this DFS they are typically present in the axial position of a sedimentary basin. In this axial position, they are likely to form a minor proportion of the basin-fill (generally <10%). Though these river systems may form significant sandstone bodies in the sedimentary record, most of the basin fill will consist of deposits from DFS.

Though significant work has been conducted in describing the fluvial geomorphology in sedimentary basins, much more effort is needed in order to better understand processes for deposition and preservation in these basins. Quantification of these systems is needed, including gradients of channel systems, morphologic metrics of the rivers (such as sinuosity, braiding indices, bar form geometry, and aspect ratios of channel forms), geomorphic controls in the drainage basins that feed the fluvial systems in the sedimentary basins, and estimations of discharge losses or gains from interaction with the groundwater system. Only through focused measurements and descriptions of fluvial systems in modern continental sedimentary basins will we be able to better understand the facies distributions that are observed from ancient continental sedimentary basins preserved in the rock record.

Acknowledgements

We appreciate very helpful reviews by Dr. Martin Stokes and three anonymous reviewers and editor Dr. Richard Marston. We also appreciate the encouragement for writing this paper from Dr. Timothy Horscroft. We acknowledge support of the sponsors of the Fluvial Systems Research Group consortium, BP, BG, Chevron, ConocoPhillips and Total.

References cited:

Allen, P.A., and Allen, J.R., 2013, Basin Analysis: Principles and Application to Petroleum Play Assessment, 3rd Edition, Chichester, Wiley-Blackwell, 642p.

Allen, P.A., Homewood, P., and Williams, G.D., 1986, Foreland basins: an introduction, *in* Allen, P.A., Homewood, P., and Williams, G.D., eds., Foreland Basins, International Association of Sedimentologists Special Publication 8, p. 3-12.

Ashworth, P.J., and Lewin, J., 2012, How do big rivers come to be different?: Earth-Science Reviews, . 114, p. 84-107.

Ashworth, P.J., Best, J.L., and Jones, M., 2004, Relationship between sediment supply and avulsion frequency in braided rivers: Geology, v. 32, p. 21-24: DOI: 10.1130/G19919.1.

Aslan, A., and Blum, M.D., 1999, Contrasting styles of Holocene avulsion, Texas Gulf Coastal Plain, USA, *in* Smith, N.D., and Rogers, J., eds., Fluvial Sedimentology VI: International Association of Sedimentologists, Special Publication 28, p. 193-209.

Aslan, A., Autin, W.J., and Blum, M.D., 2005, Causes of river avulsion: insights from the late Holocene avulsion history of the Mississippi River, U.S.A.: Journal of Sedimentary Research, v. 75, p. 650-664.

Assine, M.L., 2005, River avulsions on the Taquari megafan, Pantanal wetland, Brazil: Geomorphology, v. 70, p. 357-371.

Assine, M.L., and Silva, A., 2009, Contrasting fluvial styles of the Paraguay River in the northwestern border of the Pantanal wetland, Brazil: Geomorphology, v. 113, p. 189-199.

Assine, M.L., Corradini, F.A., Pupim, F.dN., and McGlue, M.M., 2014, Channel arrangements and depositional styles in the São Lourenço fluvial megafan, Brazilian Pantanal wetland: Sedimentary Geology, v. 301, p. 172-184, doi: 10.1016/j.sedgeo.2013.11.007.

Bartow, J.A., 1991, The Cenozoic Evolution of the San Joaquin Valley, California: U.S. Geological Survey, Professional Paper, 1501, 40p.

Bernal, C., Christophoul, F., Darrozes, J., Laraque, A., Bourrel, L., Soula, J.C., Guyot, J.L., and Baby, P., 2013, Crevassing and capture by floodplain drains as a cause of partial avulsion and anastomosis (lower Rio Pastaza, Peru): Journal of South American Earth Sciences, v. 44, p. 63-74, doi: 10.1016/j.sames.2012.11.009.

Blainey, J.B., and Pelletier, J.D., 2008, Infiltration on alluvial fans in arid environments: Influence of fan morphology: Journal of Geophysical Research, v. 113, F03008, doi: 10.1029/2007/JF000792.

Blair, T.C., and McPherson, J.G., 1994, Alluvial fans and their natural distinction from rivers based on morphology, hydraulic processes, sedimentary processes, and facies assemblages: Journal of Sedimentary Research, v. A64, p. 450-489.

Blair, T.C., and McPherson, J.G., 1998, Recent debris-flow processes and resultant form and facies of the Dolomite Alluvial Fan, Owens Valley, California: Journal of Sedimentary Research, v. 68, p. 800-818.

Blair, T.C., and McPherson, J.G., 2009, Processes and forms of alluvial fans, *in* Abrahams, A.D., and Parsons, A.J., Geomorphology of Desert Environments, 2nd edition, p. 413-467.

Blum, M.D., and Törnqvist, T.E., 2000, Fluvial responses to climate and sea-level change: a review and look forward: Sedimentology, v. 47, p. 2-48.

Bridge, J.S., 2006, Fluvial facies models: recent developments, *in* Posamentier, H.W., and Walker, R.G., eds., Facies Models Revisited: SEPM Special Publication 84, p. 85-170.

Brown, L., ed., 1993, The New Shorter Oxford English Dictionary on Historical Principles, Volume I, Oxford, Clarendon Press, 1876p.

Bryant, M., Falk, P., and Paola, C., 1995, Experimental study of avulsion frequency and rate of deposition: Geology, v. 23., p. 365-368.

Buehler, H.A., Weissmann, G.S., Scuderi, L.A., and Hartley, A.J., 2011, Spatial and temporal evolution of an avulsion on the Taquari River distributive fluvial system from satellite image analysis: Journal of Sedimentary Research, v. 81, p. 630-640, DOI: 10.2110/jsr.2011.040.

Bull, W.B., 1977, The alluvial fan environment: Progress in Physical Geography, v. 1, p. 222-270.

Bull, W.B., 1991, Geomorphic Responses to Climatic Change, Oxford, Oxford University Press, 326p.

Busby, C., and Azor Peréz, A., eds., 2012, Tectonics of Sedimentary Basins: Recent Advances: Wiley-Blackwell, 664p.

Busby, C., and Ingersoll, R.V., eds., 1995, Tectonics of Sedimentary Basins: Blackwell Science, Cambridge, 579p.

Cain, S.A. and Mountney, N.P., 2009, Spatial and temporal evolution of a terminal fluvial fan system: the Permian Organ Rock Formation, South-east Utah, USA: Sedimentology, v.56, p. 1774–1800.

Cain, S.A. and Mountney, N.P., 2011, Downstream changes and associated fluvial-eolian interactions in an ancient terminal fluvial system: The Permian Organ Rock Formation, SE Utah, USA, *in* Davidson, S.K., Leleu, S., North, C., eds, From River To Rock Record: The Preservation of Fluvial Sediments And Their Subsequent Interpretation: SEPM, Special Publication 97, p. 1–19.

Chakraborty, T., and Ghosh, P., 2010, The geomorphology and sedimentology of the Tista megafan, Darjeeling Himalaya: Implications for megafan building processes: Geomorphology, v. 115, p. 252-266, DOI: 10.1016/j.geomorph.2009.06.035.

Chakraborty, T., Kar, R., Ghosh, P., and Basu, S., 2010, Kosi megafan: Historical records, geomorphology and the recent avulsion of the Kosi River: Quaternary International, v. 227, p. 143-160, DOI: 10.1016/j.quaint.2009.12.002.

Collinson, J.D., 1996, Alluvial sediments, *in* Reading, H.G.,ed., Sedimentary Environments: Processes, Facies and Stratigraphy, Third Edition, Blackwell Publishing, Malden, MA, 688p.

Connell, S.D., Kim, W., Paola, C., and Smith, G.A., 2012, Fluvial morphology and sediment-flux steering of axial-transverse boundaries in an experimental basin: Journal of Sedimentary Research, v. 82, p. 310-325, doi: 10.2110/jsr.2012.27.

Connell, S. D., Smith, G. A., Geissman, J. W., and McIntosh, W. C., 2013, Climatic controls on nonmarine depositional sequences in the Albuquerque Basin, Rio Grande rift, north-central New Mexico: Geological Society of America Special Paper 494, p. 383-425.

Covey, M., 1986, The evolution of foreland basins to steady-state: Evidence from the western Taiwan foreland basin, Foreland Basins, *in* Allen, P.A., and P. Homewood, P., eds., Special Publication of the International Association of Sedimentologists, v, 8, p. 77-90.

Dade, W.B., and Verdeyen, M.E., 2007, Tectonic and climatic controls of alluvial-fan size and source-catchment relief: Journal of the Geological Society, London, v. 164, p. 353-358.

Davidson, S.K., and North, C.P., 2009, Geomorphological regional curves for prediction of drainage area and screening modern analogues for rivers in the rock record: Journal of Sedimentary Research, v. 79, p. 773-792, doi: 10.2110/jsr.2009.080.

Davidson, S.K., Hartley, A.J., Weissmann, G.S., Nichols, G.J., and Scuderi, L.A., 2013, Geomorphic elements on modern distributive fluvial systems: Geomorphology, v. 180-181: p. 82-95, DOI: 10.1016/j.geomorph.2012.09.008.

Davies-Vollum, K.S., and Kraus, M.J., 2001, A relationship between alluvial backswamps and avulsion cycles: an example from the Willwood Formation of the Bighorn Basin, Wyoming: Sedimentary Geology, v. 40, p. 235-249.

DeCelles, P.G., 2012, Foreland basin systems revisited: variations in response to tectonic settings, *in* Busby, C., and Azor Pérez, a., eds., Tectonics of Sedimentary Basins: Recent Advances, 1st Edition, Blackwell Publishing Ltd, p. 405-426.

DeCelles, P.G., and Cavazza, W., 1999, A comparison of fluvial megafans in the Cordilleran (Upper Cretaceous) and modern Himalayan foreland basin systems: Geological Society of America, Bulletin, v. 111, p. 1315-1334.

Denny, C.S., 1965, Alluvial fans in the Death Valley Region, California and Nevada: U.S. Geological Survey Professional Paper 466.

de Souza, O.C., Araujo, M.R., and Mertes, L.A.K., 2002, Forms and processes along the Taquari River alluvial fan, Pantanal Brazil: Zeitschrift für Geomorphologie, v. 129, p. 73-107.

Dhar, O.N., and Nandargi, S., 2002, Flood study of the Himalayan tributaries of the Ganga river: Meteorological Applications, v. 9, p. 63-68.

Dumont, J.F., 1996. Neotectonics of the Subandes-Brazilian craton boundary using geomorphological data: the Maranon and Beni basins. Tectonophysics 259, 137

Ellery, W.N., McCarthy, T.S, and Smith, N.D., 2003, Vegetation, hydrology and sedimentation patterns on the major distributary system of the Okavango Fan, Botswana: Wetlands, v. 23, p. 357-375.

ESRI, 2015. ArcGIS Desktop: Release 10.1. Redlands, CA: Environmental Systems Research Institute.

Ethridge, F.G., Skelly, R.L., and Bristow, C.S., 1999, Avulsion and crevassing in the sandy, braided Niobrara River: complex response to base-level rise and aggradation, *in* Smith, N.D., and Rogers, J., eds., Fluvial Sedimentology VI: International Association of Sedimentologists, Special Publication 28, p. 179-191.

Field, J., 2001, Channel avulsion on alluvial fans in southern Arizona: Geomorphology, v. 37, p. 93-104.

Fielding, C.R., Ashworth, P.J., Best, J.I., Prokocki, E.W., and Sambrook Smith, G.H., 2012, Tributary, distributary and other fluvial patterns: What *really*represents the norm in the continental rock record?: Sedimentary Geology, v. 261-262, p. 15-32, doi: 10.1016/j.sedgeo.2012.03.004.

Fleckenstein, J.H., Niswonger, R.G., and Fogg, G.E., 2006, River-aquifer interactions, geologic heterogeneity, and low-flow management: Ground Water, v. 44, p. 837-852, doi: 10.1111/j.1745-6584.2006.00190.x.

Fontana, A., Mozzi, P., and Bondesan, A., 2008, Alluvial megafans in the Venetian-Friulian Plain (north-eastern Italy): Evidence of sedimentary and erosive phases during Late Pleistocene and Holocene: Quaternary International, v. 189, p. 71-90, DOI: 10.1016/j.quaint.2007.08.044.

Fontana, A., Mozzi, P., and Marchetti, M., 2014, Alluvial fans and megafans along the southern side of the Alps: Sedimentary Geology, v. 301, p. 150-171, doi:10.1016/j.sedgeo.2013.09.003.

Fordham, A.M., North, C.P., Hartley, A.J., Archer, S.G., Warwick, G.L. 2010. Dominance of lateral over axial sedimentary fill in dryland rift basins. Petroleum Geoscience, 16, 299-304.

Friend, P.F., 1978, Distinctive features of some ancient river systems, *in* Miall, A.D., ed., Fluvial Sedimentology: Canadian Society of Petroleum Geologists, Memoir 5, p. 531-542.

Friend, P.F. and Moody-Stuart, M., 1972, Sedimentation of the Wood Bay Formation (Devonian) of Spitsbergen: Regional analysis of a late orogenic basin: Norsk Polarinstitutt,Nr. 157, p.1–77.

Frostick, L.E., and Reid, I., 1987, A new look at rifts: Geology Today, v. 3, p. 122-126.

Gawthorpe, R.L., and Leeder, M.R., 2000, Tectono-sedimentary evolution of active extensional basins: Basin Research, v. 12, p. 195-218.

Geddes, A., 1960, The alluvial morphology of the Indo-Gangetic Plain: its mapping and geographical significance: Institute of British Geographers, Transactions and Papers, v. 28, p. 253-276.

Gibling, M.R., Tandon, S.K., Sinha, R., and Jain, M., 2005, Discontinuity-bounded alluvial sequences of the Southern Gangetic Plains, India: aggradation and degradation in response to monsoonal strength: Journal of Sedimentary Research, v. 75, p. 369-385.

Gibling, M.R., Bashforth, A.R., Falcon-Lang, H.J., Allen, J.P., and Fielding, C.R., 2010, Log jams and flood sediment buildup caused channel abandonment and avulsion in the Pennsylvanian of Atlantic Canada: Journal of Sedimentary Research, v. 80, p. 268-287, DOI: 10.2110/jsr.2010.024.

Gibling, M.R., Fielding, C.R., and Sinha, R., 2011, Alluvial valleys and alluvial sequences: towards a geomorphic assessment, *in*North, C., Davidson, S., and Leleu, S., eds., Rivers to Rocks: SEPM (Society of Sedimentary Geology) Special Publication 97, p. 423-447.

Gilfellon, G.B., Sarma, J.N., and Gohain, K., 2003, Channel and bed morphology of a part of the Brahmaputra River in Assam: Journal of the Geological Society of India, v. 62, p. 227-235.

Gohain, K., and Parkash, B, 1990, Chapter 8: Morphology of the Kosi Megafan, *in* Rachocki, A.H., and Church, M., eds., Alluvial Fans: A Field Approach, John Wiley & Sons Ltd., p. 151-178.

Gole, C.V., and Chitale, S.V., 1966, Inland delta building activity of Kosi River: American Society of Civil Engineers, Proceedings, Journal of Hydraulics Division, Paper 4722, v. 92, p. 111-126.

Gordon, I., and Heller, P.L., 1993, Evaluating major controls on basinal stratigraphy, Pine Valley, Nevada: Implications for syntectonic deposition: Geological Society of America, Bulletin, v. 105, p. 47-55.

Goswami, D.C., 1985, Brahmaputra River, Assam, India: physiography, basin denudation, and channel aggradation: Water Resources Research, v. 21, p. 959-978.

Gumbricht, T.S., McCarthy, T.S., and Merry, C.L., 2001, The topography of the Okavango Delta, Botswana, and its tectonic and sedimentological implications: South African Journal of Geology, v. 104, p. 243-264.

Gumbricht, T., McCarthy, J., and McCarthy, T.S., 2004, Channels, wetlands and islands in the Okavango delta, Botswana, and their relation to hydrological and sedimentological processes: Earth Surface Processes and Landforms, v. 29, p. 15-29.

Gupta, A., 2007, Introduction, *in* Gupta, A., ed., Large Rivers: Geomorphology and Management. John Wiley & Sons, Ltd, Chichester, p. 1-5.

Gupta, S., 1997, Himalayan drainage patterns and the origin of fluvial megafans in the Ganges foreland basin: Geology, v. 23, p. 11-14.

Hartley, A.J., Weissmann, G.S., Nichols, G.J., and Scuderi, L.A., 2010a, Fluvial form in modern continental sedimentary basins: Distributive fluvial systems: REPLY: Geology, v. 38, e231, doi: 10.1130/G31588Y.1.

Hartley, A.J., Weissmann, G.S., Nichols, G.J., and Warwick, G.L., 2010b, Large distributive fluvial systems: characteristics, distribution, and controls on development: Journal of Sedimentary Research, v. 80, p. 167-183.

Hartley, A.J., Weissmann, G.S., Bhattacharayya, P., Nichols, G.J., Scuderi, L.A., Davidson, S.K., Leleu, S., Chakraborty, T., Ghosh, P. and Mather, A.E., 2013, Soil development on modern distributive fluvial systems: preliminary observations with implications for interpretation of paleosols in the rock record, *in*Driese, S., ed., New Frontiers in Paleopedology and Terrestrial Paleoclimatology, SEPM (Society for Sedimentary Geology) Special Publication 104, p. 149-158, DOI: 10.2110/sepmsp.104.10.

Hartley, A.J., Owen, A.E., Swan, A., Weissmann, G.S., Holzweber, B.I., Howell, J., Nichols, G.D., and Scuderi, L.A. 2015, Recognition and importance of amalgamated sandy meander belts in the continental rock record: Geology, 43, 679–682.

Harvey, A.M., 1984, Debris flows and fluvial deposits in Spanish Quaternary alluvial fans: Implications for fan morphology, *in* Koster, E.H., and Steel, R.J., eds., Sedimentology of Gravels and Conglomerates: Canadian Society of Petroleum Geologists Memoir 10, p. 123-132.

Harvey, A.M., 1987, Alluvial fan dissection: relationships between morphology and sedimentology, *in* Frostick, L., and Reid, I., eds., Desert Sediments Ancient and Modern. Geological Society, London, Special Publication, 35, p. 87-103.

Harvey, A.M., 1996, The role of alluvial fans in the mountain fluvial systems of southeast Spain: Implications of climate change. Earth Surface Processes and Landforms, v. 21, p. 543-553.

Harvey, A.M., 1997, The role of alluvial fans in arid-zone fluvial systems, *in* Thomas, D.S.G., ed., Arid Zone Geomorphology: Process, Form, and Change in Drylands, 2nd Edition, Wiley, Chichester, p. 231-259.

Harvey, A.M., 2005, Differential effects of base-level, tectonic setting and climatic change on Quaternary alluvial fans in the northern Great Basin, Nevada, USA, *in* Harvey, A.M., Mather, A.E., and Stokes, M., eds., Alluvial Fans: Geomorphology, Sedimentology, Dynamics. Geological Society, London, Special Publications, 251, p. 117-131.

Harvey, A.M., 2011, The coupling status of alluvial fans and debris cones: a review and synthesis: Earth Surface Processes and Landforms, v. 37, p. 64-76, doi: 10.1002/esp.2213.

Harwood, K., and Brown, A.G., 1993, Fluvial processes in a forested anastomosing river; flood partitioning and changing flow patterns: Earth Surface Processes and Landforms, v. 18, p. 741-748.

Hashimoto, A., Oguchi, T., Hayakawa, Y., Lin, Z., Saito, K. and Wasklewicz, T.A., 2008, GIS analysis of depositional slope change at alluvial-fan toes in Japan and the American Southwest: Geomorphology, v. 100, p. 120-130, doi: 10.1016/j.geomorph.2007.10.027.

Hawley, J.W., and Haase, C.S. (compilers), 1992, Hydrogeologic framework of the Northern Albuquerque Basin. New Mexico Bureau of Mines and Mineral Resources, Open-File Report 387, 74p.

Hawley, J. W., Haase, C. S., and Lozinsky, R. P., 1995, An underground View of the Albuquerque basin, *in* Ortega-Klett, C. T., ed., The water future of Albuquerque and the middle Rio Grande basin: New Mexico Water Resources Research Institute, p. 27-55.

Hendrickx, J.M.H., Khan, A.S., Bannicnk, M.H., Birch, D., and Kidd, C., 1991, Numerical analysis of groundwater recharge through stony soils using limited data: Journal of Hydrology, v. 127, p. 173-192.

Hirst, J.P.P., 1991, Variations in alluvial architecture across the Oligo-Miocene Huesca fluvial system, Ebro Basin, Spain, *in* Miall, A.D., AND Tyler, N., eds, The three dimensional facies architecture of terrigenous clastic sediments and its implications for hydrocarbon discovery and recovery. SEPM, Concepts in Sedimentology and paleontology 3, p. 111–121.

Hooke, R.LeB, 1967, Processes on arid-region alluvial fans: The Journal of Geology, v. 75, p. 438-460.

Horton, B.K., and DeCelles, P.G., 1997, The modern foreland basin system adjacent to the Central Andes: Geology, v. 25, p. 895-898.

Horton, B.K., and DeCelles, P.G., 2001, Modern and ancient fluvial megafans in the foreland basin system of the central Andes, southern Bolivia: implications for drainage network evolution in fold-thrust belts: Basin Research, v. 13, p. 43-63.

Houston, J., 2002, Groundwater recharge through an alluvial fan in the Atacama Desert, northern Chile: Mechanisms, magnitudes and causes: Hydrological Processes, v. 16, p. 3019-3035, doi: 10.1002/HYP.1086.

Huntington, G.L., 1980, Soil-land form relationships of portions of the San Joaquin River and Kings River alluvial depositional systems in the Great Valley of California. PhD Thesis, University of California, Davis, 147p.

Ingersoll, R.V., 2012, Tectonics of sedimentary basins, with revised nomenclature, *in* Busby, C., and Azor Pérez, a., eds., Tectonics of Sedimentary Basins: Recent Advances, 1st Edition, Blackwell Publishing Ltd, p. 3-43.

Iriondo, M., 1993, Geomorphology and late Quaternary of the Chaco (South America): Geomorphology, v. 7, p. 289-303.

Iriondo, M.H., 2007, 2. Geomorphology, *in* Iriondo, M.H., Paggi, J.C., and Parma, M.J., eds., The Middle Paraná River, Limnology of a subtropical wetland, Springer, Berlin, p. 33-52.

Iriondo, M.H., and Paira, A.R., 2007, 1. Physical Geography of the Basin, *in* Iriondo, M.H., Paggi, J.C., and Parma, M.J., eds., The Middle Paraná River, Limnology of a subtropical wetland, Springer, Berlin, p. 7-31.

Iriondo, M.H., Paggi, J.C., and Parma, M.J., eds., 2007, The Middle Paraná River, Limnology of a subtropical wetland, Springer, Berlin, 382p.

Jackson, R.G., 1978, Preliminary evaluation of lithofacies models for meandering alluvial streams, *in* Miall, A.D., ed., Fluvial Sedimentology, Canadian Society of Petroleum Geologists, Memoir 5, p. 543-576.

Jain, V., and Sinha, R., 2003, Hyperavulsive-anabranching Baghmati river system, north Bihar plains, eastern India: Zeitschrift für Geomorphologie, N.F., Supplementband 47, p. 101-116.

Jain, V., and Sinha, R., 2004, Fluvial dynamics of an anabranching river system in Himalayan foreland basin, Baghmati river, north Bihar plains, India: Geomorphology, v. 60, p. 147-170, DOI: 10.1016/j.geomorph.2003.07.008.

Jain, V., and Sinha, R., 2005, Response of active tectonics on the alluvial Baghmati River, Himalayan foreland basin, eastern India: Geomorphology, v. 70, p. 339-356, DOI: 10.1016/j.geomorph.2005.02.012.

Janda, R.J., 1966, Pleistocene history and hydrology of the upper San Joaquin River, California: PhD Thesis, University of California, Berkeley, 293p.

Jerolmack, D.J., 2009, Conceptual framework for assessing the response of delta channel networks to Holocene sea level rise: Quaternary Science Reviews, v. 28, p. 1786-1800, DOI: 10.1016/j.quascirev.2009.02.015.

Jerolmack, D.J., and Paola, C., 2007, Complexity in a cellular model of river avulsion: Geomorphology, v. 91, p. 259-270, doi: 10.1016/j.geomorph.2007.04.022.

Jerolmack, D.J., and Swenson, J.B., 2007, Scaling relationships and evolution of distributary networks on wave-influenced deltas: Journal of Geophysical Research, v. 34, L23402.

Jervey, M.T., 1988, Quantitative geological modeling of siliciclastic rock sequences and their seismic expressions, *in*, Wilgus, C.K., Hastings, B.S., Posamentier, H., Van Wagoner, J., Ross, C.A., and Kendall, C.G.St.C., eds., Sea-level Changes: An Integrated Approach, SEPM (Society for Sedimentary Geology), Special Publication 42, p. 47-69.

Jones, H.L., and Hajek, E.A., 2007, Characterizing avulsion stratigraphy in alluvial deposits: Sedimentary Geology, v. 202, p. 124-137.

Jones, L.S., and Schumm, S.A., 1999, Causes of avulsion: an overview, *in* Smith, N.D., and Rogers, J., eds., Fluvial Sedimentology VI: International Association of Sedimentologists, Special Publication, v. 28, p. 171-178.

Kale, V.S., 2002, Fluvial geomorphology of Indian rivers: an overview: Progress in Physical Geography, v. 26, p. 400-433.

Kelly, S.B. and Olsen, H., 1993. Terminal fans - a review with reference to Devonian examples: Sedimentary Geology, v. 85, p.339–374.

King, W.A., and Martini, I.P., 1984, Morphology and recent sediments of the lower anastomosing reaches of the Attawapiskat River, James Bay, Ontario, Canada: Sedimentary Geology, v. 37, p. 295-320.

Kocurek, G., 1998, Aeolian system response to external forcing factors – a sequence stratigraphic view of the Saharan region, *in* Alsharhan, A.S., Glennie, K., Whittle, G.L., and Kendall, C.G.St.C., eds., Quaternary Deserts and Climatic Change: Balkema Press, p. 327-337.

Kocurek, G., and Havholm, K.G., 1993, Eolian sequence stratigraphy: A conceptual framework, *in* Weimer, P., and Posamentier, H.W., eds., Siliciclastic Sequence Stratigraphy: Recent Developments and Applications. American Association of Petroleum Geologists, Memoir 58, p. 393-410.

Kraus, M.J., 1996, Avulsion deposits in lower Eocene alluvial rocks, Bighorn Basin, Wyoming: Journal of Sedimentary Research, v. 66, p. 364-373.

Kraus, M.J., and Davies-Vollum, K.S., 2004, Mudrock-dominated fills formed in avulsion splay channels: examples from the Willwood Formation, Wyoming: Sedimentology, v. 51, p. 1127-1144.

Kraus, M.J., and Wells, T.M., 1999, Recognizing avulsion deposits in the ancient stratigraphical record, *in* Smith, N.D., and Rogers, J., eds., Fluvial Sedimentology VI: International Association of Sedimentologists, Special Publication, v. 28, p. 251-268.

Lahiri, S., 1996, Channel pattern as signature of neotectonic movements – a case study from Brahmaputra Valley in Assam: Photonirvachak, Journal of the Indian Society of Remote Sensing, v. 24, p. 265-272.

Lahiri, S., and Sinha, R., 2012, Tectonic controls on the morphodynamics of the Brahmaputra River system in the upper Assam valley, India: Geomorphology, v. 169-170, p. 74-85.

Latrubesse, E.M., 2008, Patterns of anabranching channels: The ultimate end-member adjustment of mega rivers: Geomorphology, v. 101, p. 130-145.

Latrubesse, E.M., 2015, Large rivers, megafans and other Quaternary avulsive fluvial systems: A potential “who’s who” in the geological record: Earth-Science Reviews, v. 146, p. 1-30., doi: 10.1016/j.earscirev2015.03.004.

Latrubesse, E.M., Cozzuol, M., da Silva-Caminha, S.A.F., Rigsby, C.A., Absy, M.L., and Jaramillo, C., 2010, The late Miocene paleogeography of the Amazon Basin and the evolution of the Amazon River system: Earth-Science Reviews, v. 99, p. 99-124.

Latrubesse, E.M., Stevaux, J.C., Cremon, E.H., May, J-H.,Tatumi, S.H., Hurtado, M.A., Bezada, M., and Argollo, J.B., 2012, Late Quaternary megafans, fans and fluvio-aeolian interactions in the Bolivian Chaco, tropical South America: Palaeogeography, Palaeoclimatology, Palaeoecology, v. 356-357, p. 75-88.

Lecce, S.A., 1990, The alluvial fan problem, *in* Rachocki, A.H., and Church, M., eds., 1990, Alluvial Fans: A Field Approach, Chichester, Wiley, p. 3-24.

Leeder, M.R., and Gawthorpe, R.L., 1987, Sedimentary models for extensional tilt-block/half-graben basins, *in* Coward, M.P., Dewey, J.F., and Hancock, P.L., eds., Continental extensional tectonics: Geological Society of London Special Publication 28, p. 139-152.

Leeder, M.R., and Mack., G.H., 2001, Lateral erosion ('toe-cutting') of alluvial fans by axial rivers: implications for basin analysis and architecture: Geological Society of London, Journal, v. 158, p. 885-893.

Leeder, M.R., Mack, G.H, Peakall, J., and Salyards, S.L., 1996, First quantitative test of alluvial stratigraphic models: Southern Rio Grande rift, New Mexico: Geology, v. 24, p. 87-90.

Leier, A.L., DeCelles, P.G., and Pelletier, J.D., 2005, Mountains, monsoons, and megafans: Geology, v. 33, p. 289-292.

Leopold, L.B., Wolman, M.G., and Miller, J.P., 1964, Fluvial Processes in Geomorphology: San Francisco, Freeman, 503p.

Lesh, M.E., and Ridgeway, K.D., 2007, Geomorphic evidence of active transpressional deformation in the Tanana foreland basin, south-central Alaska, *in* Ridgeway, K.D., Trop, J.M., Glen, J.M.G., and O'Neill, J.M., eds., Tectonic Growth of a Collisional Continental Margin: Crustal Evolution of Southern Alaska: Geological Society of America, Special Paper 431, p. 573-592, DOI: 10.1130/2007.243(22).

Lettis, W.R., 1988, Quaternary geology of the northern San Joaquin Valley, *in* Graham, S.A., ed., Studies of the Geology of the San Joaquin Basin: SEPM, Pacific Section, v. 60, p. 333-351.

Levey, R.A., 1978, Bedform distribution and internal stratification of coarse-grained point bars, upper Congaree River, S.C., *in* Miall, A.D., ed., Fluvial Sedimentology: Canadian Society of Petroleum Geologists, Memoir 5, p. 105-127.

Lewin, J., and Ashworth, P.J, 2014, Defining large river channel patterns: alluvial exchange and plurality: Geomorphology, v. 215, p. 83-98, doi: 10.1016/j.geomorph.2013.02.024.

Li, F., Pan, G., Tang, C., Zhang, Q., and Yu, J., 2007, Recharge source and hydrogeochemical evolution of shallow groundwater in a complex alluvial fan system, southwest of North China Plain: Environmental Geology, v. 55, p. 1109-1122, doi: 10.1007/s00254-007-1059-1.

Mack, G.H., and Seager, W.R., 1990, Tectonic controls on facies distribution of the Camp Rice and Palomas Formations (Pliocene-Pleistocene) in the southern Rio Grande rift: Geological Society of America Bulletin, v. 102, p. 45-53.

Mack, G.H., Love, D.W., and Seager, W.R., 1997, Spillover models for axial rivers in regions of continental extension: the Rio Mimbres and Rio Grande in the southern Rio Grande Rift, U.S.A.: Sedimentology, v. 44, p. 637-652.

Mack, G.H., Seager, W.R., and Leeder, M.R., 2003, Synclinal-horst basins: examples from the southern Rio Grande Rift and southern transition zone of southwestern New Mexico, U.S.A.: Basin Research, v. 15, p. 365-377.

Mack, G.H., Seager, W.R., Leeder, M.R., Perez-Arlucea, M., and Salyardes, S.L., 2006, Pliocene and Quaternary history of the Rio Grande, the axial river of the southern Rio Grande rift, New Mexico, USA: Earth-Science Reviews, v. 79, p. 141-162.

Mack, G.H., Leeder, M.R., and Carothers-Durr, M., 2008, Modern flood deposition, erosion, and fan-channel avulsion on the semi-arid Red Canyon and Palomas Canyon alluvial fans in the southern Rio Grande Rift, New Mexico, U.S.A.: Journal of Sedimentary Research, v. 78, p. 432-442, DOI: 10.2110/jsr.2008.050.

Makaske, B., 2001, Anastomosing rivers: a review of their classification, origin and sedimentary products: Earth-Science Reviews, v. 53, p. 149-196.

Makaske, B., Berendsen, H.J.A., and Van Ree, M.H.M., 2007, Middle Holocene avulsion-belt deposits in the central Rhine-Meuse Delta, the Netherlands: Journal of Sedimentary Research, v. 77, p. 110-123, DOI: 10.2110/jsr.2007.004.

Makaske, B., Smith, D.G., and Berendsen, H.J.A., 2002, Avulsions, channel evolution and floodplain sedimentation rates of the anastomosing upper Columbia River, British Columbia, Canada: Sedimentology, v. 49, p. 1049-1071.

Makaske, B., Maathuis, B.H.P., Padovani, C.R., Stolker, C., Mosselman, E., and Jongman, R.H.G., 2012, Upstream and downstream controls of recent avulsions on the Taquari megafan, Pantanal, south-western Brazil: Earth Surface Processes and Landforms, v. 37, p. 1313-1326, DOI: 10.1002/esp.3278.

Marchand, D.E., 1977, The Cenozoic history of the San Joaquin Valley and the adjacent Sierra Nevada as inferred from the geology and soils of the eastern San Joaquin Valley, *in* Singer, M.J., ed., Soil Development, Geomorphology, and Cenozoic History of the Northeastern San Joaquin Valley and Adjacent Areas, California: University of California Press. Guidebook for Joint Field Session, Soil Science Society of America and Geological Society of America, p. 39-50.

Marchand, D.E., and Allwardt, A., 1981, Late Cenozoic Stratigraphic Units, Northeastern San Joaquin Valley, California: U.S., Geological Survey, Bulletin 1470, 70p.

May, J-H., 2011, The Rio Parapeti: Holocene megafan formation in the southernmost Amazon Basin: Geographica Helvetica, v. 66, p. 193-201.

McCarthy, T.S., 2006, Groundwater in the wetlands of the Okavango Delta, Botswana, and its contribution to the structure and function of the ecosystem: Journal of Hydrology, v. 320, p. 264-282.

McCarthy, T.S., and Cadle, A.B., 1995, Alluvial fans and their natural distinction from rivers based on morphology, hydraulic processes, sedimentary processes, and facies assemblages – Discussion: Journal of Sedimentary Research, v. A65, p. 581-583.

McCarthy, T.S., and Ellery, W.N., 1995, Sedimentation on the distal reaches of the Okavango fan, Botswana, and its bearing on calcrete and silcrete (ganister) formation: journal of Sedimentary Research, v. A65, p. 77-90.

McCarthy, T.S., Stanistreet, I.G., Cairncross, B., Ellery, W.N., Ellery, K., Oelofse, R., and Grobicki, T.S.A., 1988, Incremental aggradation of the Okavango Delta-fan, Botswana: Geomorphology, v., 1, p. 267-278.

McCarthy, T.S., Stanistreet, I.G., and Cairncross, B., 1991, The sedimentary dynamics of active fluvial channels on the Okavango fan, Botswana: Sedimentology, v. 38, p. 471-487.

McCarthy, T.S., Ellery, W.N., and Stanistreet, I.G., 1992, Avulsion mechanisms on the Okavango fan, Botswana: the control of fa fluvial system by vegetation: Sedimentology, v. 38, p. 779-795.

McCarthy, T.S., Ellery, W.N., and Ellery, K, 1993, Vegetation-induced, subsurface precipitation of carbonate as an aggradational process in the permanent swamps of the Okavango (delta) fan, Botswana: Chemical Geology, v. 107, p. 111-131.

McCarthy, T.S., Smith, N.D., Ellery, W.N., and Gumbricht, T., 2002, The Okavango Delta-semiarid alluvial-fan sedimentation related to incipient rifting, *in* Renaut, R.W., and Ashley, G.M., eds., Sedimentation in Continental Rifts, SEPM (Society for Sedimentary Geology) Special Publication 73, p. 179-193.

Miall, A.D., 1996, The Geology of Fluvial Deposits: Sedimentary Facies, Basin Analysis and Petroleum Geology: Berlin, Springer, 592p.

Miall, A.D., 2000, Principles of Sedimentary Basin Analysis, 3rd Updated and Enlarged Edition: Berlin, Springer, 616p.

Miall, A.D., 2010, Alluvial Deposits, *in* James, N.P. and Dalrymple, R.W., eds., Facies Models 4, Geological Association of Canada, GACGT6, St. John's, NL, Canada, 586p.

Milzow, C., Kgotlhang, L., Bauer-Gottwein, P., Meier, P., and Kinzelbach, W., 2009, Regional review: the hydrology of the Okavango Delta, Botswana – process data and modeling: Hydrogeology Journal, v. 17, p. 1297-1328.

Mohindra, R., Parkash, B., and Prasad, J., 1992, Historical geomorphology and pedology of the Gandak megafan, Middle Gangetic plains, India: Earth Surface Processes and Landforms, v. 17, p. 643-662.

Mohrig, D., Heller, P.L., Paola, C., and Lyons, W.J., 2000, Interpreting avulsion process from ancient alluvial sequences: Guadalope-Matarranya system (northern Spain) and Wasatch Formation (western Colorado): GSA Bulletin, v. 112, p. 1787-1803.

Moore, A.E., Cotterill, F.P.D., Main, M.P.L., and Williams, H.B., 2007, The Zambezi River, *in* Gupta, A., ed., Large Rivers: Geomorphology and Management: West Sussex, UK, John Wiley & Sons, Ltd., p. 311-332.

Munévar, A., and Mariño, M.A., 1999, Modeling analysis of ground water recharge potential on alluvial fans using limited data: Groundwater, v. 37, p. 649-659.

Nanson, G.C., 1980, Point bar and floodplain formation of the meandering Beatton River, northeastern British Columbia, Canada: Sedimentology, v. 27, p. 3-29.

Neuendorf, K.K.E., Mehl, J.P., Jr., and Jackson, J.A., 2005. Glossary of Geology (5th Edition), American Geological Institute, Alexandria, Virginia, 779p.

Nichols, G.J., and Fisher, J.A., 2007, Processes, facies, and architecture of fluvial distributary system deposits: Sedimentary Geology, v. 195, p. 75-90.

Nyburg, B., and Howell, J.A., 2015, Is the present the key to the past? A global characterization of modern sedimentary basins: Geology, v. 43, p. 643-646, doi: 10.1130/G36669.1.

O'Callaghan, J. F. and D. M. Mark, 1984. The Extraction of Drainage Networks from Digital Elevation Data: Computer Vision, Graphics and Image Processing, v. 28, p. 328-344.

Orfeo, O., and Stevaux, J., 2002, Hydraulic and morphological characteristics of middle and upper reaches of the Paraná River (Argentina and Brazil): Geomorphology, v. 44, p. 309-322.

Owen, A., Jupp, P.E., Nichols, G.J., Hartley, A.J., Weissmann, G.S., and Sadykova, D., 2015a, Statistical estimation of the position of an apex: Application to the Geologic record: Journal of Sedimentary Research, v. 85, p.142-152.

Owen, A., Nichols, G.J., Hartley, A.J., Weissmann, G.S., and Scuderi, L.A. 2015b, Quantification of a distributive fluvial system; The salt Wash DFS of the Morrison Formation, SW USA: Journal of Sedimentary Research, v. 85, p. 544-561.

Paira, A.R., and Drago, E.C., 2007, 3. Origin, evolution, and types of floodplain water bodies, *in* Iriondo, M.H., Paggi, J.C., and Parma, M.J., eds., The Middle Paraná River, Limnology of a subtropical wetland, Springer, Berlin, p. 53-81.

Pelletier, J., 2008, Quantitative Modeling of Earth Surface Processes, Cambridge, Cambridge University Press, 295p.

Pérez-Arlucea, M., and Smith, N.D., 1999, Depositional patterns following the 1870s avulsion of the Saskatchewan River (Cumberland Marshes), Saskatchewan, Canada: Journal of Sedimentary Research, v. 69, p. 62-73.

Rachocki, A., and Church, M.A., eds., 1990, Alluvial Fans: A Field Approach, Chichester, Wiley, 391 p.

Ramberg, L., Wolski, P., and Krah, M., 2006, Water balance and infiltration in a seasonal floodplain in the Okavango Delta, Botswana: Wetlands, v. 26, p. 677-690.

Rao, K.L., 1975, India's Water Wealth: Its Assessment, Uses, and Projections. Bombay, Orient Longman, 255p.

Reading, H.G., and Levell, B.K., 1996, Controls on the sedimentary rock record, *in* Reading, H.G., ed., Sedimentary Environments: Processes, Facies and Stratigraphy, 3rd Edition, Malden, MA, Wiley-Blackwell, p. 5-36.

Regard, V., Lagnous, R., Espurt, N., Darrozes, J., Baby, P., Roddaz, M., Calderon, Y., and Hermoza, W., 2009, Geomorphic evidence for recent uplift of the Fitzcarrald Arch (Peru): a response to the Nazca Ridge subduction: Geomorphology, v. 107, p. 107–117.

Reinfelds, I., and Bishop, P., 1998, Palaeohydrology, palaeodischarges and palaeochannel dimensions: research strategies for meandering alluvial rivers, *in* Benito, G., Baker, V.R., and Gregory, K.J., eds., Palaeohydrology and Environmental Change: Chichester, U.K., John Wiley & Sons, p. 27-42.

Reiser, R., Podgorski, J.E., Schmelzbach, C., Horstmeyer, H., Green, A.G., Kalscheuer, T., Maurer, H., Kinzelbach, W.K.H., Tshoso, G., and Ntibinyane, O., 2014, Constraining helicopter electromagnetic models of the Okavango Delta with seismic-refraction and seismic-reflection data: Geophysics, v. 79, p. B123-B134, DOI: 10.1190/GEO2013-0278.1.

Richards, K., Chandra, S., and Friend, P., 1993, Avulsive channel systems: characteristics and examples, *in* Best, J.L., and Bristow, C.S., eds., Braided Rivers, Geological Society Special Publication 75, p. 195-203.

Roy, N.G., Sinha, R., and Gibling, M.R., 2012, Aggradation, incision and interfluve flooding in the Ganga Valley over the past 100,000 years: Testing the influence of monsoon precipitation: Palaeogeography, Palaeoclimatology, Palaeoecology, v. 356-357, p. 38-53, DOI: 10.1016/j.palaeo.2011.08.012.

Roy, S.S., 1981, Alluvial fan model for the Himalayan piedmont deposits: Journal of the Geological Society of India, v. 22, p. 164-174.
Sambrook Smith, G.H., Best, J.L., Ashworth, P.J., Fielding, C.R., Goodbred, S.L., and Prokocki, E.W., 2010, Fluvial form in modern continental sedimentary basins: Distributive fluvial systems: COMMENT: Geology Forum, v. 38, e230, doi: 10.1130/G31507C.1.

Sarma, J.N., 2005, Fluvial process and morphology of the Brahmaputra River in Assam, India: Geomorphology, v. 70, p. 226-256.

Sarma, J.N., and Phukan, M.K., 2006, Bank erosion and bankline migration of the Brhamaputra River in Assam during the Twentieth Century: Journal, Geological Society of India, v. 68, p. 1023-1036.

Schumann, R.R., 1989, Morphology of Red Creek, Wyoming, an arid-region anastomosing channel system: Earth Surface Processes and Landforms, v. 14, p. 277-288.

Schumm, S.A., 1977, The Fluvial System: New York, John Wiley & Sons, 338p.

Schumm, S.A., Mosley, M.P., and Weaver, W.E., 1987, Experimental Fluvial Geomorphology: New York, John Wiley & Sons, 413p.

Schumm, S.A., Erskine, W.D., and Tilleard, J.W., 1996, Morphology, hydrology, and evolution of the anastomosing Ovens and King Rivers, Victoria, Australia: Geological Society of America, Bulletin, v. 108, p. 1212-1224.
Shaw, P.A., and Nash, D.J., 1998, Dual mechanisms for the formation of fluvial silcretes in the distal reaches of the Okavango Delta fan, Botswana: Earth Surface Processes and Landforms, v. 23, p. 705-714.

Shukla, U.K., Singh, I.B., Sharma, M., and Sharma, S., 2001, A model of alluvial megafan sedimentation: Ganga Megafan: Sedimentary Geology, v. 144, p. 243-262.

Singh, H., Parkash, B., and Gohain, K., 1993, Facies analysis of the Kosi megafan deposits: Sedimentary Geology, v. 85, p. 87-113.

Singh, I.B., 2007, The Ganga River, *in* Gupta, A., ed., Large Rivers: Geomorphology and Management: Chichester, John Wiley & Sons, Ltd., p. 347-371.

Singh, S., Parkash, B., Rao, M.S., Arora, M., and Bhosle, B., 2006, Geomorphology, pedology and sedimentology of the Deoha/Ganga-Ghaghara Interfluve, Upper Gangetic Plains (Himalayan Foreland Basin) – extensional tectonic implications: Catena, v. 67, p. 183-203, DOI: 10.1016/j.catena.2006.03.013.

Singh, S.K., 2007, Erosion and weathering in the Brahmaputra River system, *in* Gupta, A., ed., Large Rivers: Geomorphology and Management: Chichester, John Wiley & Sons, Ltd., p. 373-393.

Sinha, R., 1996, Channel avulsion and floodplain structure in the Gandak-Kosi interfan, north Bihar plains, India: Zeitschrift für Geomorphologie, N.F., Supplementband 103, p. 249-268.

Sinha, R., 2009, The great avulsion of Kosi on 18 August 2008: Current Science, v. 97, p. 429-433.

Sinha, R., and Tandon, S.K., 2014, Indus-Ganga-Brahmaputra Plains: the alluvial landscape, *in* Kale, V.S., ed., Landscapes and Landforms of India, Springer, Dordrecht, p. 53-63.

Sinha, R., and Friend, P.F., 1994, River systems and their sediment flux, Indo-Gangetic plains, Northern Bihar, India: Sedimentology, v. 41, p. 825-845.

Sinha, R., Gibling, M.R., Jain, V., and Tandon, S.K., 2005, Sedimentology and avulsion patterns of the anabranching Baghmati River in the Himalayan foreland basin, *in* Blum, M.D., Marriott, S.B., and Leclair, S.F., eds., Fluvial Sedimentology VII: International Association of Sedimentologists, Special Publication 35, p. 181-196.

Sinha, R., Kumar, R., Sinha, S., Tandon, S.K., and Gibling, M.R., 2007, Late Cenozoic fluvial successions in northern and western India: an overview and synthesis: Quaternary Science Reviews, v. 26, p. 2801-2822, doi: 10.1016/j.quascirev.2007.07.018.

Sinha, R., Ahmad, J., Gaurav, K., and Morin, G., 2014, Shallow subsurface stratigraphy and alluvial architecture of the Kosi and Gandak megafans in the Himalayan foreland basin, India: Sedimentary Geology, v. 301, p. 133-149, DOI: 10.1016/j.sedgeo.2013.06.008.

Slingerland, R., and Smith, N.D., 1998, Necessary conditions for a meandering-river avulsion: Geology, v. 26, p. 435-438.

Slingerland, R., and Smith, N.D., 2004, River avulsions and their deposits, Annual Review of Earth and Planetary Science, v. 32, p. 257-285, doi: 10.1146/annurev.earth.32.101802.120201.

Smith, N.D., Cross, T.A., Dufficy, J.P., and Clough, S.R., 1989, Anatomy of an avulsion: Sedimentology, v. 36, p. 1-23.

Smith, N.D., Slingerland, R.L., Perez-Arlucea, M., and Morozova, G.S., 1998, The 1870's avulsion of the Saskatchewan River: Canadian Journal of Earth Sciences, v. 35, p. 453-466.

Stanistreet, I.G., and McCarthy, T.S., 1993, The Okavango Fan and the classification of subaerial fan systems: Sedimentary Geology, v. 85, p. 115-133.

Stanistreet, I.G., Cairncross, B., and McCarthy, T.S., 1993, Low sinuosity and meandering bedload rivers of the Okavango Fan: channel confinement by vegetated levees without fine sediment: Sedimentary Geology, v. 85, p. 135-156.

Stokes, M., and Cunha, P.P., 2012, Techniques for analyzing Late Cenozoic river terrace sequences: Geomorphology, v. 165-166, p. 1-6.

Stouthamer, E., 2001, Sedimentary products of avulsions in the Holocene Rhine-Meuse Delta, The Netherlands: Sedimentary Geology, v. 145, p. 73-92.

Tandon, S.K., and Sinha, R., 2007, Geology of large rivers, *in* Gupta, A., ed., Large Rivers: Geomorphology and Management. John Wiley & Sons, Ltd, Chichester, p. 7-28.

Tandon, S.K., Gibling, M.R., Sinha, R., Singh, V., Ghazanfari, P., Dasgupta, A., Jain, M., and Jain, V., 2006, Alluvial valleys of the Ganga Plains, India, timing and causes of incision, *in* Dalrymple, R.W., Leckie, D.A., Tillman, R.W., eds., Incised valleys in time and space, SEPM Society for Sedimentary Geology, Special Publication 85, p. 15-35.

Tarboton, D. G., 1997. A New Method for the Determination of Flow Directions and Contributing Areas in Grid Digital Elevation Models: Water Resources Research, v. 33, p. 309-319.

Tooth, S., and McCarthy, T.S., 2004, Controls on the transition from meandering to straight channels in the wetlands of the Okavango Delta, Botswana: Earth Surface Processes and Landforms, v. 29, p. 1627-1649.

Törnqvist, T.E., and Bridge, J., 2002, Spatial variation of overbank aggradation rate and its influence on avulsion frequency: Sedimentology, v. 49, p. 891-905.

Weissmann, G.S., Carle, S.F., and Fogg, G.E., 1999, Three-dimensional hydrofacies modeling based on soil surveys and transition probability geostatistics: Water Resources Research, v. 35, p. 1761-1770.

Weissmann, G.S., Mount, J.F., and Fogg, G.E., 2002, Glacially driven cycles in accommodation space and sequence stratigraphy of a stream-dominated alluvial fan, Central Valley, California: Journal of Sedimentary Research, v. 72, p. 240-251.

Weissmann, G.S., Zhang, Y., Fogg, G.E., and Mount, J.F., 2004, Influence of incised-valley-fill deposits on hydrogeology of a stream-dominated alluvial fan, *in* Bridge, J.S., and Hyndman, D.W., eds., Aquifer Characterization, SEPM (Society for Sedimentary Geology), Special Publication 80, p. 15-28.

Weissmann, G.S., Bennett, G.L., and Lansdale, A.L., 2005, Factors controlling sequence development on Quaternary fluvial fans, San Joaquin Basin, California, USA, *in* Harvey, A.M., Mather, A.E., and Stokes, M.

(eds), Alluvial Fans: Geomorphology, sedimentology, dynamics: Geological Society of London, Special Publication 251, p. 169-186.

Weissmann, G.S., Hartley, A.J., Nichols, G.J., Scuderi, L.A., Olson, M., Buehler, H., and Banteah, R., 2010, Fluvial form in modern continental sedimentary basins: distributive fluvial systems: Geology, v. 38, p. 39-42.

Weissmann, G.S., Hartley, A.J., Nichols, G.J., Scuderi, L.A., Olson, M., Buehler, H., and Massengill, L., 2011, Alluvial facies distributions in continental sedimentary basins – distributive fluvial systems, *in* North, C., Davidson, S., and Leleu, S., eds., Rivers to Rocks: SEPM (Society of Sedimentary Geology) Special Publication 97, p. 327-355.

Weissmann, G.S., Hartley, A.J., Scuderi, L.A., Nichols, G.J., Davidson, S.K., Owen, A., Atchley, S.C., Bhattacharyya, P., Chakraborty, T., Ghosh, P., Nordt, L.C., Michel, L., and Tabor, N.J., 2013, Prograding distributive fluvial systems – geomorphic models and ancient examples, *in*Driese, S.G., and Nordt, L.C., eds., New Frontiers in Paleopedology and Terrestrial Paleoclimatology, SEPM (Society for Sedimentary Geology) Special Publication 104, p. 131-147, DOI: 10.2110/sepmsp.104.16.

Wells, N.A., and Dorr, J.A., Jr., 1987, Shifting of the Kosi River, northern India: Geology, v. 15, p. 204-207.

Whipple, K.X., and Trayler, C.R., 1996, Tectonic control of fan size: the importance of spatially variable subsidence rates: Basin Research, v. 8, p. 351-366.

Wilkinson, M.J., Marshall, L.G., and Lundberg, J.G., 2006, River behavior on megafans and potential influences on diversification and distribution of aquatic organisms: Journal of South American Earth Sciences, v. 21, p. 151-172, DOI: 10.1016/j.jsames.2005.08.002.

Wilkinson, M.J., Marshall, L.G., Lundberg, J.G., and Kreslavsky, M.H., 2010, Megafan environments in northern South America and their impact on Amazon Neogene aquatic ecosystems, *in* Hoorn, C., and Wesselingh, F.P., Amazonia, Landscape and Species Evolution, 1st edition, Blackwell Publishing, p. 162-184.

Wolski, P., and Murray-Hudson, M., 2006, Flooding dynamics in a large low-gradient alluvial fan, the Okavango Delta, Botswana, from analysis and interpretation of a 30-year hydrometric record: Hydrology and Earth System Science, v. 10, p. 127-137.

Wolski, P., and Savenije, H.H.G., 2006, Dynamics of floodplain-island groundwater flow in the Okavango Delta, Botswana: Journal of Hydrology, v. 320, p. 283-301.

Zak, M.R., and Cabido, M., 2002, Spatial patterns of the Chaco vegetation of central Argentina: Integration of remote sensing and phytosociology: Applied Vegetation Science, v. 5, p. 213-226.

Zani, H., Assine, M.L., and McGlue, M.M., 2012, Remote sensing analysis of depositional landforms in alluvial settings: method development and application to the Taquari megafan, Pantanal (Brazil): Geomorphology, v. 161-162, p. 82-92, doi: 10.1016/j.geomorph.2012.04.003.

Figure Captions:

Fig. 1. World map with outlines of the 10 sedimentary basins where geomorphic elements were delineated. 1 – Himalayan foreland basin, India; 2 – Andean forelandbasin in the Chaco Plain, South America; 3 – Tanana foreland basin, Alaska, USA; 4 – Okavango rift basin, Botswana and Namibia; 5 – Rio Grande rift basin, New Mexico, USA; 6 – Pantanal basin, Brazil; 7 – Southern Death Valley, California, USA; 8 – Tarim basin, China; 9 – transtensional basin, Mongolia; 10 – San Joaquin basin, California, USA.

Fig. 2.Examples of geomorphic elements in sedimentary basins. (A) A large DFS – the Magdalena River DFS, Columbia; (B)small DFS entering the Brahmaputra Valley, Himalayan foreland, Assam, India; (C)bajada (coalesced DFS), Mongolia; (D)incised DFS – Taquari DFS, Brazil; (E)axial tributary system – Paraná River, Argentina; (F)interfan tributary system between the Kosi and Baghmati DFS, India; (G)eolian geomorphic element of the Tarim basin, China; (H)lacustrine geomorphic element, Ayakkum Lake, China.

Fig. 3. Schematic diagram showing position of geomorphic elements in a sedimentary basin. The scale of the elements is dependent on the scale of the sedimentary basin, where larger basins typically hold larger geomorphic elements. If the sedimentary basin is relatively small (<30 km across), the largest DFS will typically be <30 km long and would not be classified as large DFS or megafans, but the hierarchical pattern of different DFS sizes will still be present. Modified from DeCelles and Cavazza (1999).

Fig.4. Images of the Himalayan foreland basins, India. (A) A mosaic of Landsat images with the basin outlined in yellow. (B) Delineated geomorphic elements of the basin.

Fig. 5. Images of the Andean foreland basin, Chaco Plain, South America. (A) A mosaic of Landsat images with the basin outlined in yellow. (B) Delineated geomorphic elements of the basin.

Fig. 6. Images of the Tanana foreland basin, Alaska, USA. (A) A mosaic of Landsat images with the basin outlined in yellow. (B) Delineated geomorphic elements of the basin.

Fig.7. Exposure of coarse-grained deposits from a small inter-megafan DFS located west of the Tista megafan, India.

Fig.8.(A) Overview of the inter-megafan tributary system between the Kosi and Tista megafans (large DFS), India. Where the Mahananda River exits this interfan area, it forms a large DFS, filling accommodation between the distal toes of the Kosi and Tista DFS. (B)Inset image is of the Mahananda River near the apex of its DFS.(C) Close-up image of the diffuse transition from the distributive smaller DFS to the inter-megafan tributary system.

Fig.9.(A)The incised Ganga DFS showing paleochannels radiating outward from the apex (shown in yellow) and distributive paleochannels in more distal positions (shown in dark blue). The Ganga incised valley is outlined in black and area of image in (C) is shown by white dashed box. (B) A digital elevation model of the incised Ganga DFS area. (C) The proximal areas of the Ganga incised DFS showing detail of the radiating paleochannels that were described by Shukla et al. (2001).

Fig.10.DFS of the Brahmaputra Valley surrounding the axial Brahmaputra River. The Burhi Dihing DFS to the south has very different character than the small DFS that are entering the basin from the north.

Fig.11. Rivers entering the Brahmaputra Valley portion of the Himalayan foreland basin develop DFS that have braided river form. These rivers coalesce to form the axial Brahamaputra River on the left side

of this image. The DFS farthest to the left is formed wherethe Brahmaputra River enters the sedimentary basin.

Fig. 12.(A) Landsat mosaic of the upper Bermejo River DFS, with arrows showing the apex and the transition from low sinuosity to high sinuosity at ~140km location. (B) Graph of width (blue) vs. sinuosity (red) with distance down-DFS. (C) Graph of width (blue) vs. elevation (red) showing river profile with distance down-DFS. The equation for the trendline on elevation is shown.

Fig. 13.(A) The Paraguay River leaves the axial position of the Pantanal basin and enters the Chaco Plain, forming a large DFS before becoming the axial river to the south of this DFS. (B) The Paraná River enters the Chaco Plain from the east, forming a large DFS before it joins the Paraguay River to become the axial river in the Chaco Plain foreland.

Fig. 14.Images of the Okavango rift basin, Botswana and Namibia. (A) A mosaic of Landsat images with the basin outlined in yellow. (B) Delineated geomorphic elements of the basin.

Fig. 15. Images of the Rio Grande rift basin, New Mexico. (A) A mosaic of Landsat images with the basin outlined in yellow. (B) Delineated geomorphic elements of the basin.

Fig. 16. Landsat mosaic of the Tarim basin. The Hotan River crosses the western side of the basin, and paleochannels appear to form a large DFS as substrate under the dunes.

Fig. 17. Landsat image of the southern portion of Death Valley, California, USA, showing the axial Amargosa River DFS.

Fig. 18. Flooded area on the Taquari DFS is shown by black regions in this image. Notice how the water leaves the river and is sent onto the floodplain on the DFS surface, never returning to the main channel.

Fig. 19. A spring line (approximated by the dashed line) is observed on the Pilcomayo DFS where paleochannels below the spring line are filled with water (shown in black) and agriculture is present above the springline where soils are better drained.

Fig.20.The meanderbelt forms on the Taquari DFS. (A) The meanderbelt has an amalgamated form in the incised valley where avulsions are dominated by chute and neck cutoff avulsions. (B) The meanderbelt on the open fan is not amalgamated. Levees along this reach are shown in lighter blue color surrounding the main channel.

Fig.21.The Beni River DFS, Bolivia. (A) Landsat mosaic of the Beni DFS. (B) SRTM elevation of the Beni River DFS area showing incision of the distal channel belts through the Fitzcarrald Arch and the raised meanderbelts and alluvial ridges on the active DFS. (C) Close-up of the Beni River meanderbelt on its DFS, with an abandoned meanderbelt shown in yellow to the east of the modern meanderbelt.

Fig. 22. The Kosi DFS showing that the active channelbelt width decreases down-DFS, as identified by the presence of water (black in this image) and unvegetated or lightly vegetated bars (light colored in this image).

Fig. 23.(A)An elevation map(DEM) of the Amazon basin, derived from the SRTM dataset. (B) Curvature analysis of the basin elevations enhances the visualization of the dendritic pattern (e.g., erosional) that is present in this basin.

Table 1

Table 1

Aerial coverage of geomorphic elements in selected sedimentary basins

	Large DFS	Small DFS	Bajada / piedmont	Exposed interfluve on DFS	Incised valley in DFS	TOTAL DFS	Axial tributary	Interfan tributary	TOTAL TRIBUTARY	Lacustrine	Eolian	TOTAL	TOTAL FLUVIAL AREA
Himalayan Foreland													
Area (km^2)	94235	2587	84999	129509	42608	353938	25246	2325	27571	0	0	381509	381509
% basin	24.7	0.7	22.3	33.9	11.2	92.8	6.6	0.6	7.2	0	0		
% fluvial area	24.7	0.7	22.3	33.9	11.2	92.8	6.6	0.6	7.2				
Andean Foreland - Chaco Plain													
Area (km^2)	702791	7363	58421	0	0	768575	14467	1353	15820	0	0	784395	784395
% basin	89.6	0.9	7.4	0.0	0.0	98.0	1.8	0.2	2.0	0.0	0.0		
% fluvial area	89.6	0.9	7.4	0.0	0.0	98.0	1.8	0.2	2.0				
Tanana Foreland													
Area (km^2)	4961	131	576	0	0	5668	293	72	365	0	0	6033	6033
% basin	82.2	2.2	9.5	0.0	0.0	93.9	4.9	1.2	6.1	0.0	0.0		
% fluvial area	82.2	2.2	9.5	0.0	0.0	93.9	4.9	1.2	6.1				
Okavango Rift													
Area (km^2)	59862	150	1267	0	0	61279	605	0	605	3350	0	65234	61884
% basin	91.8	0.2	1.9	0.0	0.0	93.9	0.9	0.0	0.9	5.1	0.0		
% fluvial area	96.7	0.2	2.0	0.0	0.0	99.0	1.0	0.0	1.0				
Rio Grande Rift													
Area (km^2)	0	0	823	1725	170	2718	323	0	323	0	0	3041	3041
% basin	0	0	27.1	56.7	5.6	89.4	10.6	0	10.6	0	0		
% fluvial area	0	0	27.1	56.7	5.6	89.4	10.6	0	10.6				
Pantanal Basin													
Area (km^2)	27044	294	11434	64636	659	104067	4951	2568	7519	984	0	112570	111586

% basin	24.0	0.3	10.2	57.4	0.6	92.4	4.4	2.3	6.7	0.9	0.0		
% fluvial area	24.2	0.3	10.2	57.9	0.6	93.3	4.4	2.3	6.7				
Southern Death Valley													
Area (km^2)	153	684	123	0	0	960	27	5	32	58	0	1050	992
% basin	14.6	65.1	11.7	0	0	91.4	2.6	0.5	3	5.5	0		
% fluvial area	15.4	69	12.4	0	0	96.8	2.7	0.5	3.2				
Tarim Basin													
Area (km^2)	102427	12535	81537	0	0	196499	26547	0	26547	6060	291797	520903	223046
% basin	19.7	2.4	15.7	0	0	37.7	5.1	0	5.1	1.2	56		
% fluvial area	45.9	5.6	36.6	0	0	88.1	11.9	0	11.9	2.7	130.8		
Mongolia Basin (N4330E10270 from Weissmann et al. 2010)													
Area (km^2)	0	0	6742	0	0	6742	109	0	109	0	469	7320	6851
% basin	0	0	92.1	0	0	92.1	1.5	0	1.5	0	6.4		
% fluvial area	0	0	98.4	0	0	98.4	1.6	0	1.6				
San Joaquin Basin													
Area (km^2)	8255	0	5191	7669	369	21484	709	0	709	851	0	23044	22193
% basin	35.8	0	22.5	33.3	1.6	93.2	3.1	0	3.1	3.7	0		
% fluvial area	37.2	0	23.4	34.6	1.7	96.8	3.2	0	3.2				

Table 2

Table 2

DFS surface areas, drainage basin areas, and average DFS gradient for selected DFS in the Himalayan and Andean foreland basins

River name, apex latitude and longitude	DFS surface area (km^2)	Drainage basin area (km^2)	DFS average gradient
Himalayan Foreland Basin – Ganges Plain – Large DFS			
Ganga, 29.374˚N, 78.039˚E	56,664	23,136	0.0023[a]
Sarda and Ghaghra (combine near apex), 28.834˚N, 80.109˚E	79,518	18,260	0.00015
Rapti, 28.06˚N, 81.73˚E	10,585	6,011	0.00036
Gandak, 27.44˚N, 83.909˚E	26,757	85,709	0.00029[a]
Kosi, 26.53˚N, 86.938˚E	12,839	58,274	0.00056[a]
Tista, 26,69˚N, 88.407˚E	18,227	8,230	0.00022[a]
Son, 24.75˚N, 84.07˚E	8,361	65,930	0.00041[a]
Himalayan Foreland Basin – Ganges Plain – Large DFS in inter-megafan position			
Mechi, 26.78˚N, 88.19˚E	594	123	0.0045
Balan, 26.723˚N, 86.504˚E	1,279	125	0.0016
Kamla, 26.84˚N, 86.15˚E	3,954	1,545	0.00058
Bagmahti, 27.13˚N, 85.480˚E	3,954	1,545	0.00043
Himalayan Foreland Basin – Brahmaputra Valley – South Side DFS			
Noadihang, 27.49˚N, 96.22˚E	3219	2417	0.0036[a]
BurhiDihing, 27.25˚N, 95.416˚E	1816	3900	0.00081[a]
Dikhow, 26.80˚N, 94.81˚E	602	[b]	0.0011
Himalayan Foreland Basin – Brahmaputra Valley – North Side DFS			
Subanseri, 27.53˚N, 94.26˚E	1,147	26,139	0.0019[a]
JiyaDhol, 27.57˚N, 94.45˚E	408	290	0.0043
Sisi, 27.66˚N, 94.69˚E	185	192	0.0022
Simen, 27.73˚N, 94.86˚E	144	737	0.0030
Chaco Plain - Andean Foreland Basin – Large DFS (megafans)			
Rio Paraná, 27.482˚S, 57.034˚W	46,743	924,072	0.000065[a]
Rio Paraguay, 19.685˚S, 57.515˚W	12,042	374,749	0.000056[a]
Rio Grande, 18.91˚S, 63.402˚W	29,304	59,532	0.00056[a]
Rio Parapeti, 20.022˚S, 63.189˚W	79,146	7,453	0.0016[a]
Rio Pilcomayo, 21.552˚S, 63.011˚W	216,115	319,687	0.00036[a]
Rio Bermejo, 23.293˚S, 64.074˚W	83,475	52,956	0.00034[a]
Rio Salado, 25.108˚S, 64.16˚W	184,819	39,521	0.00077[a]
Chaco Plain - Andean Foreland Basin – Large DFS in inter-megafan position			
Rio Carapari/Itiyura, 22.208˚S, 63.612˚W	5,417	1,579	0.00244[a]
Rio Piray, 17.813˚S, 63.253˚W	6,001	2,453	0.0025
Unknown, 24.759˚S, 64.292˚W	3,080	942	0.0025
Unknown, 24.548˚S, 64.175˚W	1,226	677	0.0020
Unknown, 20.346˚S, 63.021˚W	1,266	1,488	0.0038
Unknown, 20.583˚S, 62.982˚W	1,154	536	0.00285
Unknown, 20.77˚S, 63.019˚W	1,698	298	0.00295

Unknown, 21.892˚S, 63.453˚W	1,281	560	0.0036

[a] Apex location and gradient from Hartley et al. (2010b).
[b]Drainage basin area not estimated.

Figure (Color) 1
Click here to download high resolution image

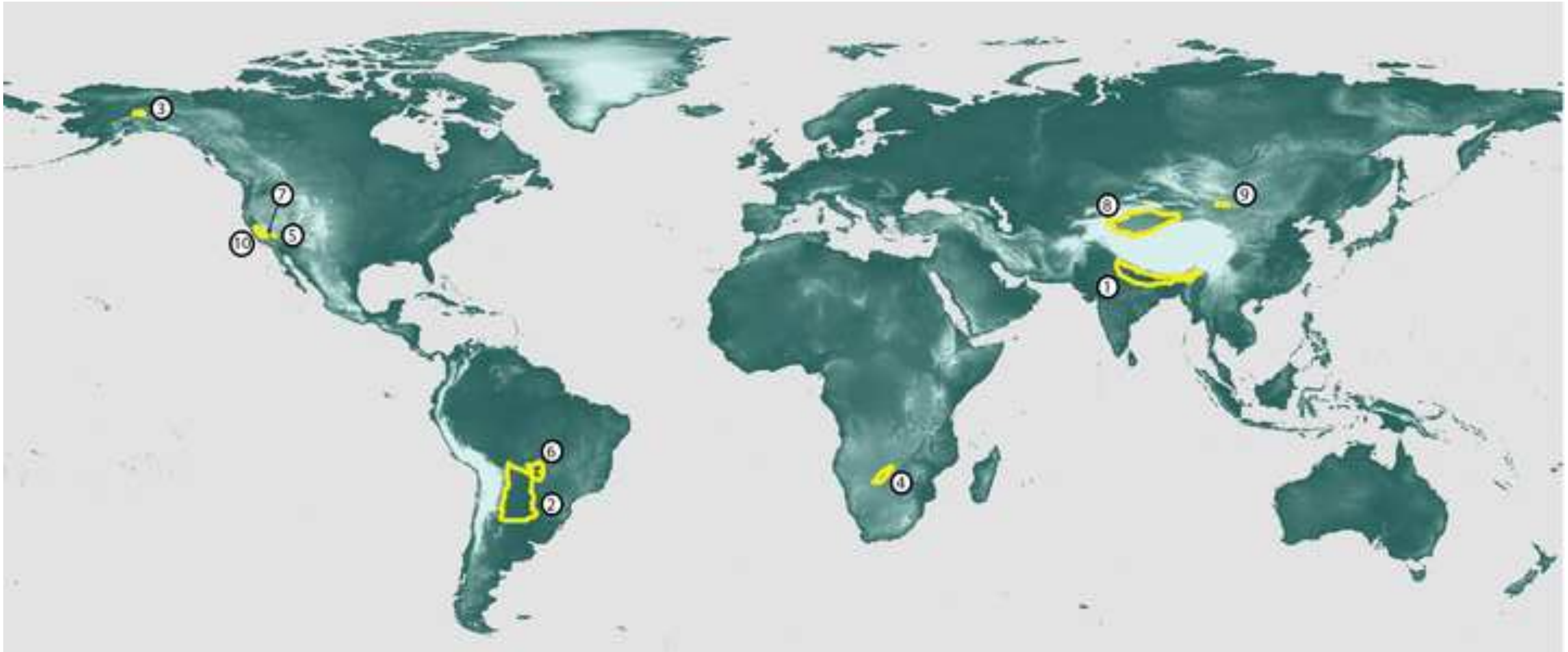

Figure (Color) 2 part 1

Click here to download high resolution image

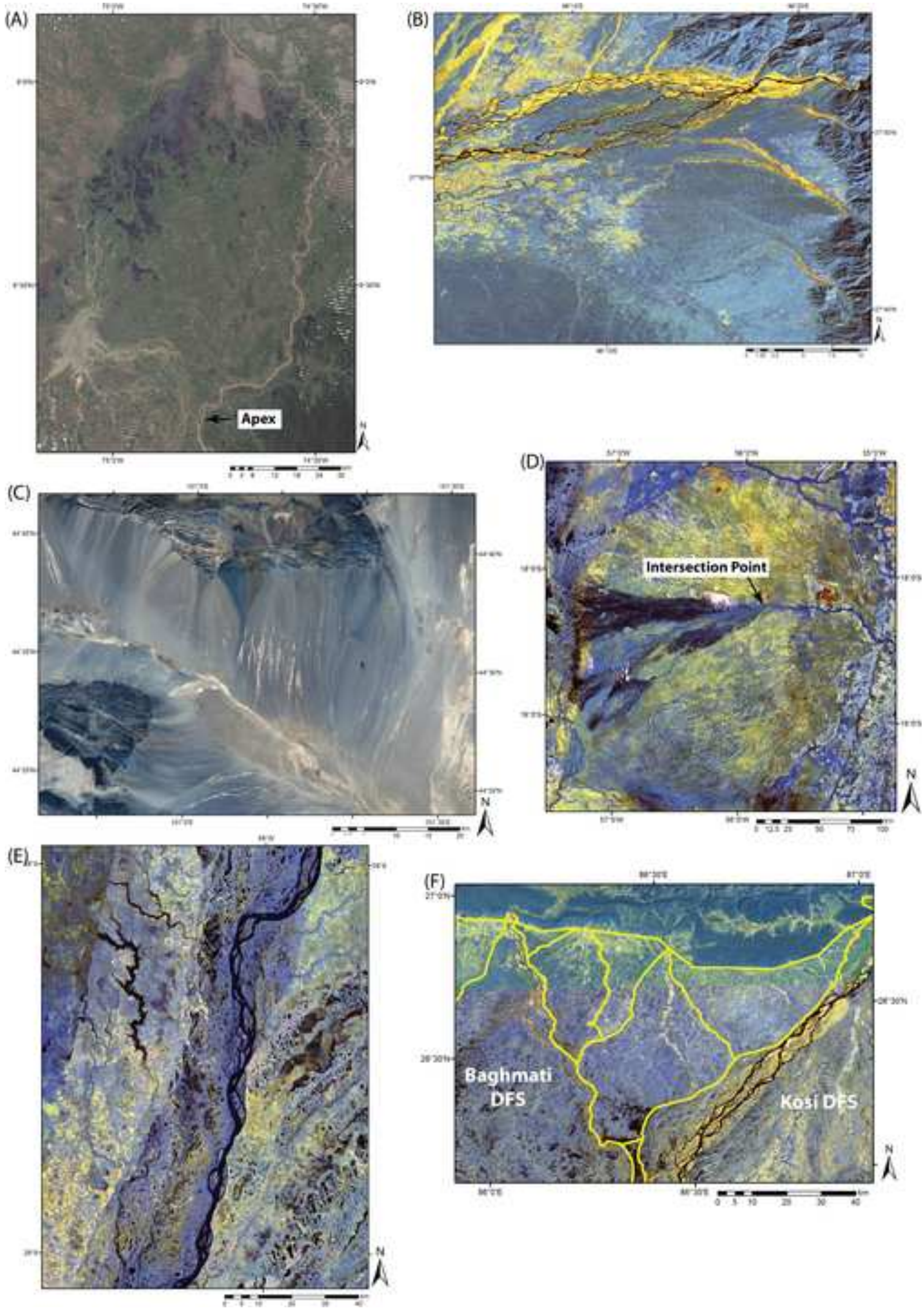

Figure (Color) 2 part 2
Click here to download high resolution image

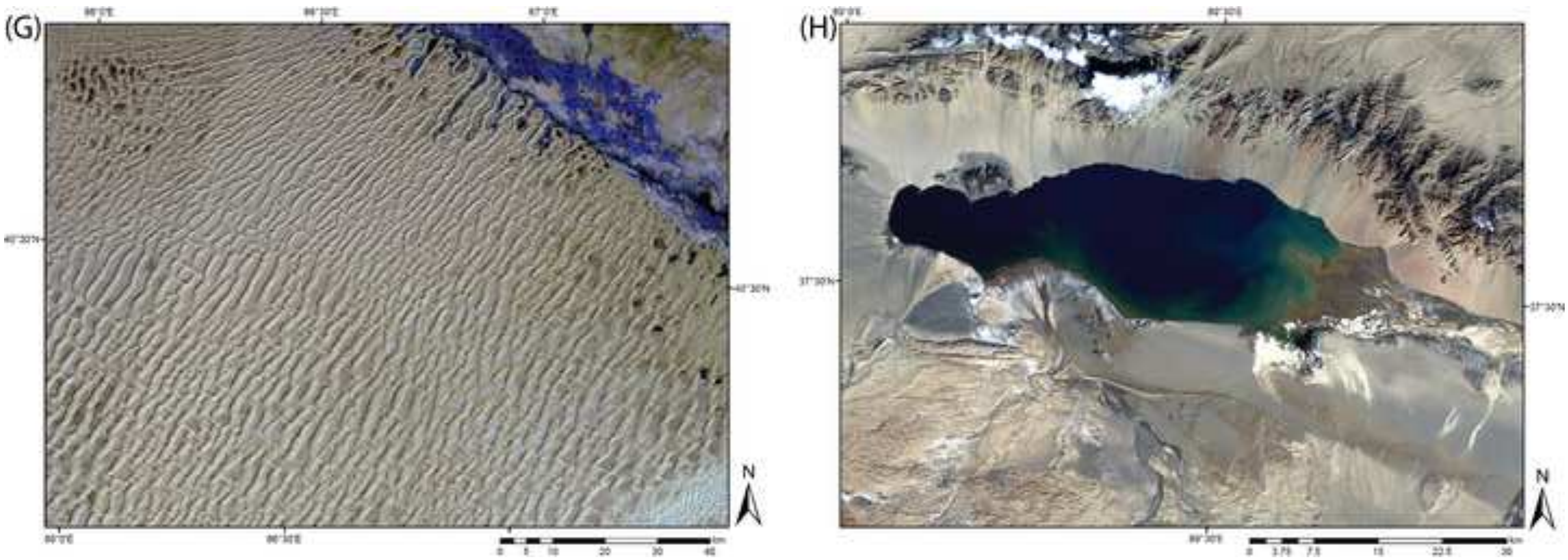

Figure (Color) 3
Click here to download high resolution image

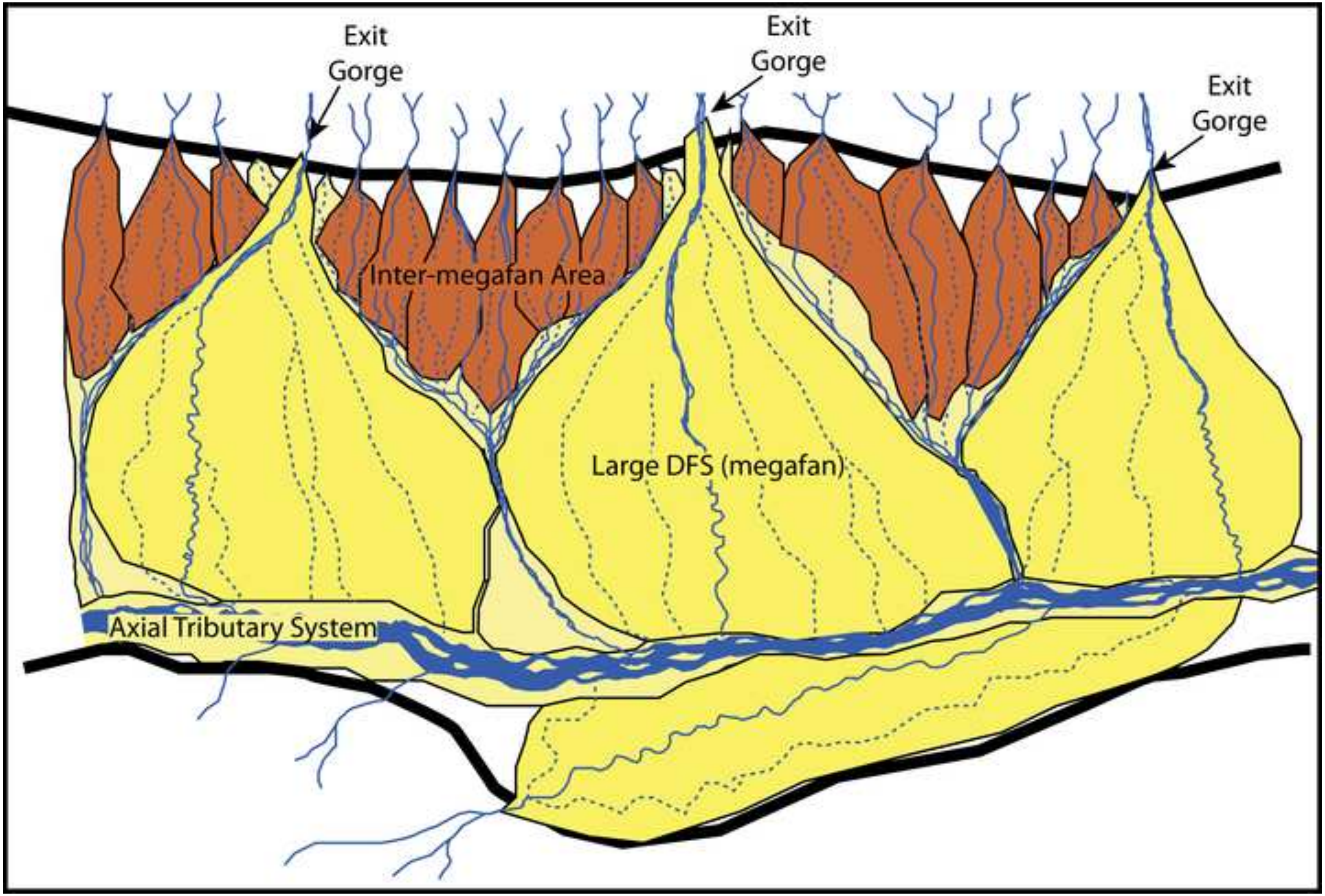

Figure (Color) 4
Click here to download high resolution image

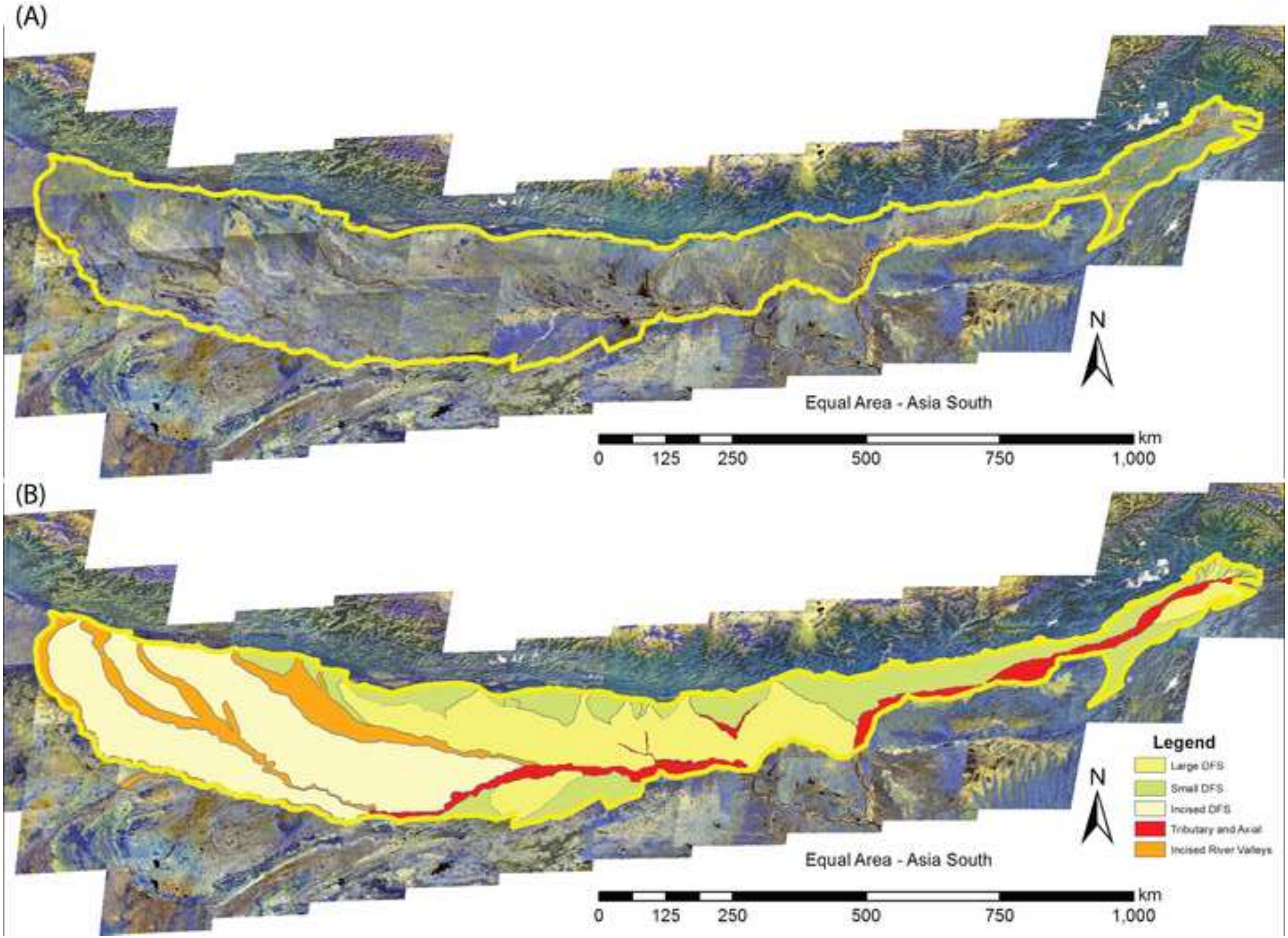

Figure (Color) 5
Click here to download high resolution image

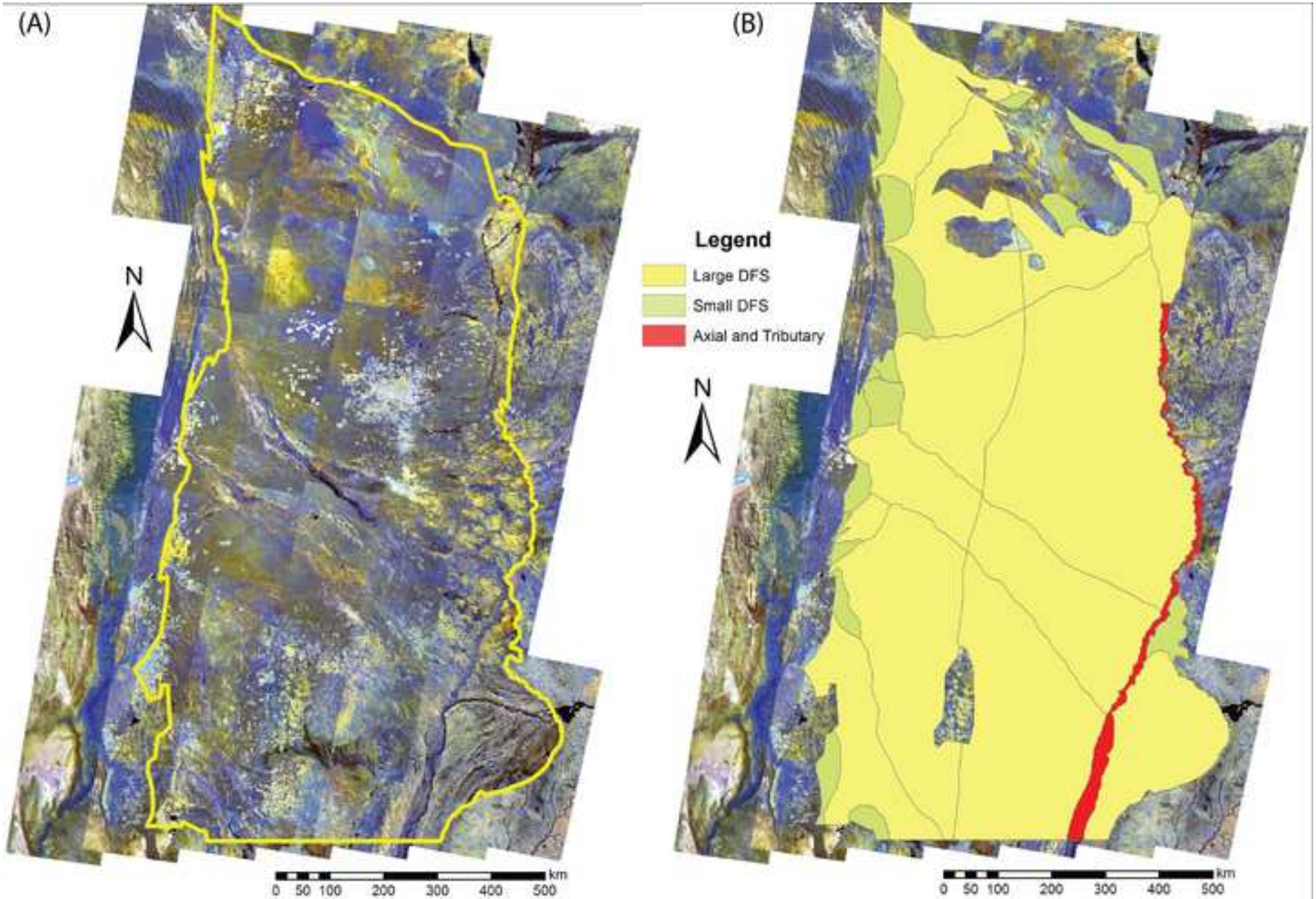

Figure (Color) 6
Click here to download high resolution image

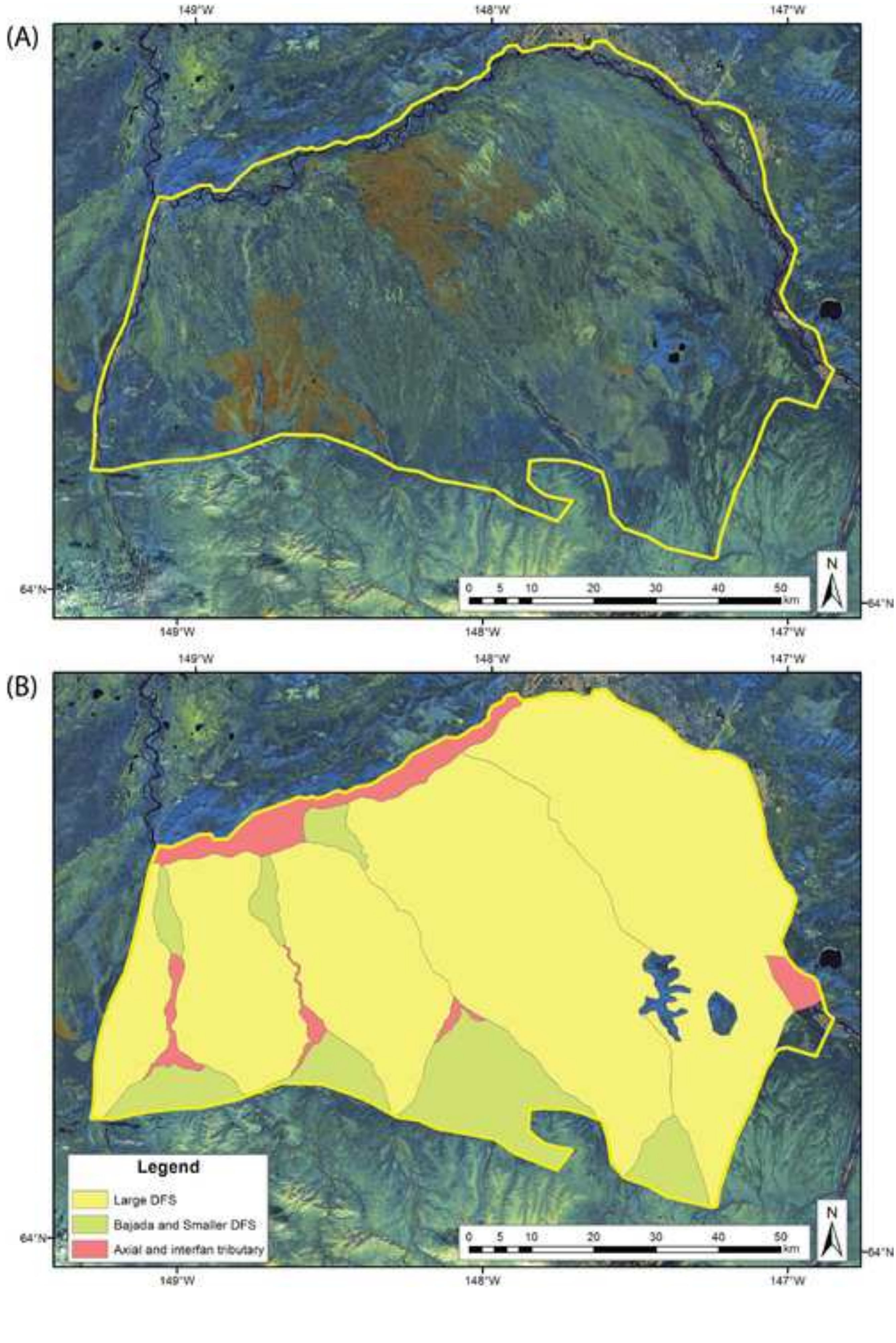

Figure (Color) 7
Click here to download high resolution image

Figure (Color) 8

Click here to download high resolution image

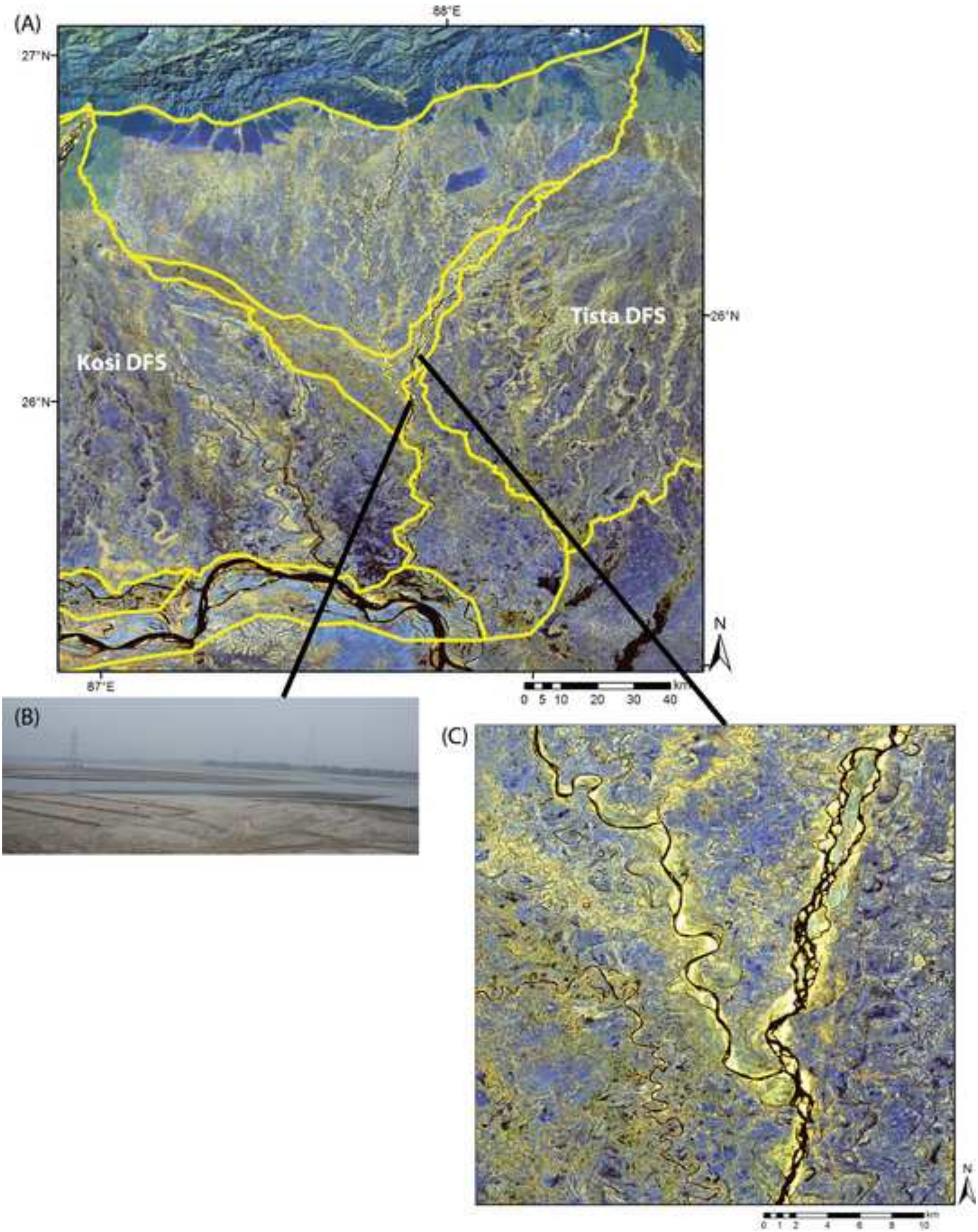

Figure (Color) 9
Click here to download high resolution image

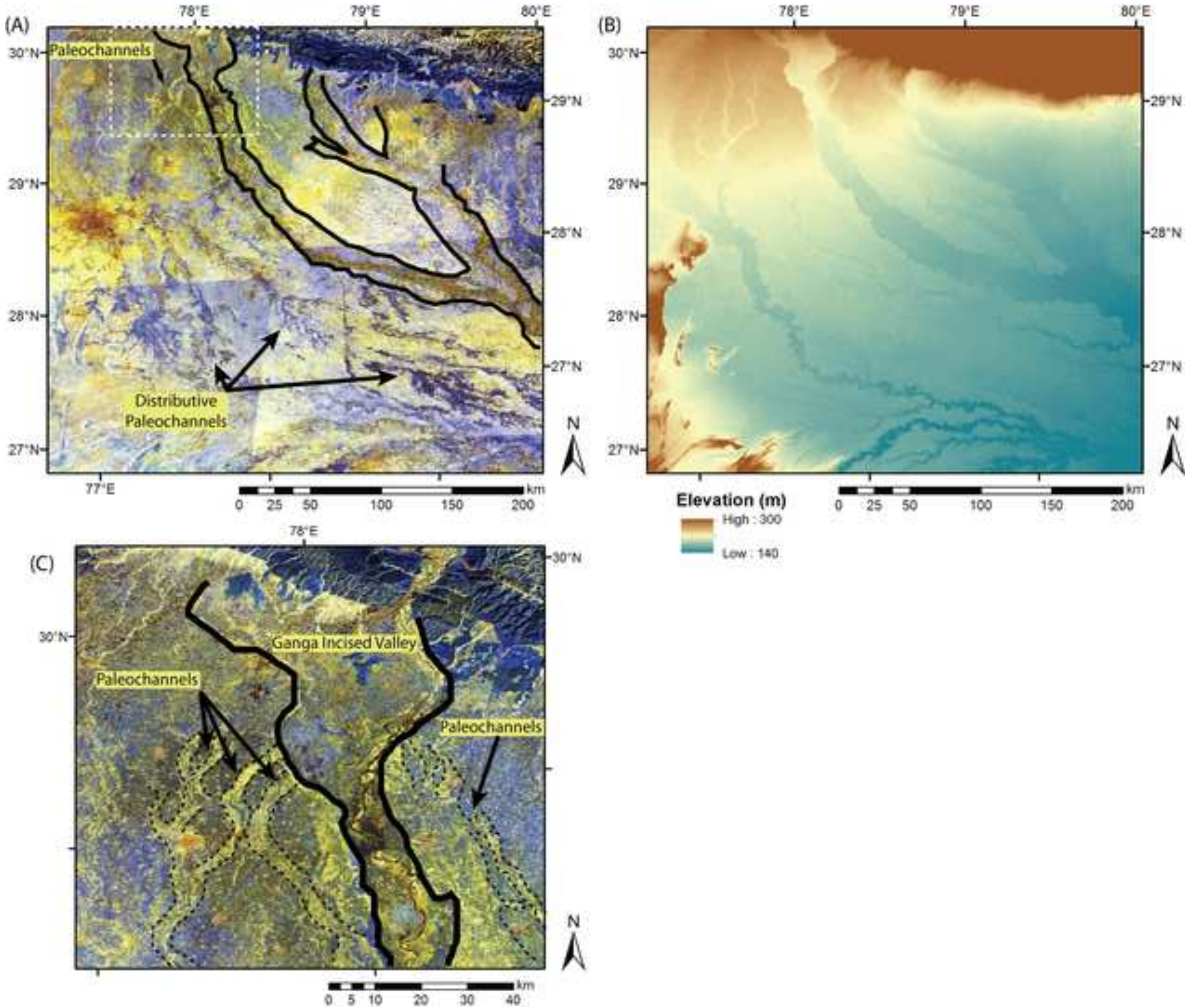

Figure (Color) 10
Click here to download high resolution image

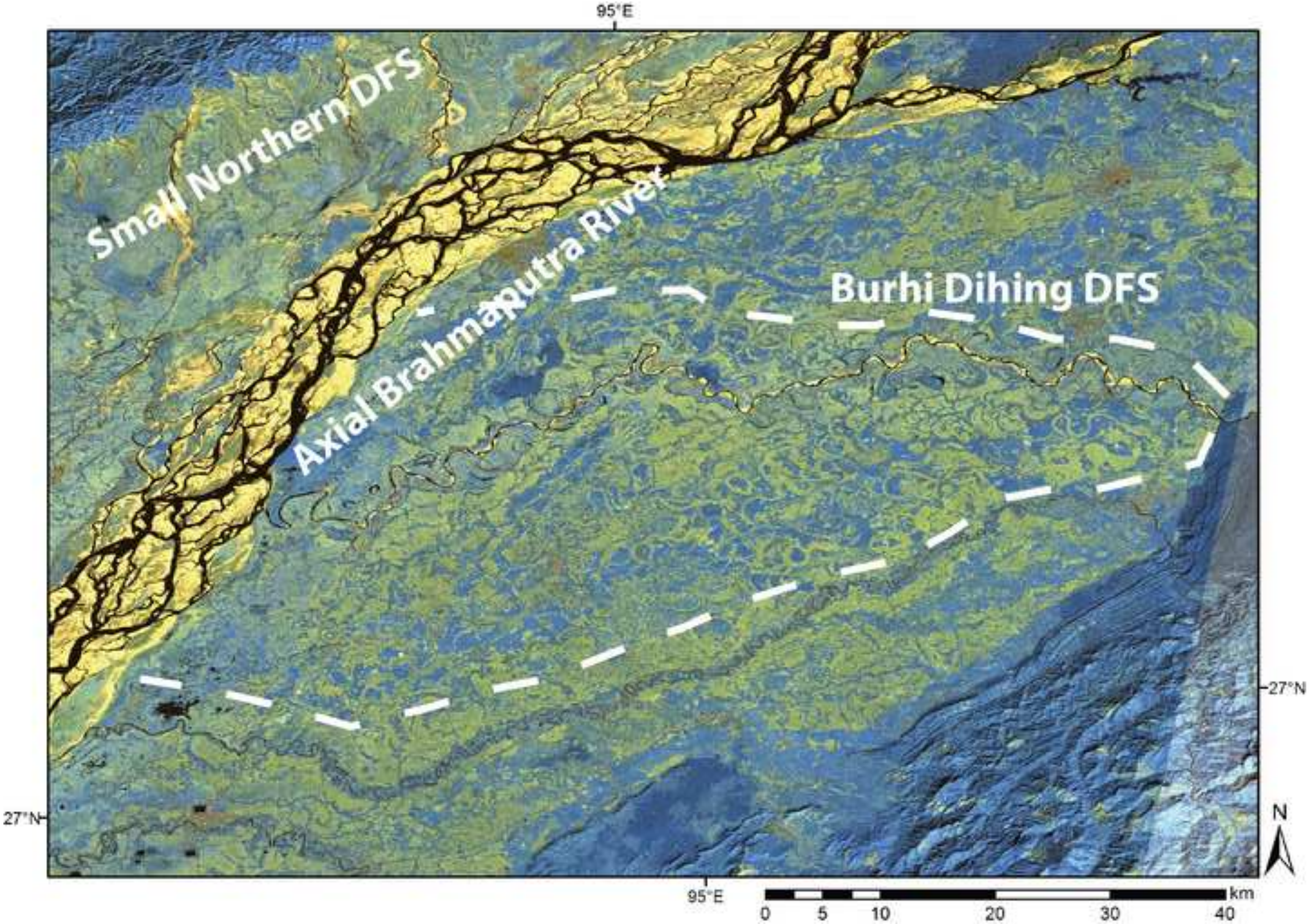

Figure (Color) 11
Click here to download high resolution image

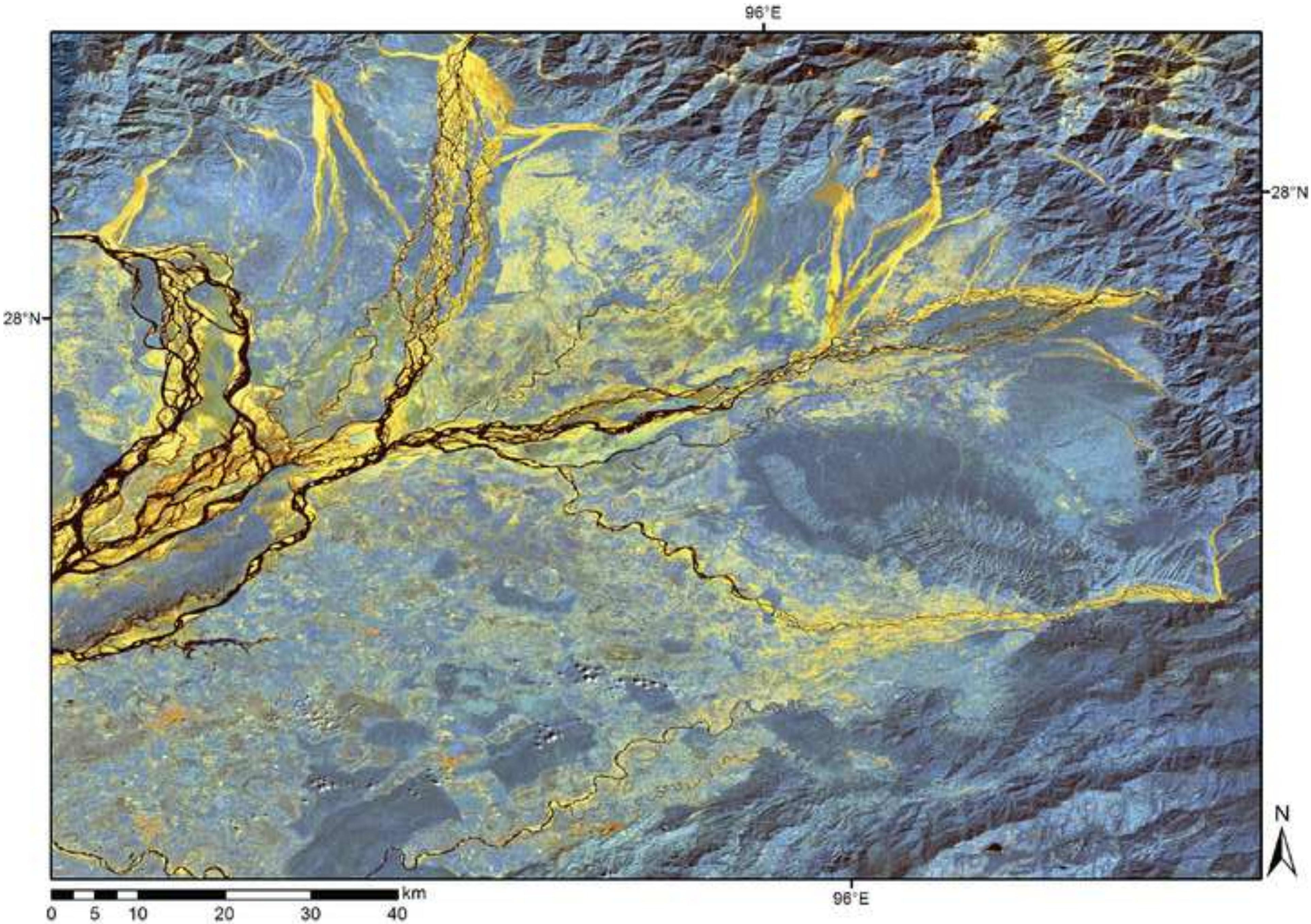

Figure (Color) 12

Click here to download high resolution image

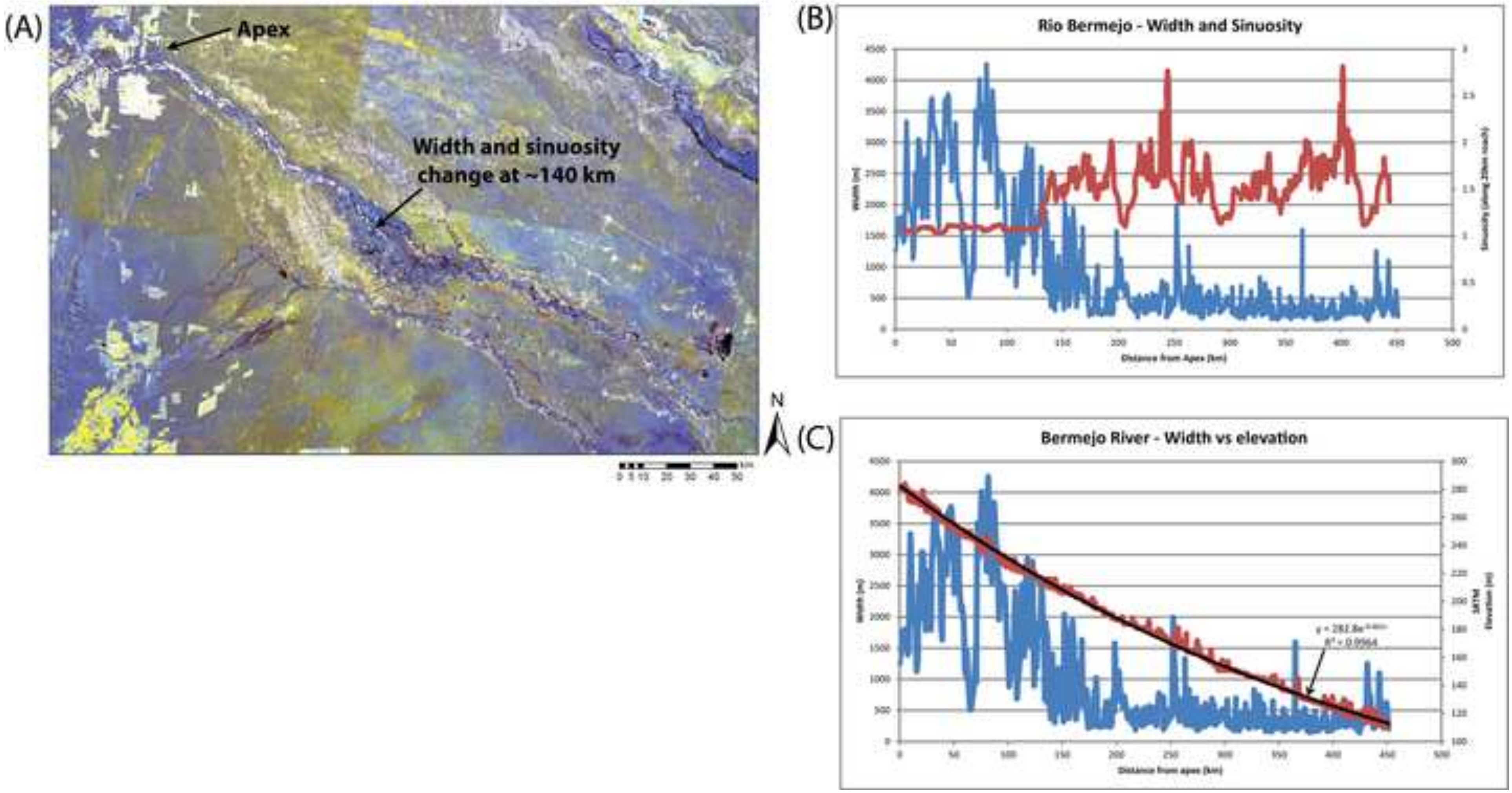

Figure (Color) 13
Click here to download high resolution image

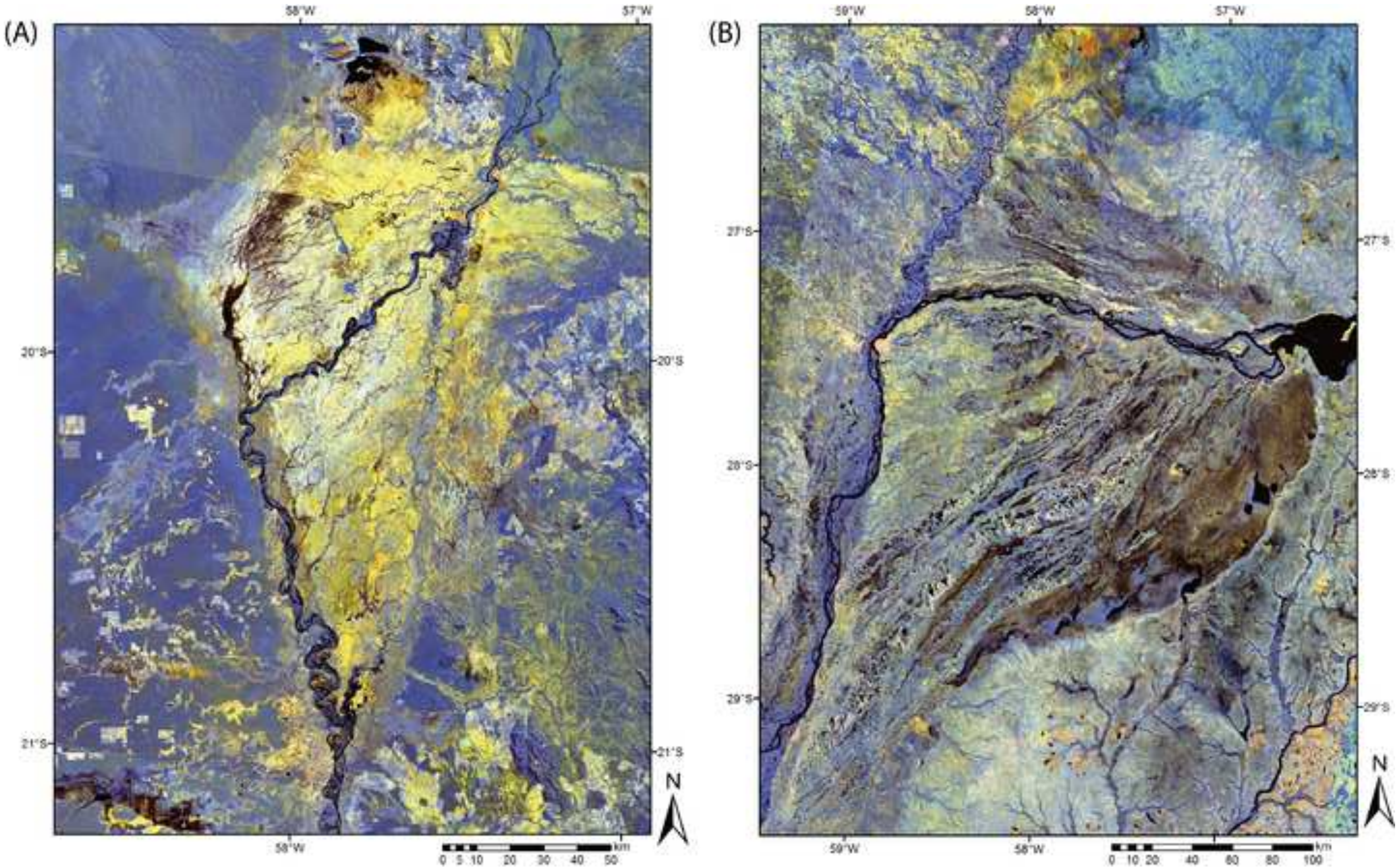

Figure (Color) 14

Click here to download high resolution image

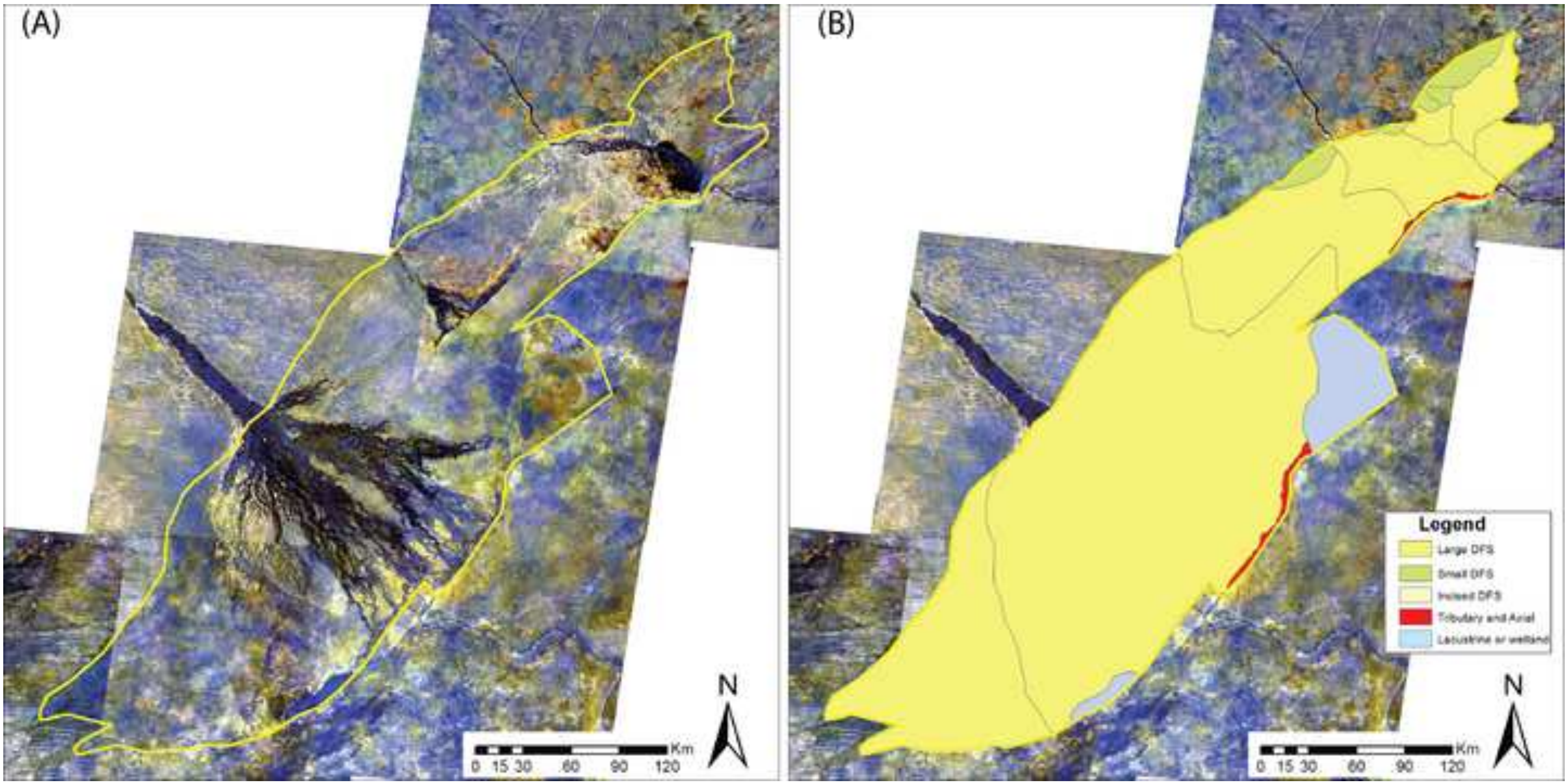

Figure (Color) 15
Click here to download high resolution image

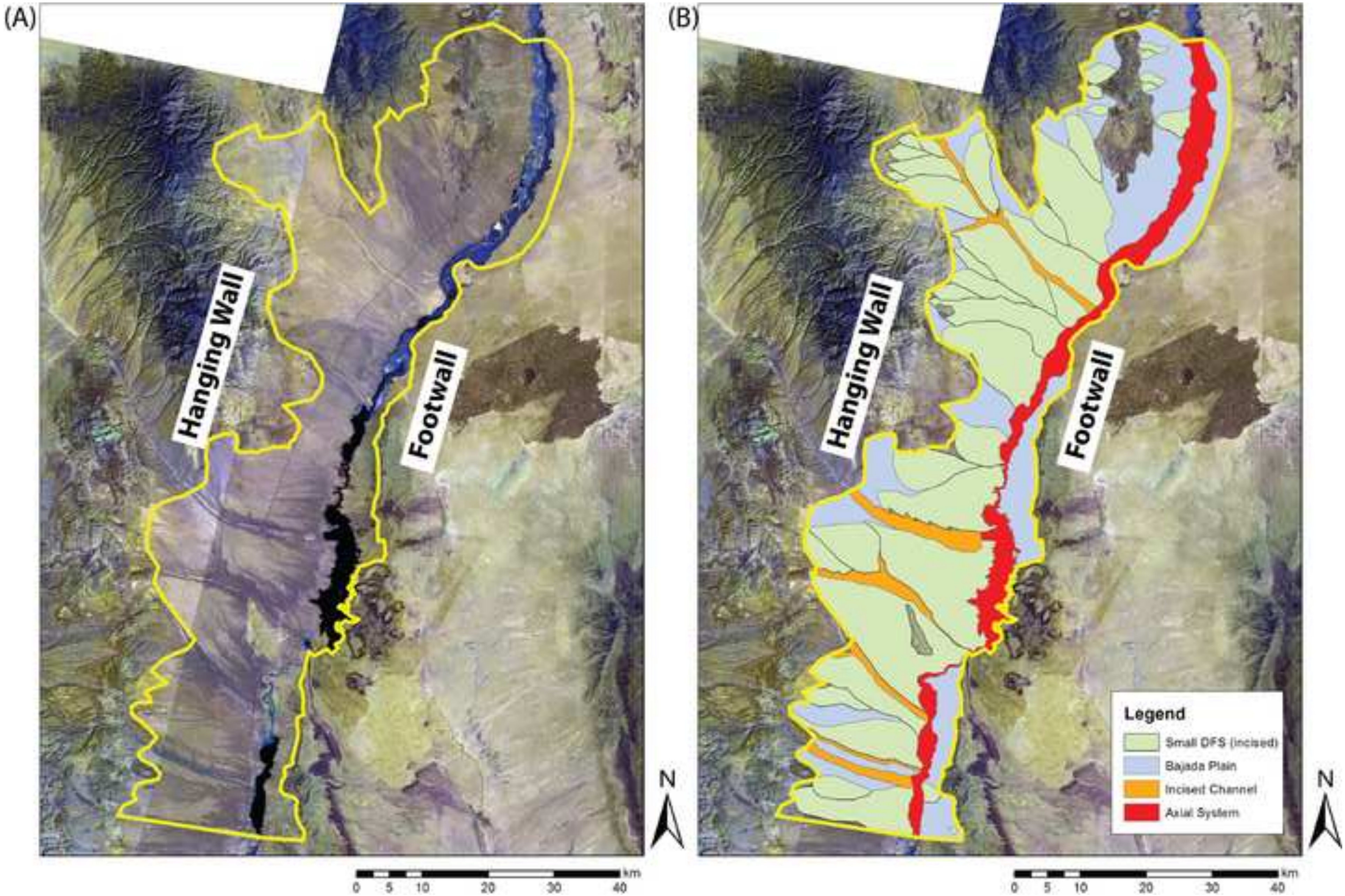

Figure (Color) 16
Click here to download high resolution image

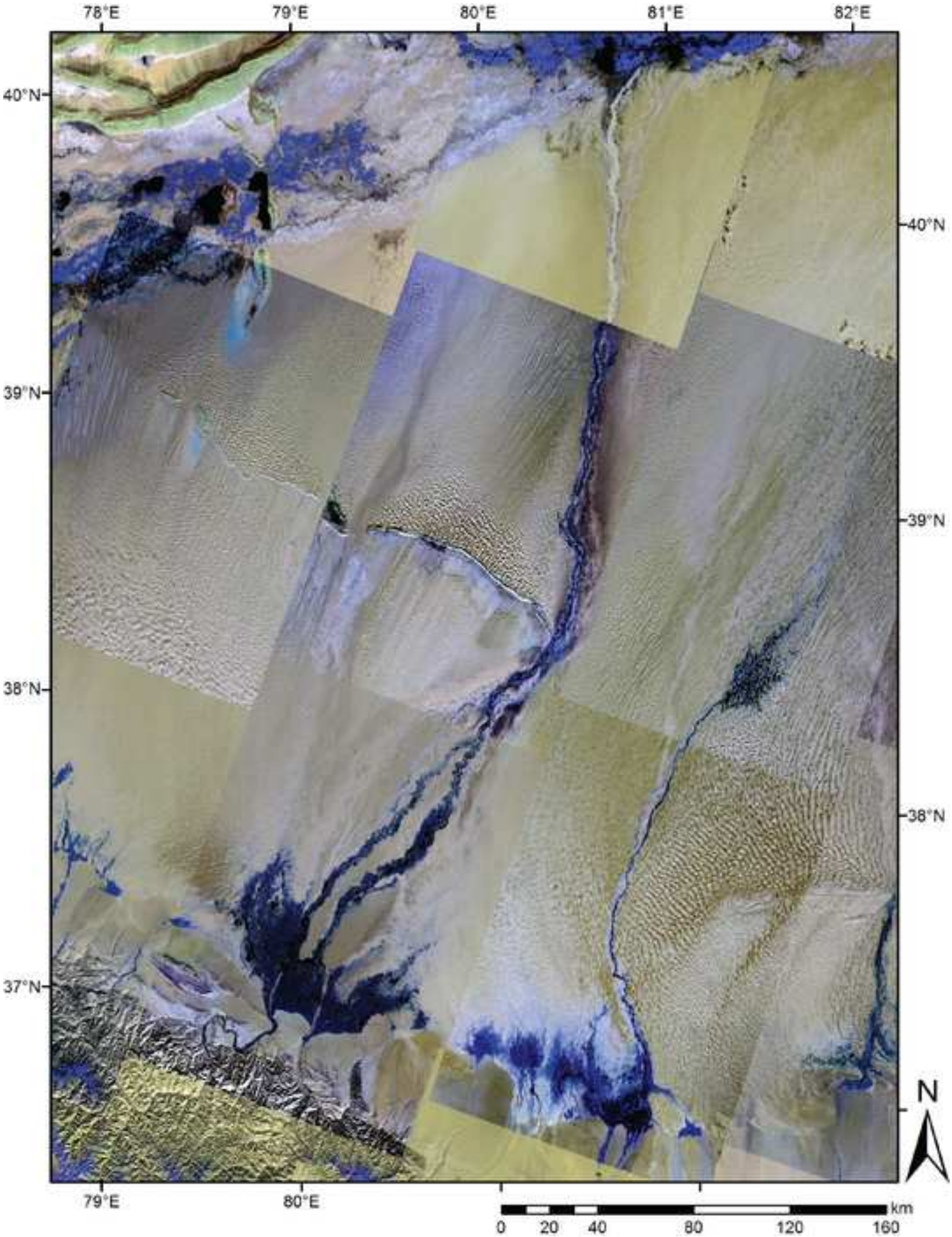

Figure (Color) 17
Click here to download high resolution image

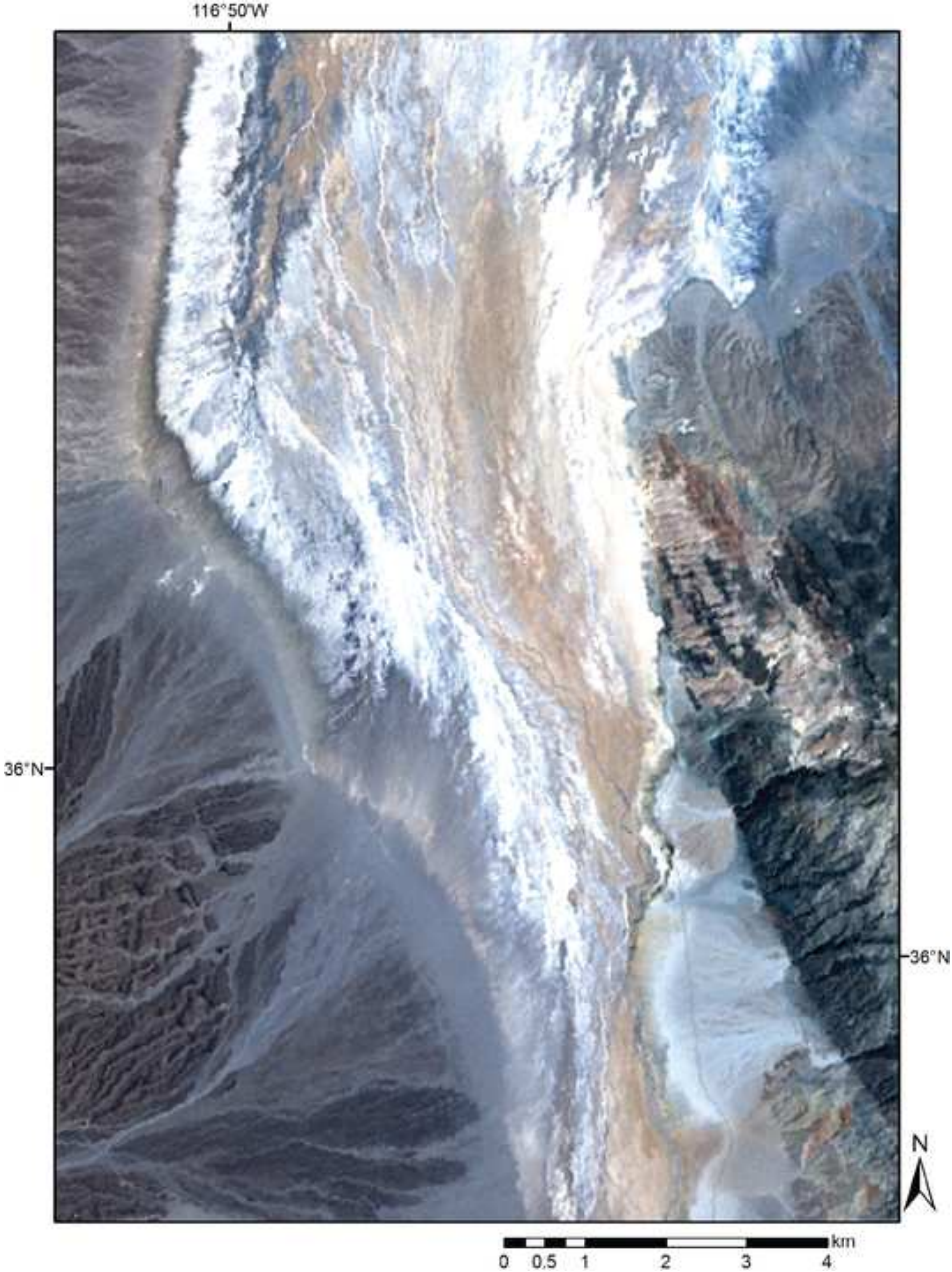

Figure (Color) 18
Click here to download high resolution image

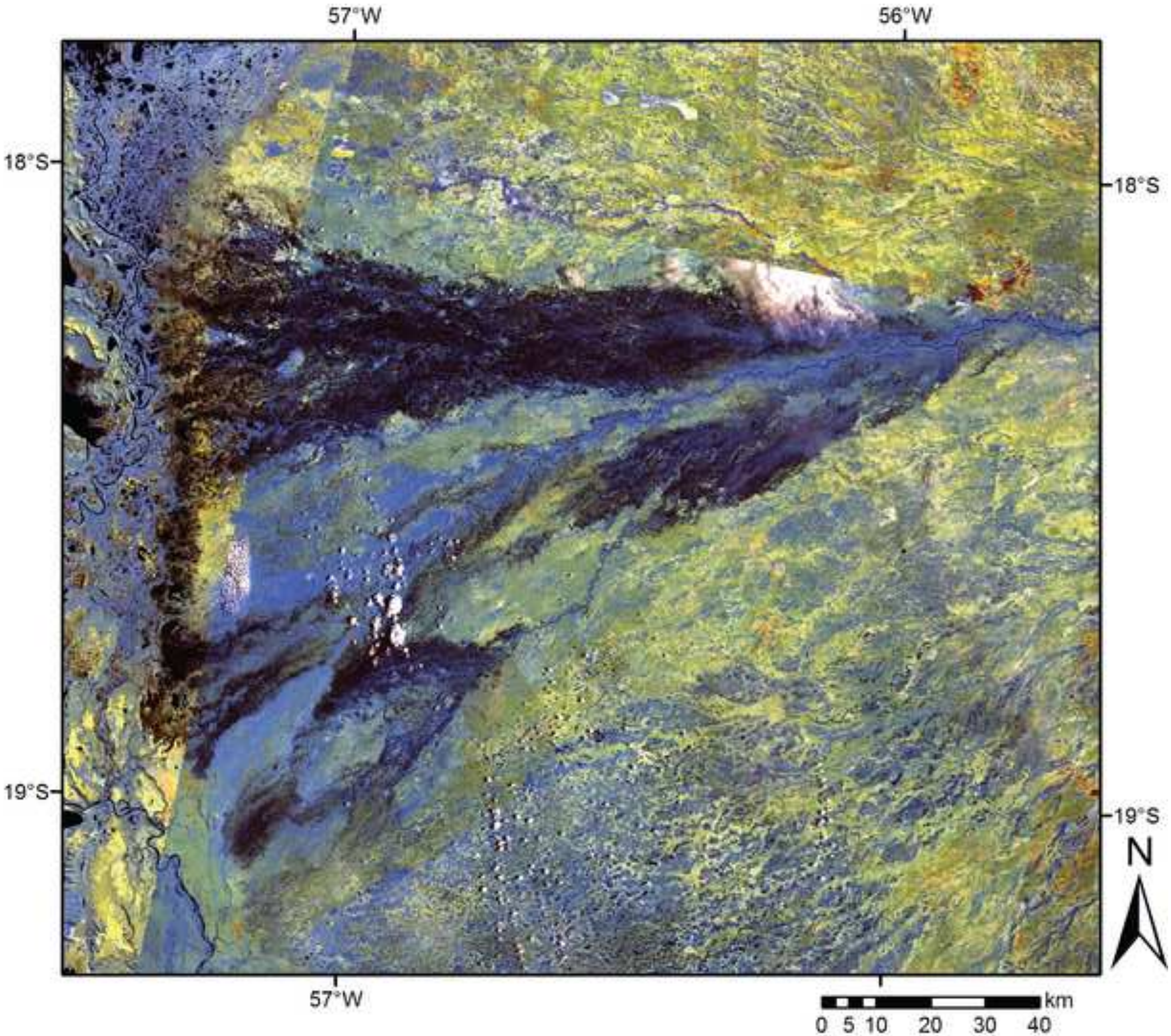

Figure (Color) 19
Click here to download high resolution image

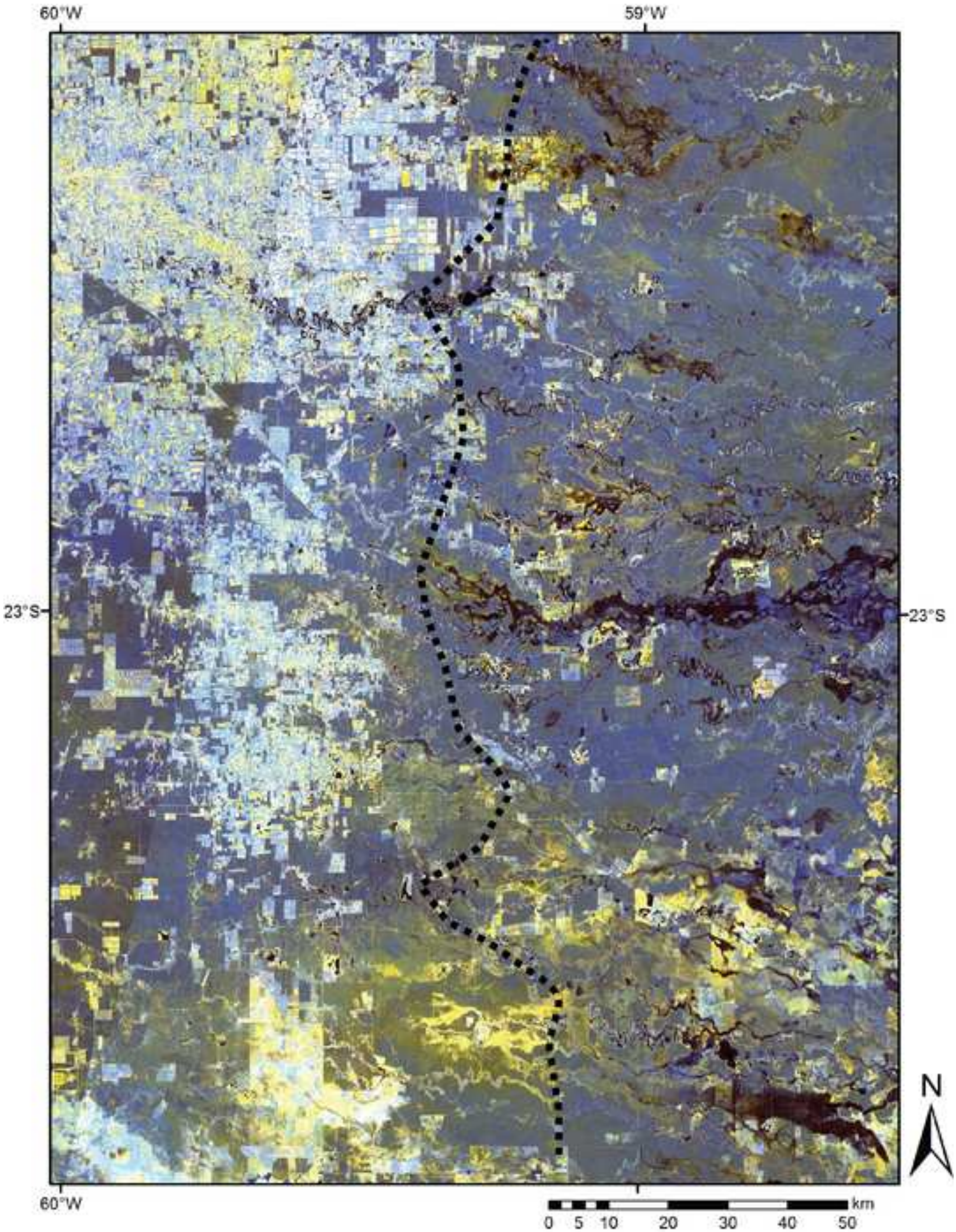

Figure (Color) 20
Click here to download high resolution image

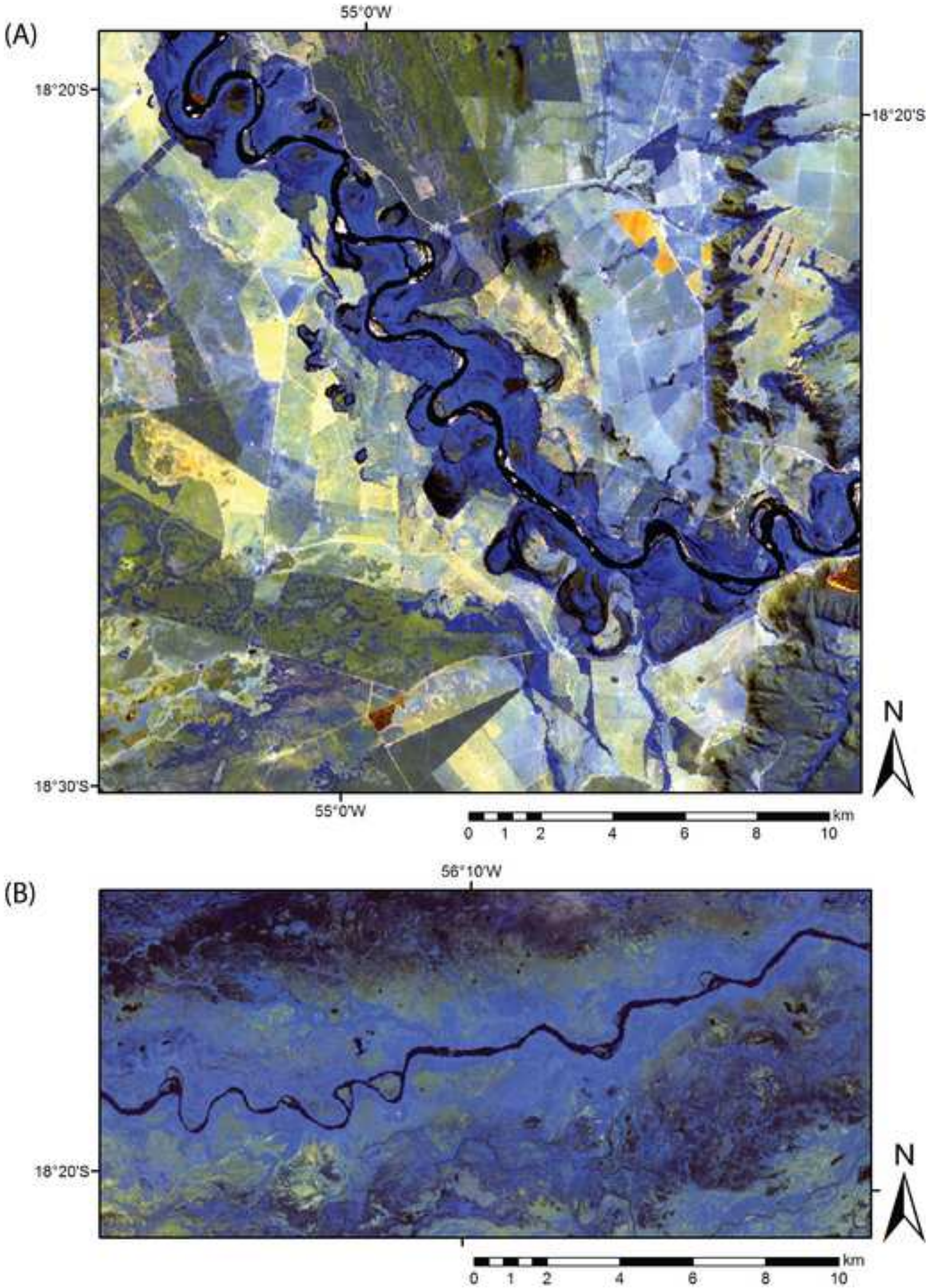

Figure (Color) 21

Click here to download high resolution image

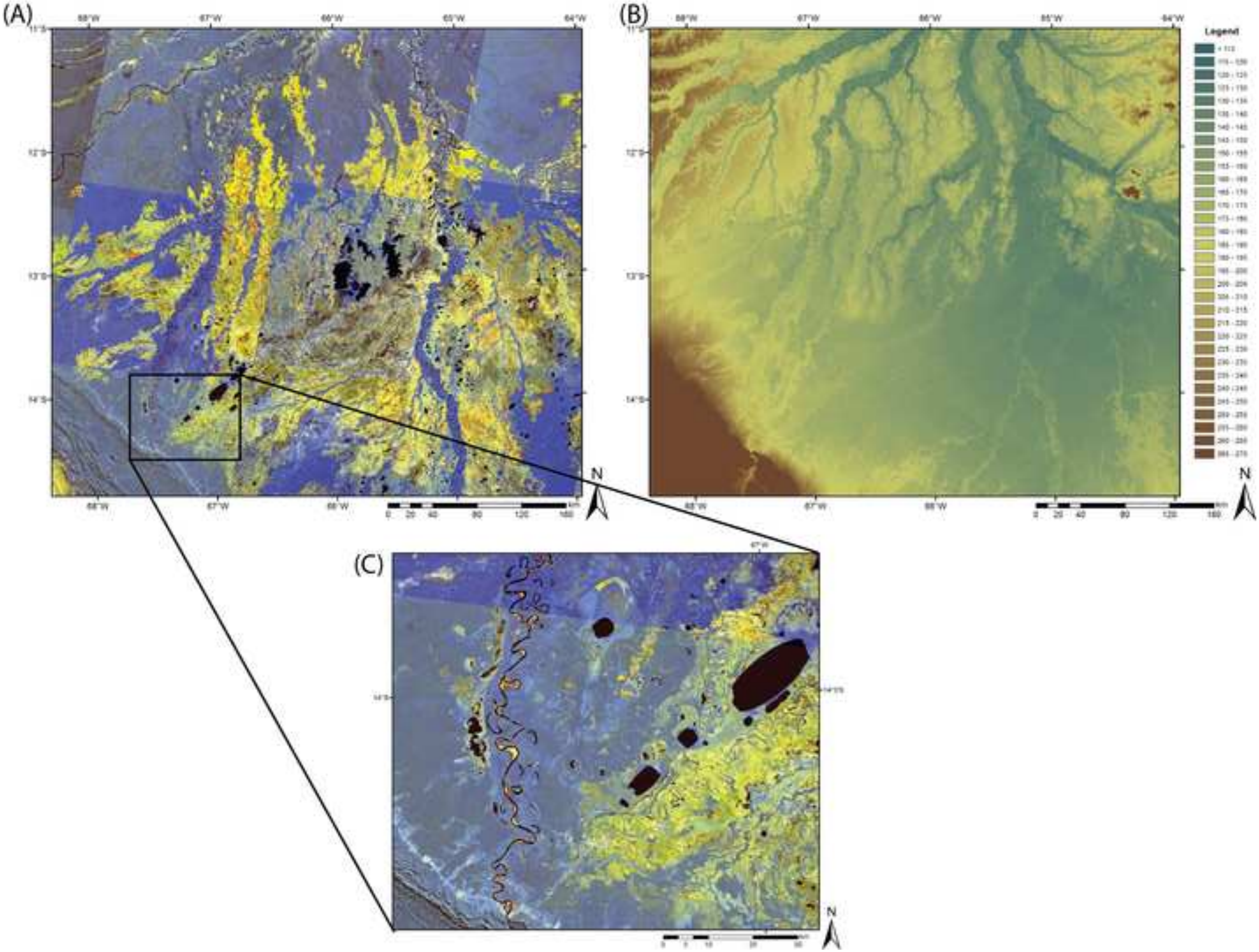

Figure (Color) 22
Click here to download high resolution image

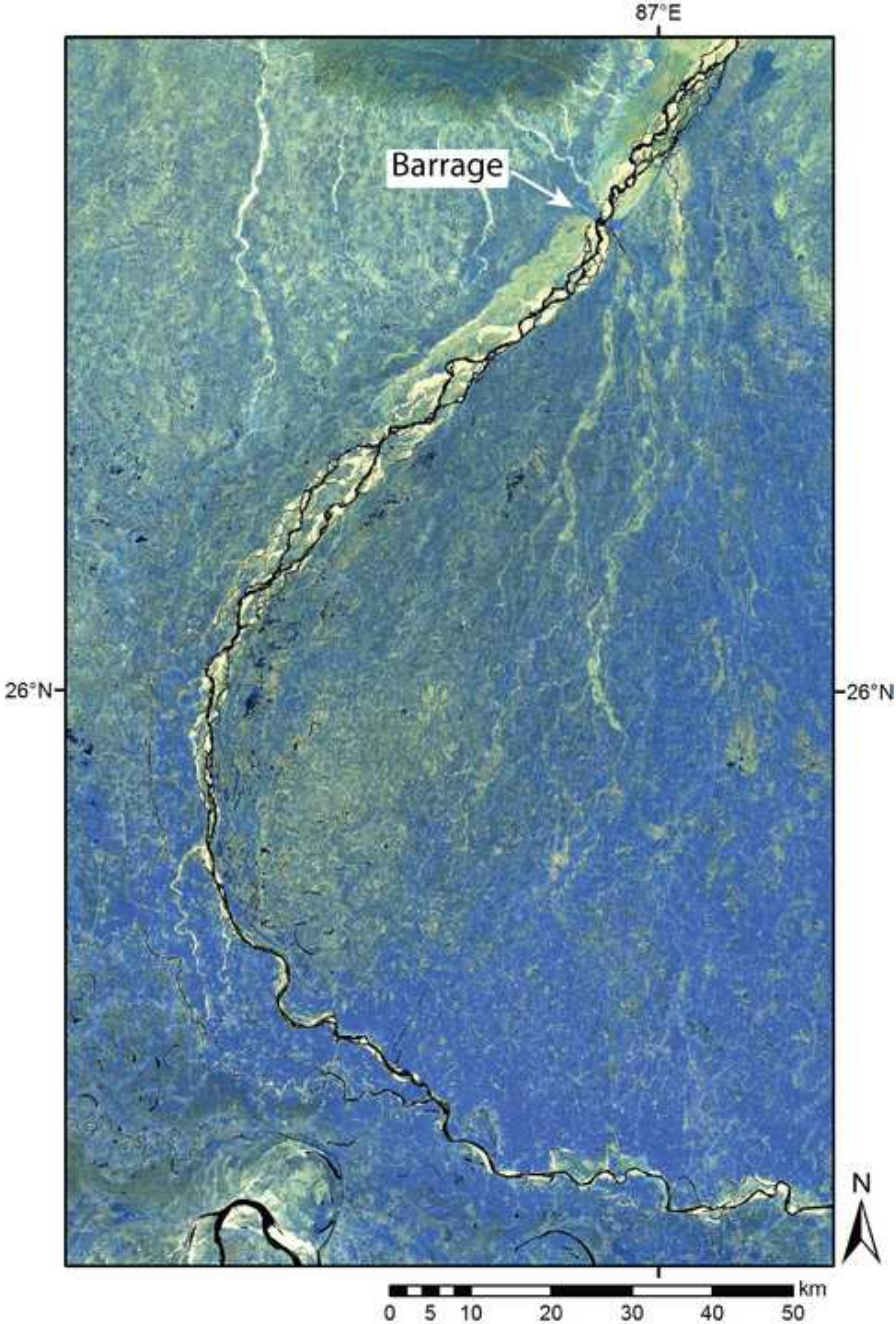

Figure (Color) 23
Click here to download high resolution image